National Library of Canada
Acquisitions and Bibliographic Services Branch
395 Wellington Street
Ottawa, Ontario
K1A 0N4

Bibliothèque nationale du Canada
Direction des acquisitions et des services bibliographiques
395, rue Wellington
Ottawa (Ontario)
K1A 0N4

Your file Votre référence

Our file Notre référence

NOTICE

The quality of this microform is heavily dependent upon the quality of the original thesis submitted for microfilming. Every effort has been made to ensure the highest quality of reproduction possible.

If pages are missing, contact the university which granted the degree.

Some pages may have indistinct print especially if the original pages were typed with a poor typewriter ribbon or if the university sent us an inferior photocopy.

AVIS

La qualité de cette microforme dépend grandement de la qualité de la thèse soumise au microfilmage. Nous avons tout fait pour assurer une qualité supérieure de reproduction.

S'il manque des pages, veuillez communiquer avec l'université qui a conféré le grade.

La qualité d'impression de certaines pages peut laisser à désirer, surtout si les pages originales ont été dactylographiées à l'aide d'un ruban usé ou si l'université nous a fait parvenir une photocopie de qualité inférieure.

Canada

ISOTOPE HYDROGEOLOGY AND AQUEOUS GEOCHEMISTRY

of

SELECTED BRITISH COLUMBIA HOTSPRINGS

by

Robert John Phillips

A thesis
submitted to the School of Graduate Studies
in partial fulfillment of the requirements
for the degree of M.Sc. in Geology

UNIVERSITY OF OTTAWA
OTTAWA, CANADA, 1994.

ISBN 0-315-95968-1

UNIVERSITÉ D'OTTAWA
UNIVERSITY OF OTTAWA

Abstract

Hydrogeochemical analyses of the thermal waters at Hotsprings Cove, west coast Vancouver Island, reveal the presence of a stable geothermal reservoir. Temperature (50.5°C), and aqueous geochemical data are nearly identical to those dating back to 1898. δ^{18}O-D plots indicate local recharge for these thermal waters, whereas radiocarbon isotopes suggest mean residence times of several thousand years and modification by sulphate-reducing bacteria.

Bromide/chloride ratios, when considered with tritium and ^{34}S data, are indicative of minor seawater mixing near the discharge zone. Binary mixing models, with local recharge waters and local seawater as end-member components, point to maximum local seawater contributions of about 1% and 4% for Hotsprings Cove and associated Mate Island thermal waters, respectively. Most chemical and isotopic geothermometer estimates are < 90°C. The Ahouset hotspring, located 12 km south of Hotsprings Cove has low total dissolved solids, a pH of 10.05, and a different geochemistry. Helium gas isotope data, although consistent with proximity to local and regional intrusions, indicate minor but significant mantle-derived gas contributions to the geothermal flow system.

Data from the Selkirk Range show a consistent sodium-sulphate geochemistry among the three hotsprings sampled in the Kuskanax Batholith. All waters have low bicarbonate content. ^{14}C values in excess of 100 pmc at the Nakusp hotspring imply incorporation of ^{14}C-

active DIC from soil zone organics entrained during recharge, with possible additional ^{14}C contributions occurring due to sulphate reduction and incorporation of soil zone organics during mixing with non-thermal groundwaters near discharge. ^{14}C-derived mean residence times for the sulphide-rich waters of Halcyon hotspring are also short; possibly ~1000 years. Geothermometer estimates for all three springs are consistent and fall into two groups, one group near ~90° C and the other between 115° C and 155°C. High heat flow, steep topography, and proximity to the CRFZ are likely increasing the volume of volatiles in these locally-recharged thermal waters as evidenced by nearly 400 times the atmospheric volume of helium gas in Halcyon. These Omineca Belt hotsprings all have radiogenic He-isotope signatures, but minor input of deep-seated volatiles cannot be ruled out

Helium isotope samples from hotsprings in the Mt. Meager area of the Coast Plutonic Complex have $(^3He/^4He)/(^3He/^4He)_{air}$ ratios near 6, indicative of volcanogenic helium input. Helium isotope ratios from geothermal waters sampled within different tectonic belts of the southern Canadian Cordillera are regionally consistent, and show good correlation with helium data for hotsprings located in similiar tectonic regimes to the south in the United States.

Acknowledgements

Many thanks are owed for the encouragement and support required to undertake, carry out and complete this thesis study. First thanks go to the late Dr. Brian Rust and Dr. Ralph Kretz of the University of Ottawa who introduced me to geosciences as an undergraduate and then encouraged and assisted me to return to graduate studies.

Thanks are also due to many different laboratory people for their excellent service and the quality of analytical data provided, including Dr. W.B.Clarke of McMaster University, and John Loop, Gilles St. Jean, Margaret Maclaren and Natalie Morissette at the University of Ottawa. Dr. Stephan Weiss of FRG labs in Germany, who provided helium analyses, and Dr. Conrad Gregoire and associated staff of the GSC, who provided Dionex analyses, are thanked for their support and their "deep graduate student discounts" which are too generous to detail. The staff of the Department of Geology at the University, including Hélène De Gouffe, and Sylvie Downing are thanked for their continuous, good-natured, expert support, as are fellow grad-students Kevin Telmer, Mark Mihalasky, Mark Shore, Imasiku Nyambe, Mathew Leybourne, Dr. Julian "Augustus Nobel" Murton, Yusef Al-Mooji and William "The Badger" Bajalli.

Thanks are also in order to Dr. F.A. Michel of Carleton University, for examining the thesis with his usual thoroughness and attention to detail. Mention must be made of his

graduate and undergraduate courses in hydrogeology, which have nurtured a "steady stream" of inspired students and budding hydrogeologists over the years and provided teaching assistantships for a "continuous flow" of graduate students. Thanks also to Dr. Peter Fritz for his encouragement and timely examination and review of the manuscript, and to Dr. Trevor Lewis of the Pacific Geoscience Centre for his brief but invaluable consultations following my seminar presentation to the Canadian Geothermal Energy Association . Thank you as well to Canadian taxpayers and goverment departments, particularly the Geological Survey of Canada and Energy Mines and Resources Canada , for DSS contract 2354-0-0167/01-XSB.

More than thanks are in order to my multi-talented supervisor Dr. I.D. Clark, who accepted and financed me for this project, introduced me to isotope hydrogeology, and was a constant source of encouragement and information. I'll long remember being tossed about in a boat at the mouth of Hotsprings Cove,in waters agitated by post-hurricane force winds, looking for an offshore gas vent and wondering if Ian (in his scuba gear) would ever rise from the depths of the Pacific to supervise again. His energy and enthusiasm for scientific research is contagious. To quote Dr. Jack Souther with regard to his geothermal research techniques, "He lives, eats and breaths this stuff".

Final thanks to my family; my parents Ken and Roberta Phillips and my children, Sebastien and Manna, who continually encouraged and supported me. Eternal thanks to my wife Lydia who supported our family, buoyed my spirits when they were low, and first encouraged me to move on from my job as a bus-driver and pursue what I really wanted.

Table of Contents

3 Selkirk Range Hotsprings; Halcyon, St. Leon, and Nakusp

4 Regional Geotectonic Comparision of Geothermal Areas

List of Figures

List of Tables

Selkirk Range hotsprings *Page*

Regional geotectonic summary

List of Plates

1 Introduction

1.1.1 Hotspring Occurrences

Hotsprings are defined as waters emanating from naturally occurring springs where the discharge temperature is at least 5°C above the mean annual air temperature (White 1957). The origin of these thermal springs as well as their source of heat have likely been a subject of wonder and mystery since human-beings first eased themselves into their hot, soothing waters.

Hotsprings occur naturally in a variety of locations and settings and have a long history of use for therapeutic baths and health spas throughout the world (Waring, 1965). In North America, thermal waters have been popularized as spas and tourist attractions by locations such as Yellowstone Park in the United States, and Banff and Harrison Hotsprings in Canada.

Canadian hotsprings are concentraed in the Cordillera, with approximately 150 located thus far in British Columbia and the Yukon (see for example Elworthy, 1925, Souther and Halstead, 1973, McDonald 1978). Proximity to the active convergent continental plate margin has produced a distinct assemblage of tectonic "belts" within the Cordillera as shown in Fig.1.1. These tectonic belts roughly parallel the convergent margin, and host most of Canada's natural thermal waters as well as British Columbia's often spectacular mountain vistas.

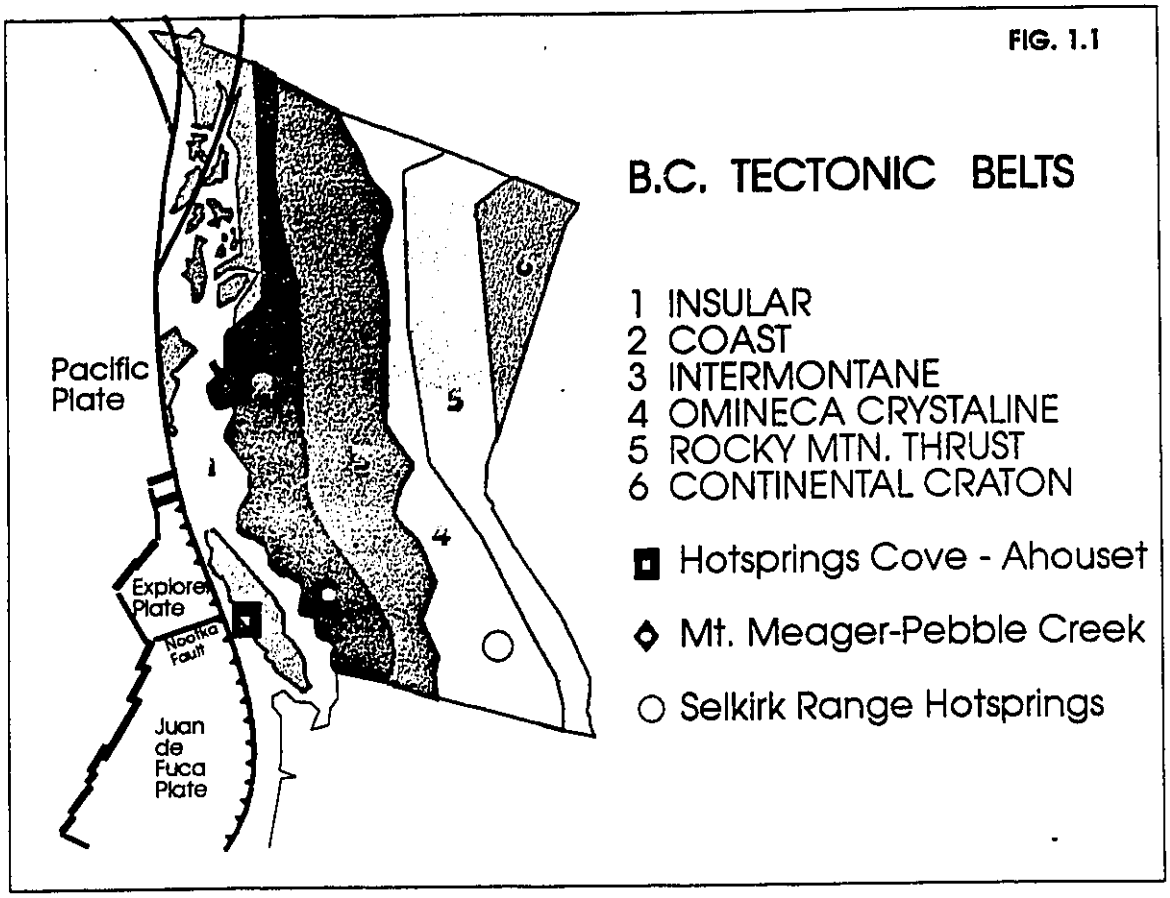

Documentation of geothermal flow systems includes geochemical and hydrogeological characterization of parameters such as the chemical constituents of the waters, their "age" or mean residence time, their flow history including recharge, discharge and possible mixing with non-thermal waters as well as estimation of the maximum reservoir temperatures where the fluids reside prior to discharge (Fournier, 1990). Delineation of these characteristics aid in determining the development potential of a given geothermal reservoir. For example, is it suitable for exploitation as a high or low-temperature resource, or is it preferable to discourage development and leave the thermal waters to flow from their natural vent?

1.1.2 Thermal Water Use in Canada

While the United States has a number of active commercially-productive geothermal fields, Canada has to date but one deep well discharging high-temperature geothermal fluids, MC-1 at Mount Meager B.C. (Jessop et al, 1991). Abundant hydroelectric power, slow global economic growth, and relatively stable world oil prices since 1980 have slowed funding and commercial development of geothermal facilities capable of producing electricity in Canada. However direct use of hotsprings for bathing and therapeutic purposes is as popular as ever, while installation of various heat-pump technologies continues, encouraged by highly successful projects such as those at Springhill N.S. and Carleton University in Ontario (Jessop et al., 1991). Additionally, several Canadian studies have recommended use of low-temperature geothermal waters (<100°C) for space-heating, domestic hot-water supply, or fish hatcheries (see for example Clark 1985, NSBG 1988).

1.1.3 Origin and Scope of Project

This project, initiated by Dr. Ian Clark of the University of Ottawa, and partially funded by Energy, Mines and Resources and N.S.E.R.C., is a continuation of the documentation and scientific inquiry into hotsprings and geothermal resources which commenced near the turn of the century (Clapp 1913, Elworthy 1925), and evolved further during the energy crisis of the 1970's. Section 2 is concerned with thermal waters from Vancouver Island, part of the Insular Belt of the Canadian Cordillera, while Section 3 examines hotsprings from the Selkirk Range of the Omineca Belt. One of the most intriguing aspects of the project concerns, in Sections 2.6 and 4, the analysis and interpretation of helium gas isotopes, sampled for the first time from Canadian thermal waters.

This noble gas data, used as a regional tectonic interpretational tool in Section 4, raises as many questions as it answers about the nature and potential origin of our geothermal fluids. Thermal waters from the the Coast Plutonic Complex, including samples from the Mount Meager-Pebble Creek area, are examined along with those from the Omineca and Insular Belts. This new information may serve not only as part of the continuing scientific inquiry and documentation of Canadian thermal resources, but also as a source of future pondering for those fortunate enough to soak in our soothing, natural hotspring waters.

1.2 Study Objectives

The objectives of study are threefold. The first two aspects involve the characterization of hotsprings from two different regions; the west coast of Vancouver Island area of the Insular Belt north of Tofino, and the Selkirk Range of the Omineca Belt south of Revelstoke. The third objective, a regional geotectonic comparision, incorporates data from both of the above two studies as well as new data from the Mount Meager-Pebble Creek geothermal area of the Coast Plutonic Complex. These objectives are summarized below.

1.2.1 Specific objectives of study are to:

1. Characterize the isotope hydrogeology, gas and aqueous geochemistry of Insular Belt geothermal flow systems at Hotsprings Cove and Ahouset

2. Characterize, as above, Omineca Belt geothermal flow systems in the Selkirk Mountains at Halcyon, St. Leon and Nakusp hotsprings

3. Compare the above-named geothermal systems and the Mount Meager-Pebble Creek geothermal area with respect to geologic and tectonic setting.

1.3. Field Sampling Program

1.3.1 Sampling Dates and Locations

West coast Vancouver Island geothermal sites were sampled on Dec 6 and 7, 1990. Mount Meager-Pebble Creek samples were collected the following summer on July 8 and 16 respectively, while the Selkirk Range sites and Harrison Hotsprings were sampled during the first week of September 1991. Sample site locations for each region are shown in their respective chapters.

1.3.2 Sample Type and Collection Method

Wherever possible, samples were collected from waters flowing directly from the thermal vent, facilitated through use of a funnel with tygon tubing attached. Sample containers are first rinsed twice with the waters to be collected. Purpose of sample, sample type, volume, container, collection method, and other details relating to collection are shown in Table 1.1.

Mention should be made of sampling procedure for collecting sulphide and sulphate fractions from thermal waters. The technique involves addition of cadmium acetate during sample collection. This precipitates out cadmium sulphide CdS, which can then be collected on a 45 μ filter, prior to converson to silver sulphide. The silver sulphide sample is converted to sulphur dioxide gas for mass spectrometric analysis. The fluid remaining after the initial extraction of CdS is retained and barium chloride ($BaCl_2$) is then added to precipitate out the sulphate fraction as $BaSO_4$. The barium sulphate is converted to sulphur dioxide gas prior to mass spectrometric analysis of its ^{34}S component. (see Table 1.1)

TABLE 1.1	Sampling Program					
Purpose of Sample	**Phase**	**Sample type**	**Volume**	**Container**	**Sampling Method**	**Comments**
Characterize aqueous geochemistry	water	Anions	50 mls	Nalgene	on site filtration, 0.45µm	Storage at 4°C
	water	Cations	50 mls	Nalgene	as above & acidify to pH 2.5	
	water	Alkalinity	50 mls	Grad.Cyl.	fill at vent, then acid titrate	Hach field test kit
	water	Silica	25 mls	Nalgene	dilute to 10% with DI water	25mls HS + 225mls DI
Characterize gas geochemistry	gas	gas	700ml	Glass	displace thermal water	Funnel and tygon tubing used to maximize gas input for all gas samples
	diss. gas	dissolved gas	700ml	Glass	displace thermal water	
Characterize Isotope Hydrogeology	water/gas	Helium/Neon gas	?mls	Cu tube	Funnel-tube over vent	2 min. flow-thru of thermal water then clamp quickly both ends
	water	O-18-D	50 mls	Nalgene	unfiltered , flowing water	
	water	sulfide/sulfate for S-34	2litres	Nalgene	add CdS , then fill	Extract CdS filtrate, add BaCl2 extract BaSO4.
	DIC/water	Carbon -13	20 litres	Nalgene	fill, add NaOH, BaChloride	Alkalize to pH 10, then add Barium Chloride
	DIC/water	Carbon-14	20 litres	Nalgene	fill, add NaOH, BaChloride	Same as Carbon-13
	water	Tritium	50-500 mls	Nalgene	fill at vent	

Noble gas samples were collected in 30 cm lengths of 0.95 mm diameter copper tubes which were then crimped at both ends to prevent helium loss through diffusion (Weiss, 1968). Bulk gas samples were collected in glass bottles which were first filled with the thermal water being sampled. Gas bubbles from the thermal vent were then allowed to displace the resident water and the container was capped while still submersed. These gas samples were then transported and stored inverted, with a minimum 3cm layer of residual thermal water as an airlock. Plates showing helium and gas sampling apparatus are part of Appendix A..

1.4 Analytical Program

Due to a variety of sample types, sample analyses were carried out at a number of different laboratories. Analytical details and equipment specifications are shown in Table 1.2.

1.4.1 Stable Isotope Techniques

All stable isotope analyses were by gas mass spectrometer. Results are expressed as delta permil differences from known standards. ^{18}O contents in water were measured following conversion to CO_2 gas and referenced to standard mean ocean water (SMOW) according to the fractionation factor $\delta_{CO2\text{-}H2O} = 1.14143$ established by Friedman and O'Neil (1977). Analytical precision for all analyses are given with results of analyses. ^{13}C and ^{14}C are prepared as gases under vacuum at 25° C following H_3PO_4 attack on precipitated dissolved inorganic carbon samples (DIC). Values are presented as permil differences from PDB (Bellemnite from Peedee Formation). ^{14}C values are expressed as percent modern carbon (pmC), defined as 95% of the activity of the NBS oxalic acid standard in 1950.

TABLE 1.2	Analytical Program			
Purpose of Analysis	**Analysis of :**	**Laboratory**	**Analytical Method**	**Comments**
Characterize aqueous geochemistry	Anions	Geological Survey Canada Ottawa, Ont.	Dionex HPLC	all samples run undiluted except seawater samples
	Cations	University of Otttawa Geochemistry Lab	Inductively Coupled Plasma-Atomic Emission Spectroscopy	Argon plasma stream; Thermo Jarrell Ash Atomscan 25 ICP-AES
	Alkalinity	Field analysis on site	Acid titration to Known Endpoint 0.16 M Hydrosulphuric Acid	Hach Field Titration Kit Methyl Bromo-Cresol Indicator
	Silica	University of Otttawa Geochemistry Lab	ICP-AES	Analyses multiplied by factorof 10 due to field dilution of samples
Characterize gas geochemistry	gas	University of Otttawa Chemistry Department	Gas Chromatography	
	dissolved gas	University of Otttawa Chemistry Department	Gas Chromatography	
Characterize Isotope Hydrogeology	Helium/Neon gas	Dept. of Physics McMasterUniversity	Branch tube mass spectrometry	isotope dilution ; sample flow thru <80 mesh activated C @ -186°C
	Helium	Institut Fur Hydrologie GSF, Munich, Germany	Branch tube mass spectrometry	
	O-18	University of Ottawa Stable Isotope Lab	Gas mass spectrometry VG-SIRA12 mass spectrometer	Carbon dioxide gas equilibration with water sample per SMOW
	Deuterium	University of Otttawa Stable Isotope Lab	Gas mass spectrometry VG-SIRA12 mass spectrometer	
	sulfide/sulfate for S-34	University of Otttawa Stable Isotope Lab	Gas mass spectrometry VG-SIRA12 mass spectrometer	Barium sulphate precipitate converted to sulphur dioxide gas
	Carbon -13	University of Otttawa Stable Isotope Lab	Gas mass spectrometry VG-SIRA12 mass spectrometer	carbon dioxide gas from DIC
	Carbon-14	Isotrace Radiocarbon Lab University of Toronto	Accelerator Mass Spectrometry	gas proportonal counting on purified carbon dioxide gas
	Tritium	University of Waterloo Waterloo, Ont.	Liquid scintilation counting	Liquid scintilation counting following electrolytic enrichment

Sulphate and sulphide samples were analysed for ^{34}S in SO_2 following standardized procedures after conversion to silver sulphide using KIBA reagent. $^{13}C/^{12}C$, $^{18}O/^{16}O$, $^{34}S/^{32}S$, and $^{2}H/^{1}H$ mass spectrometric determinations were carried out on a VG-SIRA 12 gas source mass spectrometer at the Stable Isotope Facility, University of Ottawa.

Measurement of helium isotope ratios was carried out at McMaster University utilizing high-sensitivity branch tube mass spectrometry. Helium and neon concentrations were measured using the isotope dilution technique where measured additions of pure ^{3}He and ^{22}Ne are introduced to a known fraction of the gas sample. All helium and neon samples were passed through a <80 mesh activated charcoal column, cooled to -186° C, allowing approximately 99.95% He introduction with negligible Ne loss.

1.4.2 Geochemistry

Analyses of aqueous geochemical components were carried out at laboratories of the Ottawa Carleton Geosscience Centre at University of Ottawa laboratories using standard analytical techniques (see also Table 1.2). Anionic constituents of water samples were analyzed at the Geological Survey of Canada laboratories in Ottawa.

2 *West Coast Vancouver Island Hotsprings; Hotsprings Cove and Ahouset*

2.1 Introduction

The allure of the sea and tranquillity of a wilderness setting are found together at Refuge Cove along with the soothing and fascinating geothermal waters of the Hotsprings Cove hotspring. Those seeking the hotspring waters for a relaxing dip can experience the power and beauty of the sea in the same breath. The 50°C thermal waters find their own way down the 10 metre ocean-side rock-face to the sea in Refuge Cove. There, they mix with the waters of the Pacific Ocean in just the right proportions to make a warm and relaxing mineral bath in the naturally-occurring, bedrock-enclosed, tide-water basins (Plates 2.1a&b next page).

These geothermal waters are just as fascinating from a scientific perspective. In addition to their interest geochemically with respect to flow history and dissolved species distribution, these Insular Belt hotsprings show strong evidence of releasing mantle-derived noble gases along with their aqueous components.

2.1.1 Location and Access

The Hotsprings Cove hotspring, also known as the Sharp Point or Ramsey hotspring, is located in Maquinna provincial park on the west coast of Vancouver Island (Fig. 2.1.1a), about 33 km north of Tofino. Access is by charter boat or floatplane. The Hesquiat Indian band also operates a water-taxi service to the reserve located on the west side of Hotsprings Cove (also known as Refuge Cove) where lodging is available. The Ahouset hotspring, a 25°C low-flow spring is located between Tofino and Hotsprings Cove on the southeast corner of Flores Island (for location see Fig. 2.2.1c).

Plates 2.1a & b ***Hotsprings Cove thermal waters meet the sea.***

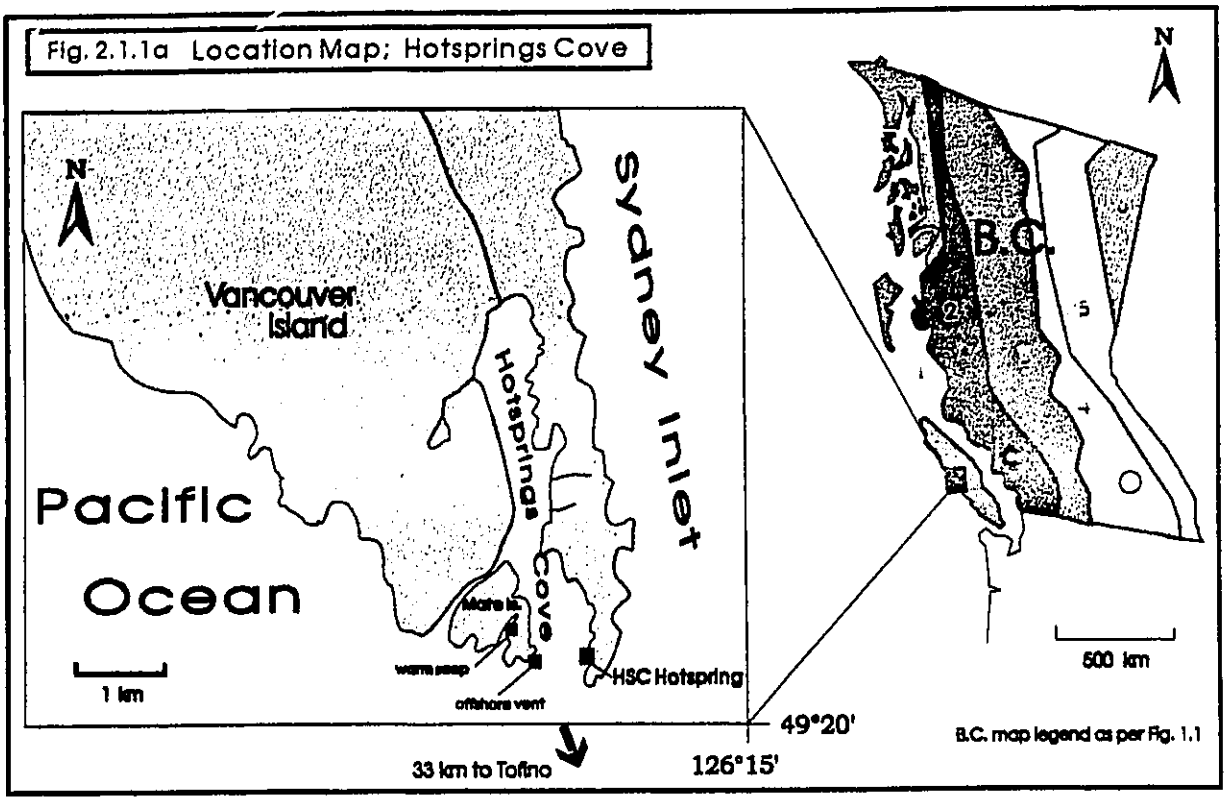

2.1.2 Climate, Physiography, and Hydrology

Mean annual air temperature in the study area is about 9° C and climate is typical of a northern temperate rainforest with approximately 3300 mm. of precipitation annually, much of it falling between October and March as shown in Fig. 2.1.2a (Environment Canada, 1980). Additionally, fog frequently occurs when winds are calm, particularly in late summer, when it may last for weeks (Jeletzky, 1953). The persistent humidity combined with mild temperatures encourages lush growth of vegetation and establishment of a soil zone rich in organic matter. Timber in the area of Nootka and Clayoquot Sound, much of it old-growth, is highly coveted by both logging companies and conservationists.

Fig. 2.1.2a

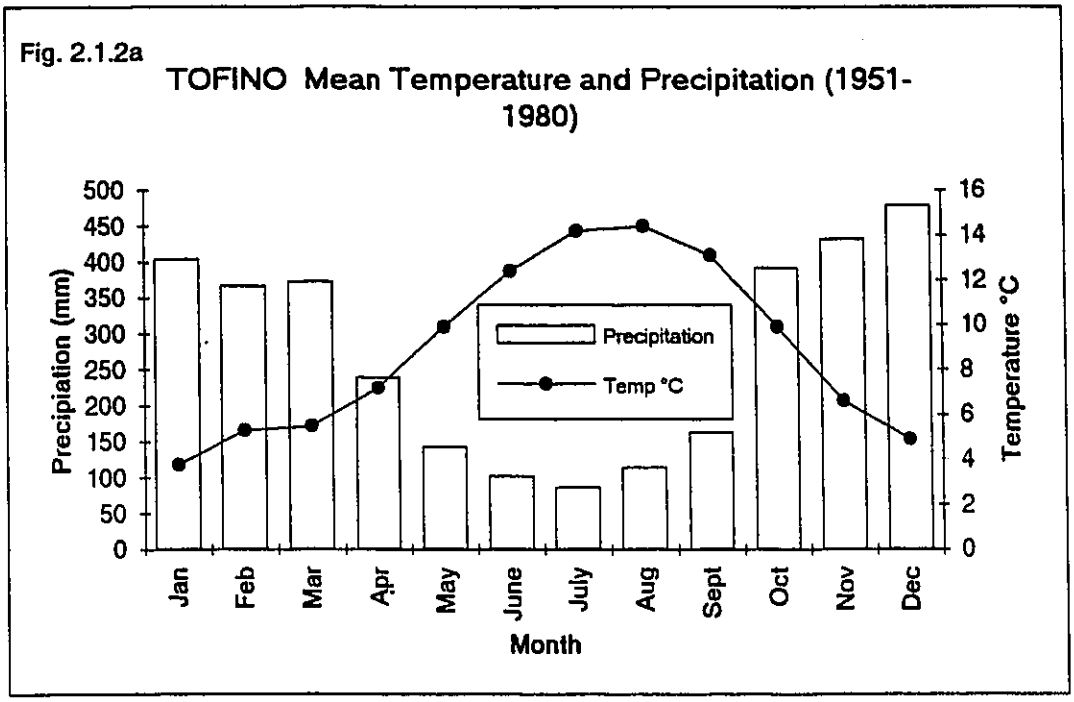

The physiography of the region, sculpted by two major glaciations in the past 50,000 years, is typified by a relatively subdued topography, with most elevations below 1500 m, and a coast-line indented by fiords and fiord-like inlets and channels (Muller, 1981). Mean topographic increases in the Hotsprings Cove (HSC) and Ahouset map area are in the order of 95 m/km (500 ft per horizontal mile) , or roughly 10% vertical gradients. North of HSC, a local topographic high of ~850 m (2784 ft.) occurs near Stewardson Point. Flores Island has two principle peaks, Steamer Mountain and Mount Flores, both of which are near to 800 m elevation (2500 ft.).

The abundant rainfall supplies runoff waters for the many creeks and streams and rivers along the coast. The narrow headlands and inlets of the area are usually drained by creeks and streams, rather than major rivers, due to their proximity to the Pacific Ocean.

Strong winds are common especially in the afternoons (Jeletzky, 1953), when onshore winds and seaspray may contribute particulate seasalt to coastal recharge areas.

2.1.3 Previous work

Previous geochemical work on the Hotspring Cove hotspring by Clapp (1913) included detailed chemical analyses, and a comparison of water samples collected that year with a sample collected in 1898. Elworthy (1925) reviewed Clapp's work and interpretation of the origin of the thermal waters, as did Souther and Halstead (1973), who also sampled and compared analyses. These analyses and analyses of this study are shown in Section 2.3.1. Nevin Sadlier-Brown Goodbrand Consultants sampled at Hotsprings Cove on four occasions from 1975 to 1988. Their findings included location of both a local tidal-flat warm spring, and an offshore vent, the latter detectable only in very calm waters.

2.2 Geology

2.2.1 Physical and tectonic setting

The study area, located within the Insular Belt of the Canadian Cordillera is near the western margin of the North American plate and has been subjected to periods of intense volcanism, plutonism, and more recently, at least two major glaciations. The rocks of the Insular Belt show evidence of intensive tectonism though widespread fault sets, shear zones, intrusive plutons, and volcanics. These principle structural elements are generated largely as a result of the convergence of the North American Plate with the present day Juan de Fuca plate (see Riddihough 1991, and Section 2.2.2). Hotsprings Cove and Ahouset are just south of the poorly-defined edges of the Nootka Fault Zone and additionally are in close proximity to both the Tofino Fault and the West Coast Fault.

Two major fault sets dominate the southwest-dipping homocline of Early Mesozoic intruded rocks which typify this region. One fault set strikes northerly and westerly and is of Mesozoic age. The second major set are Late Mesozoic to Tertiary, strike northwesterly and northeasterly and again are steep to vertical. (Jeletzky 1953, Muller 1981). On a regional scale, central Vancouver Island is part of an area which has been uplifted approximately 2 km during the last 10 million years (Mathews, 1991), while the West Coast Fault (WCF) and Tofino Fault (TF) strike subparallel to the Pacific coast and are considered to be thrust faults which may become active during periods of high tectonic activity (Hyndman and Wang,1993). These regional features are shown below in Fig.2.2.1a. .

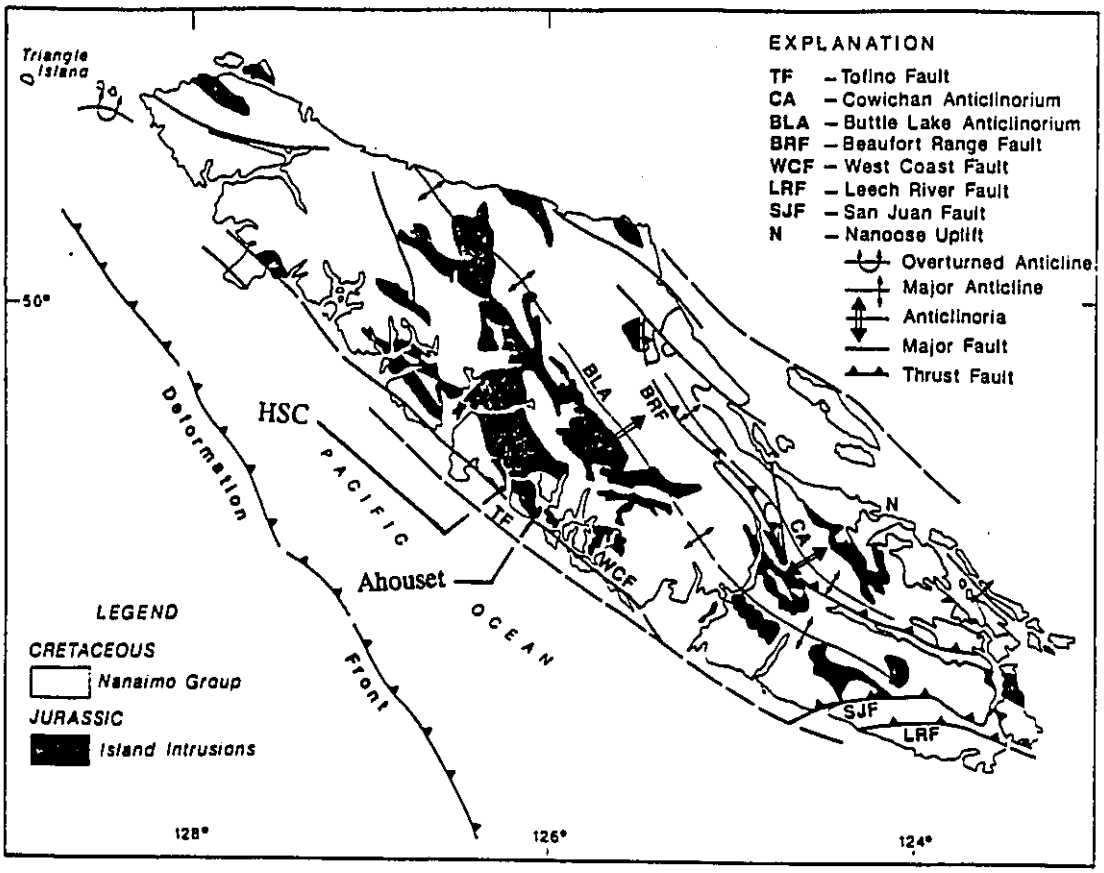

Fig. 2.2.1a. Main folds, faults and plutons on Vancouver Island (from Gabrielse, 1991)

The West Coast Fault, which separates the Pacific Rim Complex from the West Coast Complex (pers. comm. C.J. Yorath) diverges offshore just north of Tofino. Though absent from earlier maps (eg. Muller and Carson, 1969; Muller et al., 1980), recent publications show the WCF and TF, two deep-seated thrust faults, combining to form a lens-shaped "wedge", approximately 70 km long and up to ~12 km wide as shown in Fig. 2.2.1b below. The northern tip of the intersection of these two major faults is located just offshore of Flores Island near the the Ahouset hotspring (see Fig. 2.2.1c).

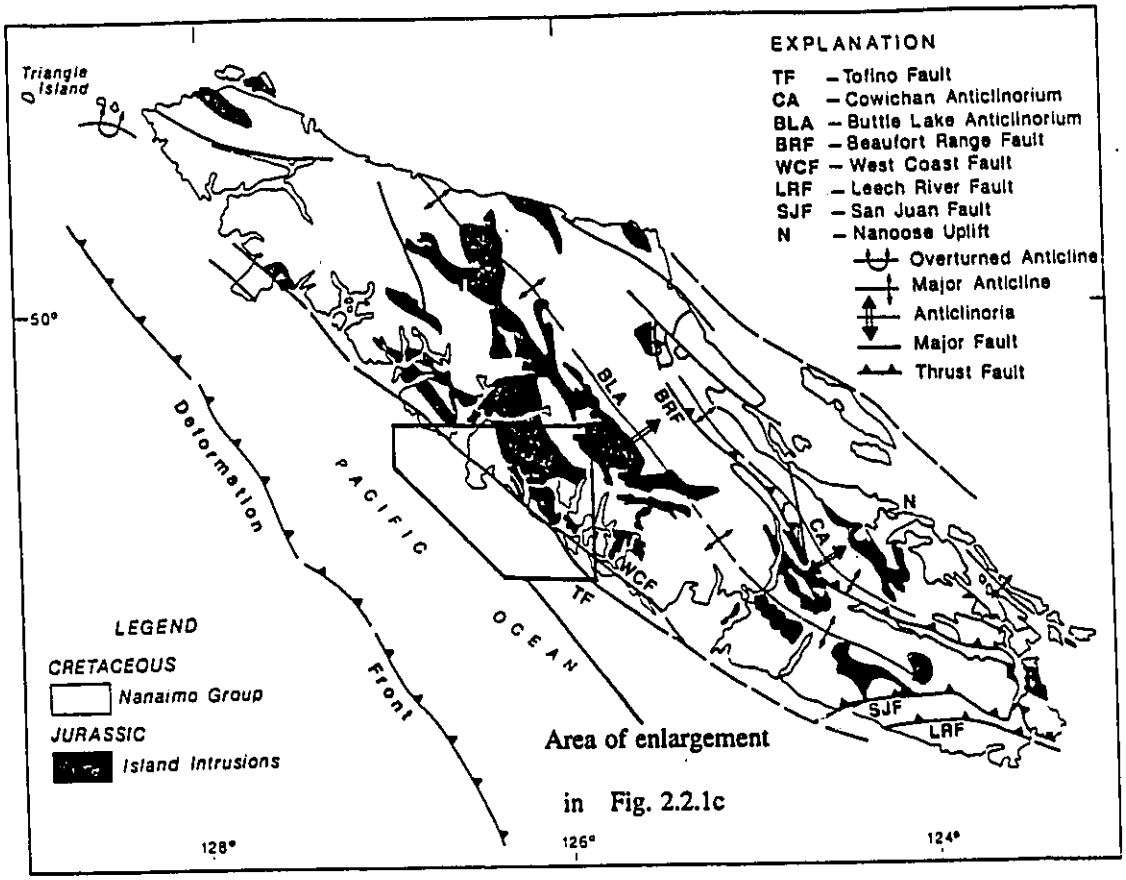

Fig. 2.2.1b. Main folds and plutons on Vancouver Is. with intersecting WCF-TF-RCF (after Gabrielse 1991, Read et al. 1991)

Other recent regional maps (Read et al., 1991) show the West Coast-Tofino Fault wedge extension intersecting with the Refuge Cove Fault (RCF on geology map). The Refuge Cove Fault passes directly through the discharge area of Hotsprings Cove. Still other maps show the northern extension of the WCF-TF reappearing onshore on the Hesquiat Peninsula between the West Coast Complex and Hesquiat Formation units where the fault repetition sequence occurs. Fig.2.2.1d shows a structural cross-section through the WCF-TF 'wedge' and includes the subducted Juan de Fuca oceanic plate. Further regional tectonic discussion is part of Section 4.

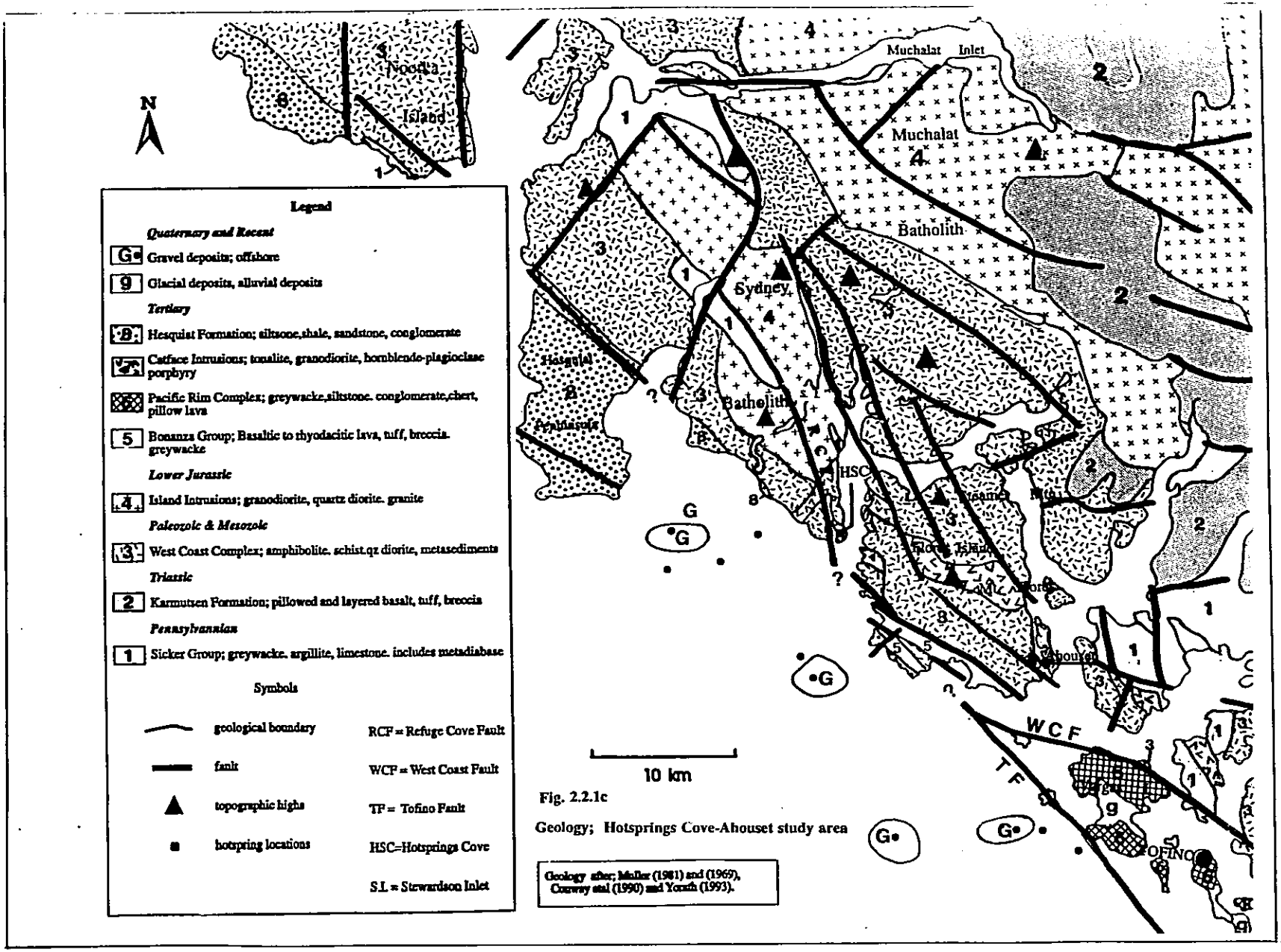

Fig. 2.2.1c

Geology; Hotsprings Cove-Ahouset study area

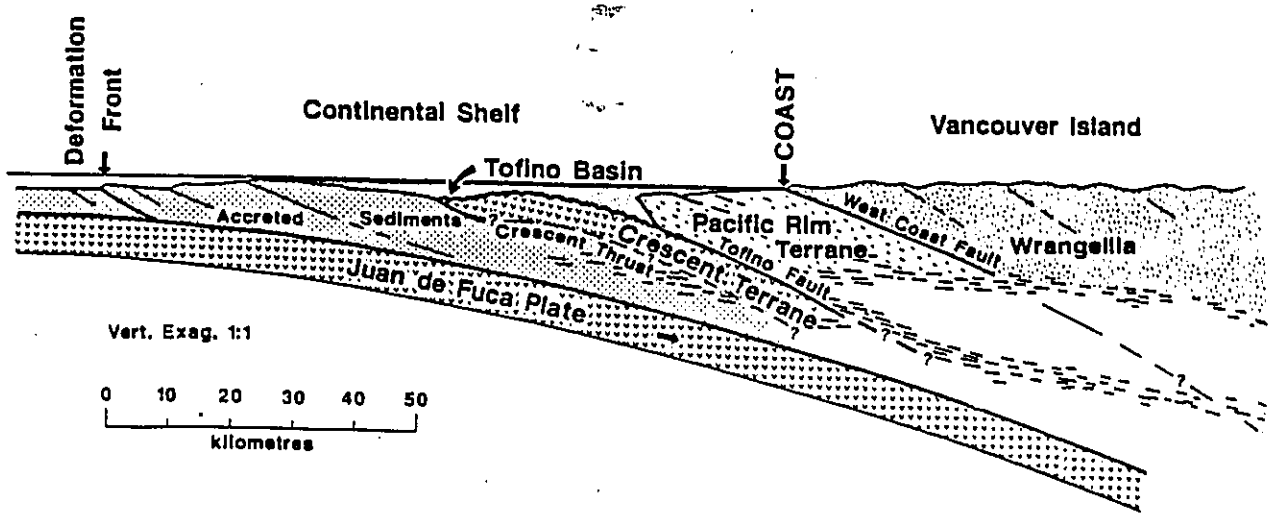

Fig.2.2.1d Structural cross-section through Tofino Basin (after Hyndman, 1990)

2.2.2 Seismicity, tectonism, and major faults

Seismicity on the west coast of Vancouver Island is due principally to interactions involving the Juan de Fuca plate, the Pacific and America plates, and the relatively new (~ 4 Ma old) Explorer Plate (see Fig. 2.2.2a). Major faults in this tectonically-dynamic terrain are not restricted, however, to the WCF and TF which are approximately parallel to the subduction front, but include the NE-SW trending Nootka transform fault. The Nootka transform fault, is actually a wide and imprecisely-defined fault *zone* which, due to complex plate motions, is migrating northerly, up the coast (pers. comm. Robin Riddihough).

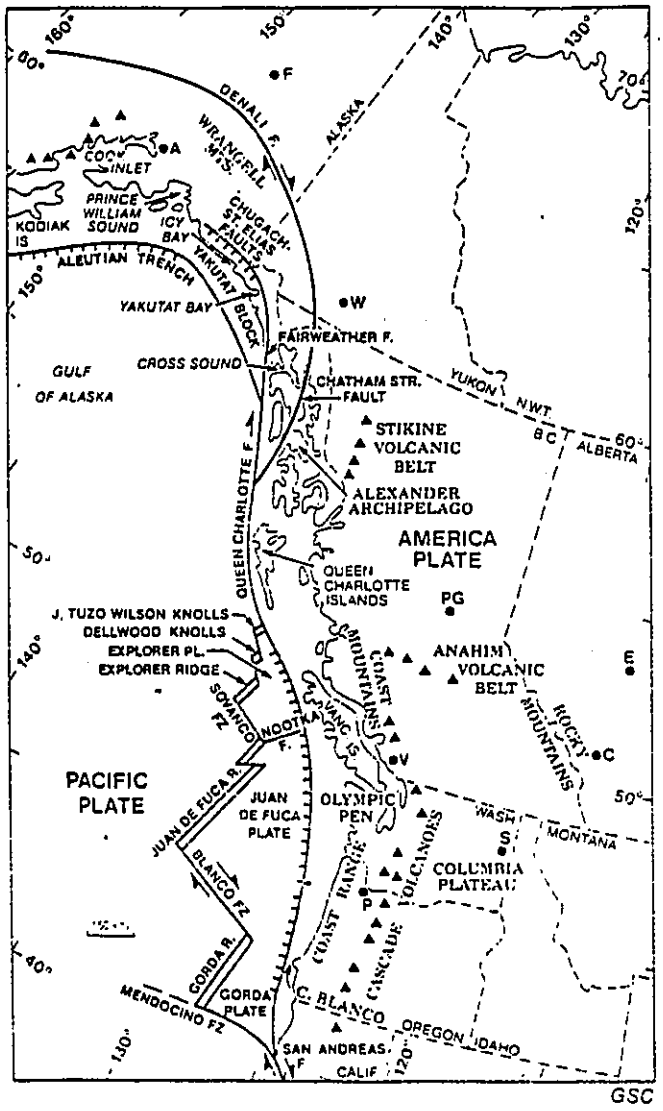

Fig. 2.2.2 Western North America tectonic plates (after Riddihough and Hyndman, 1991)

This fault zone extends from the triple junction point[1] at the Juan de Fuca Ridge, to Nootka Island, about 50 km north of HSC. The Nootka Fault Zone (NFZ) marks the division between the Juan de Fuca and Explorer plates (Hyndman, 1979). The Explorer plate has a rotational motion at present and a convergence rate of ~2 mm/a as opposed to ~ 4 mm/a for the Juan de Fuca plate (Riddihough and Hyndman, 1991).

[1] - triple juncton point between Juan de Fuca, Explorer and America plates.

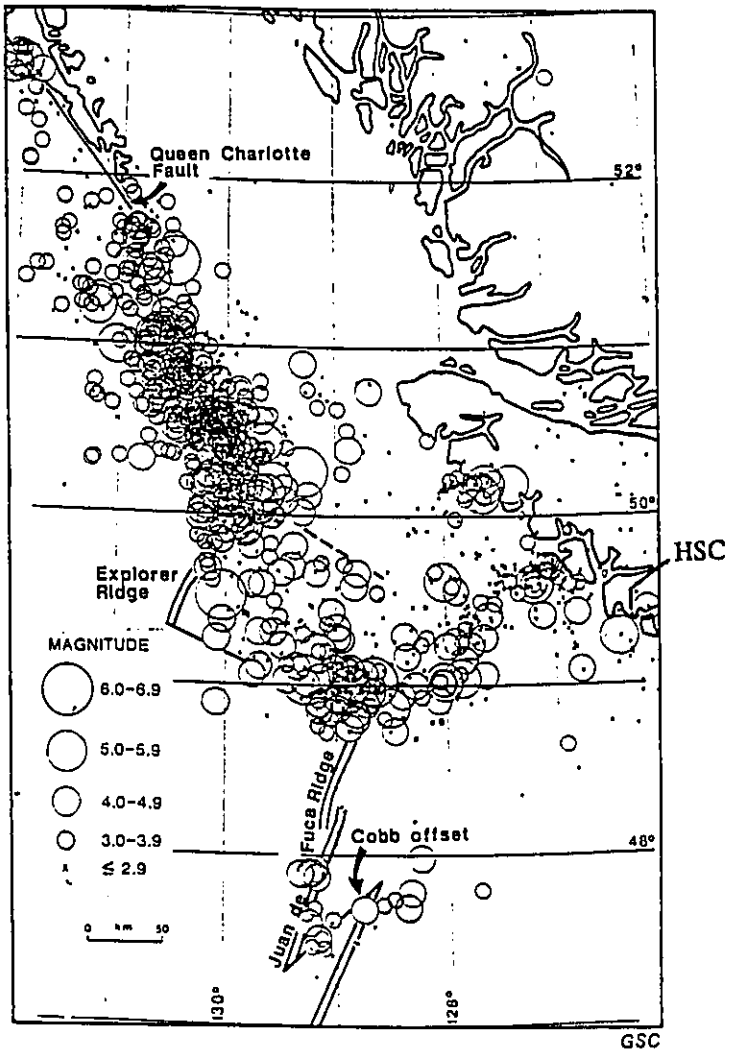

Fig.2.2.2b Seismicity of HSC and Ahouset area 1972-1984 (after Riddihough and Hyndman, 1991)

Fig. 2.2.2b shows seismic events along the west coast of Vancouver Island from 1972 to 1984 (Riddihough and Hyndman, 1991). Trends of earthquake epicenters appear to define not only the Nootka Fault Zone but also the trend of the WCF-TF and the subduction front. Other localized epicenters occur at or near the Refuge Cove Fault.

2.2.3 Rock types

The oldest rocks in the region, named by Clapp in 1912, are the Late Paleozoic Sicker Group, composed of clastics, cherts, and basaltic flows which are capped by limestone units. Notably, the Sicker Group or portions of it, are often found at higher elevations, apparently uplifted during batholithic intrusions and left as roof pendants, for example, adjacent to the Sydney Batholith, north of Hotsprings Cove (Fig. 2.2.1c).

The Upper Triassic Vancouver Group (~ 225-180 Ma) underlie much of the map area. They grade from pelites into pillow basalts of the Karmutsen Formation and then into carbonaceous clastics atop the group. The basalts of the Karmutsen Fm, up to 6 km in thickness on some parts of Vancouver Island, underlie much of the Nootka Sound region and were likely deposited following volcanic arc rifting which occurred during the Paleozoic (Muller, 1981). They are found as outcrop in the local map area only on the eastern edge of Flores Island.

Muller considered that the Permian-Triassic West Coast Complex, the Island Intrusions and also the Bonanza Group rocks to be the result of three successive stages of the same volcano-plutonic process. Pre-Jurassic Sicker and Vancouver Group rocks were apparently metamorphosed and migmatized into gneissic rocks of the West Coast Complex. Similarly, the Sydney and Muchalat Early Jurassic Batholiths, which are part of the Island Intrusions, may be derived from the plastic flow of pre-existing strata in the manner described by Roddick for rocks of the Coast Plutonic Complex (Roddick, 1965). An amphibolite unit of the West Coast Complex outcrops on Mate Island and to the west of Hotsprings Cove, while

gneissic and sheared quartz diorite of the complex outcrops on the headland of Sharp Point and hosts the main discharge of the HSC hotspring. Bonanza Group volcanic rocks outcrop in the map area in only one location, the southwest corner of Flores Island.

The Early Tertiary Catface Intrusions occur as small, fine-grained, stocks and sills and have been frequently studied due to their association with gold and porphyry copper deposits. They are K-feldspar-poor granitoid rocks and porphyries where plagioclase frequently comprises more than 50% of the mineralogy, the remainder made up of quartz, biotite, and hornblende with accessory epidote (Stevenson, 1950).

Originally termed Sooke Intrusions by Clapp, these small plutons were renamed by Muller, after the Catface Range of Clayquot Sound, to avoid confusion with the Sooke Fm and Sooke gabbros of southern Vancouver Island. Although the Catface Intrusions are difficult to differentiate from Island Intrusions in the field, a number of potassium-argon (K-Ar) age estimates have been determined for samples from both the Hotsprings Cove Stock and the Flores Island Catface Intrusion. They are 32.5 (+/- 3.9) and 35.1 (+/- 2.1) million years (Ma) for the Hotsprings Stock and 35.1 (+/- 2.1) for Flores Island (Wanless et al., 1974, Wanless et al., 1978), dates consistent with observation that these intrusions cut Eocene deposits (Clapp, 1912) but are nowhere found in contact with Oligocene-Miocene epoch Carmanah Group rocks (Jeletzky, 1953). The latter group is represented in the local map area by the sedimentary units of the Hesquiat Formation. These units overlie two thin bands of Escalante Fm strata on the Hesquiat Peninsula which are separated by West Coast Complex rocks, apparently a result of fault repetition (Muller,1981).

Most of the terrain in the study area is dominated either by outcrop, or by a thick layer of organic matter formed under the optimal growth conditions of this northern temperate rain-forest. Quaternary deposits are dominant only in the southeastern corner of the map area near Tofino and on Vargas Island, where alluvial sands and gravels are found. Offshore continental slope and shelf surficial deposits have been mapped on a 5 km^2 grid, following grab sampling of sediments using a mini-submarine (Conway et al. 1990). A Modified Folk Classification was used to define sediment types. The very few gravel locations that were found appear to define two principle lineation directions; one set of lines are subparallel to the Nootka Fault Zone, while the other principle 'lineation' is aligned with the WCF-TF system.

2.2.4 Glaciation

The Fraser glaciation reached its peak about 15,000 years B.P. (before present), but had less impact on the physiography than did the preceding "Mountain Glaciation" which peaked about 40,000 years B.P. (Clague, 1977; Muller, 1981).

During this period, a massive ice sheet continuous with the mainland covered much of Vancouver Island. The map area shows evidence of previous ice accumulation at up to 1200 m elevation near the head of Muchalat Inlet. Throughout the rest of the area and along the coast, the ice sheet was 450 - 600 m. thick, advancing as fiord-bound outlet glaciers. The deeply- incised fiords and inlets of the Nootka Sound map area are a reflection of this glacial sculpting.

2.2.5 Occurrence of Hotsprings

The Hotsprings Cove hotspring, discharges 50.5° C sodium chloride waters, at a flow rate of ~5 l/s, from a vertical fissure in sheared quartz-diorite (Plate2.2a). It is located about 15 m above the high tide mark on the west side of the narrow Sharp Point penninsula (see Fig.2.1.1a). The hotspring vent also discharges a steady stream of gas bubbles. A moderate odour of hydrogen sulphide is noticeable as the site is approached along the log walkway, which winds through the dense northern temperate rainforest.

The Ahouset low flow hotspring discharges about 0.2 l/s of low TDS NaCl water at a temperature of ~23° C. A prolific, thick growth of filamentus *Cyana formidium* algae has overgrown the shallow discharge vent (Plate 2.2b). The Ahouset hotspring is located on the southeastern corner of Flores Island about 20 m uphill from the shoreline.

The Mate Island warm seep is located on a tidal flat in a rocky inlet on Mate Island (Plate 2.2c). Its 25.4° C waters trickle out from a small pocket on the flat and are warm enough to support a small growth of algae. The vent is below sealevel except for times near to low-tide. A submarine vent, likely associated with the Hotsprings Cove geothermal system, is located offshore from Mate Island in about 15 m of water (Plate 2.2d)

Plate 2.2a (top) Gas sampling Hotsprings Cove vent set in sheared quartz diorite

Plate 2.2b The low flow Ahouset spring; 22.7° C, pH 10.05

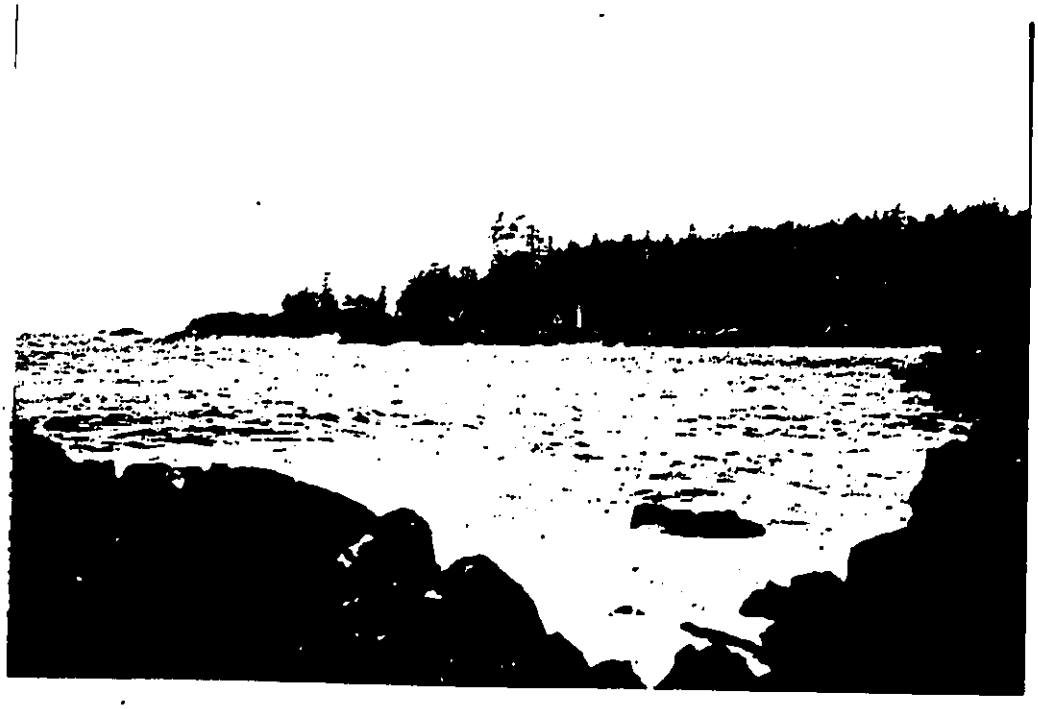

Plate 2.2c (top) Mate Island 25.4° C tidal flat warm seep

Plate 2.2d Looking WSW from HSC towards offshore vent (see arrow) and Mate Is.

2.3 Aqueous geochemistry

2.3.1 Introduction

In addition to being the only known substantial geothermal occurrence on Vancouver Island, the Hotsprings Cove site is the oldest quantitatively-documented geothermal vent in Canada and has exhibited remarkable geochemical stability over the past century. Table 2.3.1 shows the major dissolved constituents and aqueous geochemistry for analyses dating back to 1898.

Table 2.3.1 ***Hotsprings Cove Geochemical Analyses 1898 - 1990***

Year	*1898*	*1975*	*1975*	*1990*
Author	*Clapp*	*Souther&Halstead*	*N.S.B.G.*	*This study*
Temperature	52	50.5	50.5	50.3
pH	n.r.	8.35	n.r.	8.71
Dissolved constituents (ppm)				
Na	137	141	144	149
Ca	20	18	16.5	22
K	2	2	2.1	2
Mg	1	0.1	0.05	0.1
Cl	217	206	224	224
HCO3-	nr	22.3	32.1	38.6
SO4--	35	36	28.5	31
SiO2	59	53	49	51
TDS	471	478	496	518

n.r. - not reported

It is notable that the temperature, as measured in 1898 (and remeasured in 1912 by Clapp during the study in which he also reanalyzed the sample collected in 1898), has declined slightly as has the dissolved silica content. At the same time the total dissolved solids (TDS) have increased. While these changes may be partially due to changes in analytical technique, it is also possible that the reservoir is cooling, or that variable amounts of mixing with local seawater may be occurring resulting in increased salinity and slightly lower discharge temperature. Future documentation should clarify this possibility.

2.3.2 Ionic constituents

All of the west coast Vancouver Island thermal waters sampled can be characterized as sodium chloride waters with minor calcium and sulphate components. Table 2.3.2 shows the ionic constituents, first in weight fractions (ppm) and then as milliequivalents per litre. Cationic-anionic mass balance calculations are shown in Table 2.3.2c. All waters are near the 5% mark with respect to balancing, within the range of acceptable analytical error.

The dominance of the sodium chloride component may be partly attributed to input from marine waters either through aerosol deposition in the recharge environment or at discharge points. The possibility of mixing of the thermal waters with a minor fraction of local seawater is discussed in Section 2.3.6. Considering the low bicarbonate and calcium concentrations in all samples, it is possible that the thermal waters are at saturation with respect to calcite. Mineral solubility data, modelled with Solmineq geochemical software designed for geothermal waters, are in agreement with this and also show oversaturation with respect to a number of silicate and clay minerals.

Table 2.3.2a **Hotsprings Cove - Ahouset**

Aqueous Geochemistry

Anions (ppm)

	Temp	pH	Eh	TDS	NO3-	F-	Cl-	Br-	SO4--	HCO3-	CO3 --
HSC 1	50.3	8.71	-246	524	b.d.*	1.55	224	1.10	31.05	38.8	1.3
Ahouset	22.7	10.05	-133	156	b.d.	0.98	10.1	0.01	11.72	35.7	33.6
Mate Island	25.4	8.98	-143	959	b.d.	1.94	465	2.27	42.80	60.4	48.6

* - below detection

Cations ppm

	Ca++	Mg++	Fe++	Ba++	Sr++	K+	Na+	Li+	Al+++	B+++	SiO2
HSC 1	22.7	0.08	0.12	0.004	0.15	2.00	149.00	0.05	0.02	2.29	50.1
Ahouset	1.91	0.12	0.05	0.083	0.01	0.20	42.50	0.00	0.03	0.05	18.9
Mate Island	25.9	12.18	0.18	0.004	0.27	7.80	272.00	0.08	0.04	2.74	16.8

Table 2.3.2b ***Anions (meq/l**)***

	Temp	pH	Eh	NO3-	F-	Cl-	Br-	SO4--	HCO3-	CO3 --	meq sum
HSC 1	50.30	8.71	-246.00	b.d.	0.08	6.32	bd	0.65	0.64	0.04	7.73
Ahouset	22.70	10.05	-133.00	b.d.	0.05	0.28	bd	0.24	0.59	1.12	2.28
Mate Island	25.40	8.98	-143.00	b.d.	0.10	13.12	bd	0.89	0.99	1.62	16.72

**milliequivilants/litre

Cations (meq/l)

	Ca++	Mg++	Fe++	Ba++	Sr++	K+	Na+	Li+	Al+++	B+++	meq sum
HSC 1	1.13	0.01	0.0043	0.0001	0.0034	0.051	6.48	0.008	0.002	0.636	8.32
Ahouset	0.10	0.01	0.0017	0.0012	0.0002	0.005	1.85	0.000	0.003	0.015	1.98
Mate Island	1.29	1.00	0.0065	0.0001	0.0061	0.199	11.83	0.011	0.004	0.760	15.11

Table 2.3.2c ***Cation anion mass balances***

((cations -anions)/(cations + anions))

			% difference
HSC 1	(8.32 -7.73)/(8.32+7.73)	→ 0.0373	3.73%
Ahouset	similarly	→ -0.0713	-7.13%
Mate Island	" "	→ -0.0504	-5.04%

Note for detection limits see Table 3.3.2

Table 2.3.2d **Mineral Solubility**

	HSC	Ahousei	Mate Island
Temperature (°C)	50.3	22.7	25.4
Mineral			
Albite	3.182	1.414	3.189
Muscovite	7.317	3.048	7.689
Calcite	0.243	0.423	0.950
Aragonite	0.052	0.281	0.810
Dolomite	-1.056	1.355	2.911
Ca-Smectite	4.384	0.439	3.865
Mg- Smectite	4.111	0.360	3.950
K- Smectite	3.805	-0.500	3.481
Talc	2.016	11.022	9.281
Chalcedony	0.948	0.204	0.519
Quartz	0.895	0.534	0.719
Anhydrite	-2.827	-4.338	-2.797
Gypsum	-3.461	-5.453	-2.507

* solubility is expressed as Log IAP/KT; where IAP= ion activity product, KT = mineral solubility product.
Positive values indicate oversaturation, negative values indicate undersaturation.

2.3.3 Gas and dissolved gas

Table 2.3.3a below shows gas and dissolved gas analyses for all west coast Vancouver Island thermal waters. The oxygen content of the HSC sample analyzed at NRC should be regarded as suspect as accidental uprighting of the sample bottle occurred during extraction of the gas aliquot. The methane content in the two samples is quite consistent however, as is the predominance of nitrogen and lack of carbon dioxide. The gas constituents point to a highly reducing environment virtually devoid of oxygen. The low CO_2 concentration is consistent with absence of carbonate rocks in the predominantly silicic regional terrain. The high volume of methane gas at Mate Island may be due primarily to the decomposition of tidal-flat organic matter.

Table 2.3.3a ***Gas and Dissolved Gas***

Hotspring	Nitrogen	CO2	Oxygen	CH4	Other Gases	
					Hellum	Hydrogen
HSC	99.76	<.03	0.02	0.17	0.01	0.002
Ahouset*	no data	no data	no data	no data	see Section 2.6	no data
Mate Island	86.80	nd	1.70	11.50	nd	nd
HSC 90 (NRC)	97.10	nd	2.70	0.25	nd	nd

* No visible gas discharge. Dissolved gas container leaked nd - not detected

2.3.4 Eh and Redox conditions

The measured Eh values and sulphur species distribution are interesting in that they both point to reducing conditions. The HSC thermal waters have in fact reached Eh values where sulphate reduction can occur, oxygen atoms being stripped from the sulphate ion to form dissolved sulphide ions (HS^-) or hydrogen sulphide gas (H_2S); the latter immediately noticeable by the "rotten-egg" odour present in the vicinity of the hotspring. Fig 2.3.4a below shows the Eh values at which various redox buffering reactions occur. For alkaline

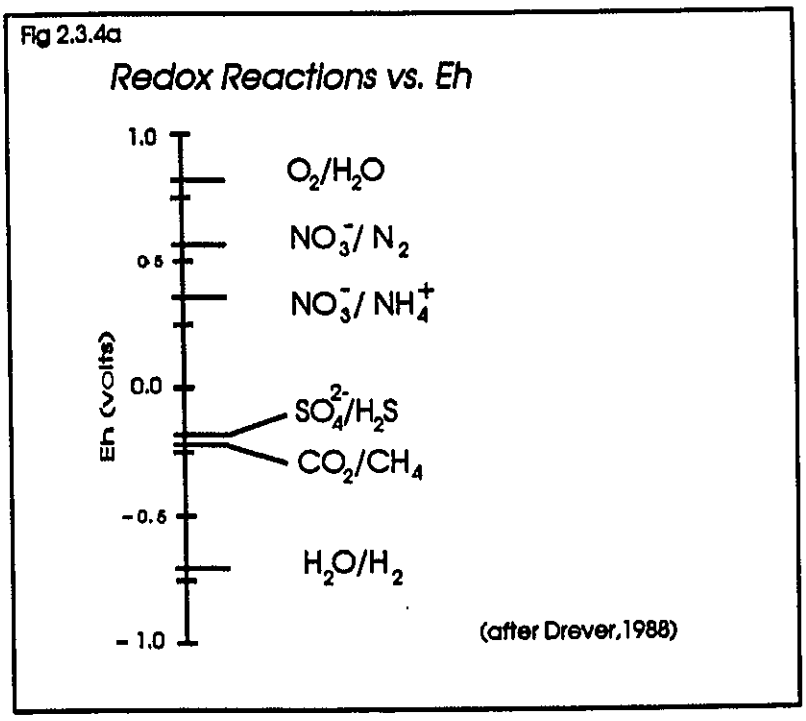

pH conditions however, the SO_4^{--}/H_2S couplet shown above is replaced by the SO_4^{--}/HS^- oxidation-reduction pair. The stability fields for these sulphide-sulphate species is shown in Fig. 2.3.4b. Note that a solution near pH 8.7 and Eh -0.270 volts is very near to the SO_4^{--}/HS^- boundary curve, consistent with the presence of both of these sulphur species in the thermal waters.

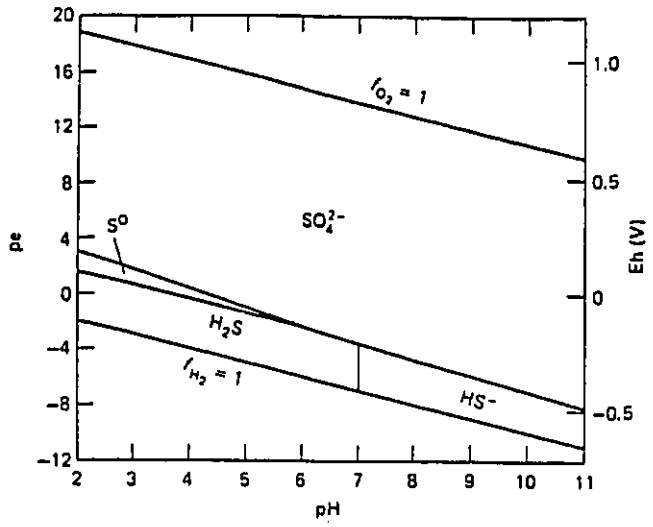

Fig. 2.3.4b Stability fields for dissolved sulphur species (from Drever, 1988)

The ratio of the activity of the sulphide - sulphate redox couplet can in fact be used to calculate an Eh value for HSC and Ahouset using the following equations:

(Eqn 2.3.1) $SO_4^{2-} + 8e^- + 9\ H^+ = HS^- + 4\ H_2O$ (Drever, 1988)

The Eh expression for the above reaction at 25° C is:

(Eqn 2.3.2) $Eh = E^0 + 0.059/8 \log (a_{SO4-}\ a^{10}_{H+} / a_H\ a^4_{H20})$ (Drever.1988)

where a = chemical activity and E^0 (for Eqn. 2.3.1) at 25° C = +300 mV

The activity of H_2O will be unity as it is in its standard state with a neutral charge.

Table 2.3.4a ***Eh Calculaton using the Sulphide - Sulphate Redox Pair***

To calculate Eh from the HS- - SO4-- redox couplet, the following equation can be used:

Eh = E0 + 0.059/8 log((aSO4--(a9H+))/ aHS-); @25°C, E0=.3V

* (mmols) ***Chemical Activity and Eh***

	*HS-**	*SO4--**	*H+*	*log calc'n*	*Calc Eh (volts)*	*Field Eh (volts)*
HSC	0.000261	0.002886	1.95E-09	-77.346	-0.27043	-0.246
Ahouset	5.51E-04	0.000119	8.91E-11	-91.1154	-0.37198	-0.133
Mate Island	0.00026	0.000282	3.94E-09	-75.6029	-0.25757	-0.143

As shown in Table 2.3.4a, the calculated Eh value for HSC is very close to the measured value, while the Ahouset and Mate Island calculated values are lower than those measured. Minor oxidation upon discharge, or in a zone of mixing near the discharge zone could account for the slightly lower field value at HSC, while Mate Island and Ahouset would appear to have appreciable input from more oxygenated waters (Table 2.3.3a), or have other redox couplets influencing the Eh. The fact that the above equation was written for STP conditions may also account for some discrepancy.

2.3.6 Mixing and Dilution

The validity of geochemical and isotopic techniques involved in the interpretation of a geothermal site is influenced by any mixing or dilution of the geothermal waters which may have occurred. For example, the addition of any seawater, shallow non-thermal groundwaters, or other source will affect both the geochemical and isotopic geochemical signatures of the system.

Studies of Canadian hotsprings at Mt. Meager and Mt. Edziza (Clark et al., 1982; Clark, 1985) revealed up to 10 % dilution through mixing with shallow non-thermal groundwaters. In the present study, carbon isotope and hydrochemical data for HSC indicate that these waters are relatively evolved and of considerable age, with mean residence times in the order of thousands of years (Section 2.4.4).

A potential contradiction to this evidence is the presence of a minor amount of tritium in the HSC waters (Table 2.4.4a). For, even if analytical precision of +/- 0.8 tritium units (T.U.) is considered, the tritium concentration of 1 T.U. for HSC may be indicative of some component of mixing or dilution with modern waters. Furthermore, the presence of bromide in both the HSC and Mate Island thermal waters may suggest the incorporation of some component of seawater as this conservative element is generally below detection in groundwaters but present in oceanic waters at ~ 67 mg/l (Drever, 1988).

One possible mixing is that of thermal and marine waters, and requires establishing the salinity of the local coastal seawater. While global oceans have very uniform total

dissolved solids (TDS) and conservative ion concentrations, coastal seawaters are frequently diluted with precipitation and runoff from local rivers and streams. The chloride concentration of the tidal flat sample from Mate Island (see Table 2.3.6a) will be used to calculate the extent of seawater dilution by local runoff waters. The sample has a chloride concentration of 11,000 ppm, while oceanic-seawater chloride is stable for well-mixed basins at 19,350 ppm (Drever 1988). Direct calculation yields:

11000 ppm Cl-/19,350 ppm Cl- = 0.5685 = fraction seawater in tidal pool.

Thus the local coastal seawater, represented by the tidal pool sample from Mate Island, is comprised of approximately 57% seawater with the remaining 43% freshwater. Verification of the seawater Br/Cl ratio,(which should be retained if the analytical results are valid) is shown below using the figuires from Table 2.3.6 a ;

38.09 ppm Br-/11,000 ppm Cl- = .0035 Br/Cl.

Hence, conservation of these ions at the standard seawater ratio of 0.0035 is demonstrated, and we may proceed using the tidal pool to represent local seawater. Table 2.3.6 a shows that while both the HSC and Mate Island thermal waters have Br/Cl ratios slightly higher than the seawater ratio of 0.0034, they are virtually identical to each other at 0.0049, strong evidence that they are part of the same geothermal system. The Mate Island sample location and its NaCl concentration higher than that of HSC are indicators of seawater mixing for this tidal-flat thermal seep.

Now if both HSC and Mate Island are part of the same geothermal reservoir then they should plot on a mixing line along with local seawater. For the purpose of determining a mixing line we can select the Na+ and Cl- ions, both of which are usually conservative (Drever,1988). Sodium concentrations can be plotted versus chloride for the local precipitation and runoff waters, oceanic and local seawater, and thermal waters (samples and concentrations from Table 2.3.2 a). Fig 2.3.6a reveals the mixing line for a two component or binary mixture with local seawater and precipitation as end-members. The Mate Island thermal waters fall neatly on the mixing line, the HSC sample has a slight enrichment in Na+, indicative of sources of sodium other than marine. Mixing lines for other conservative elements are shown in Fig 2.3.6b. Regression statistics for these mixing lines are included as part of Appendix A.

If bromide concentrations are considered, then mixing ratios for the thermal waters can be approximated (Clark, 1985). If we use the tidal pool to represent local seawater, as discussed above, and assume that all Br- is due to seawater mixing, then the thermal waters of HSC and Mate Island will have incorporated:

1.1 ppm Br/38.1 ppm Br = 2.8 % local seawater content for HSC,

and 2.27 ppm Br/38.1 ppm Br = 6.0 % local seawater for Mate Island.

These estimates however are too high for seawater mixing. The Br/Cl ratio is 0.0049 for both, and about 30% higher than the seawater ratio. Thus there is insufficient chloride in

Fig. 2.3.6a

HSC - Mate Island - Seawater Mixing line

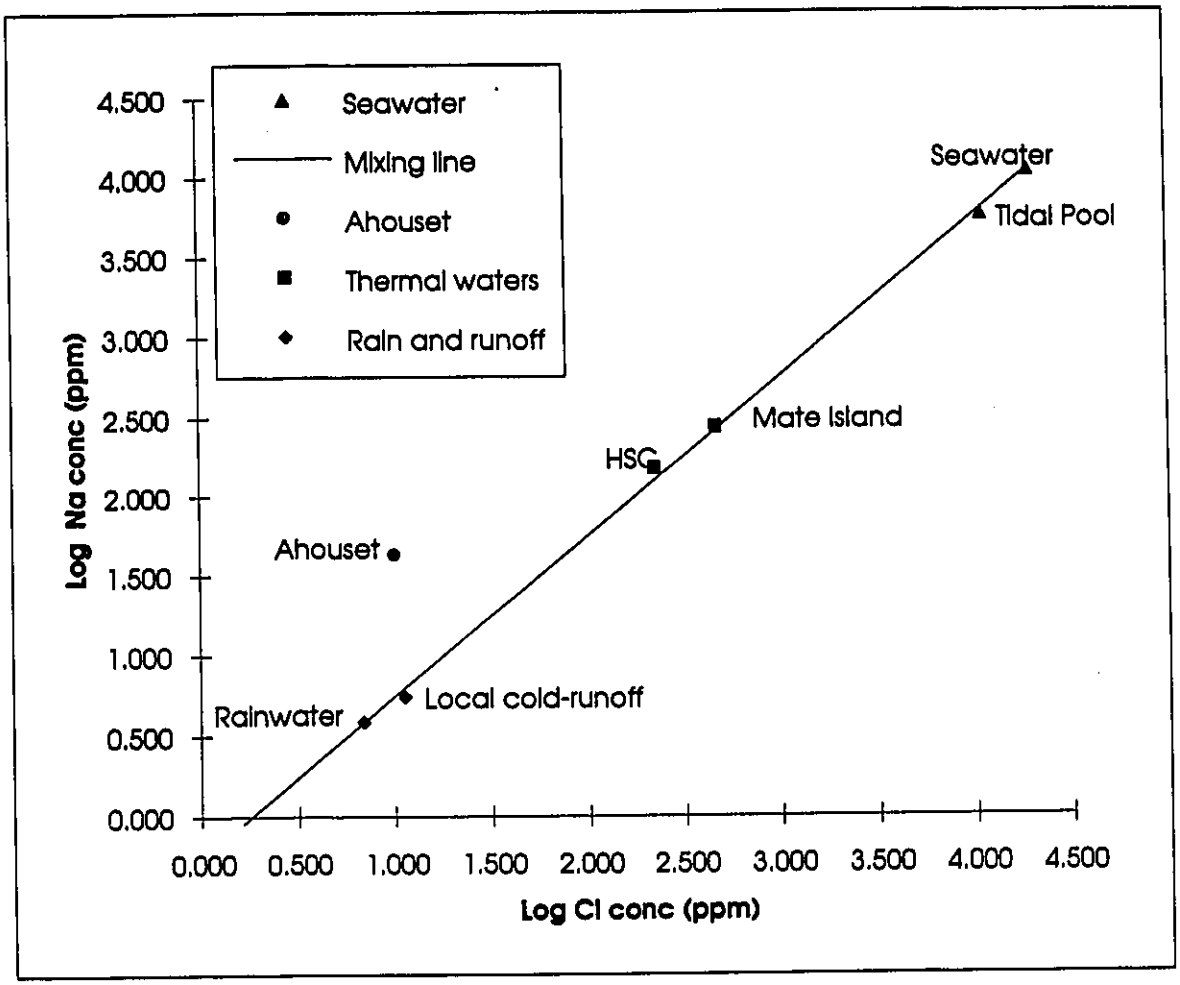

Table 2.3.6a

	Temp	pH	Eh	Na	Cl-	Br-	log Na	log Cl	Br-/Cl-
HSC	*50.3*	*8.71*	*-246*	*149.0*	*224.0*	*1.098*	*2.173*	*2.350*	*0.0049*
Mate Island	*25.4*	*8.98*	*-143*	*272.0*	*465.0*	*2.269*	*2.435*	*2.667*	*0.0049*
Tidal pool	*nd*	*nd*	*nd*	*5759.0*	*11000.0*	*38.857*	*3.760*	*4.041*	*0.0035*
Local runoff	*nd*	*nd*	*nd*	*5.5*	*11.3*	*bd*	*0.740*	*1.053*	*na*
Local rainwater	*nd*	*nd*	*nd*	*3.9*	*6.9*	*bd*	*0.585*	*0.836*	*na*
Seawater	*nd*	*nd*	*nd*	*10760.0*	*19350.0*	*67.000*	*4.032*	*4.287*	*0.0035*
Ahouset	*22.7*	*10.05*	*-133*	*42.5*	*10.1*	*0.050*	*1.628*	*1.002*	*0.0050*

nd - no data; bd - below detection

Fig. 2.3.6 b

*HSC - Mate Island - Seawater Mixing Lines**

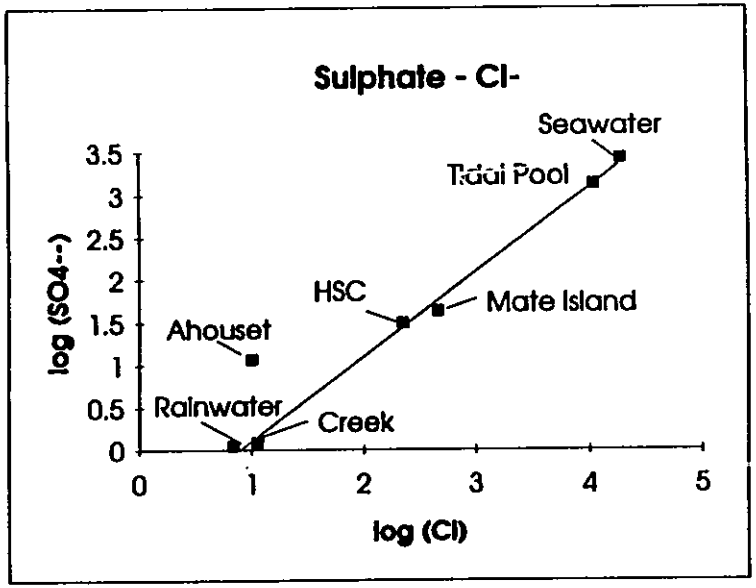

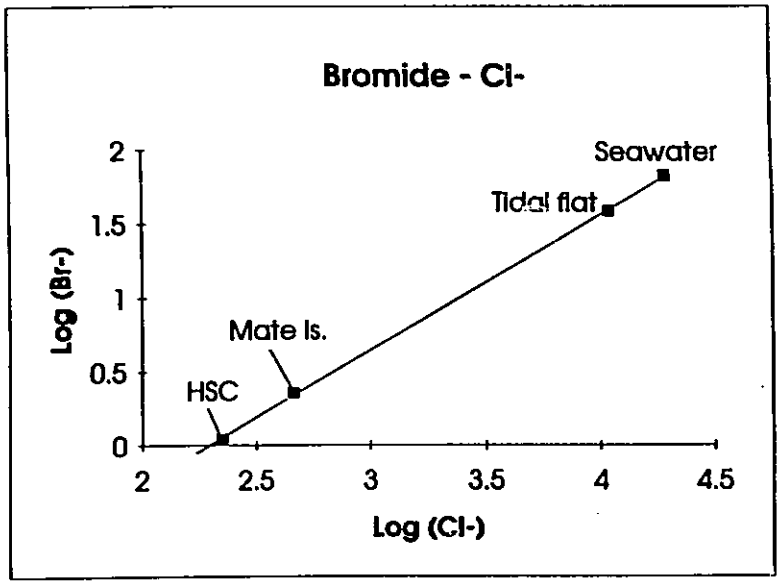

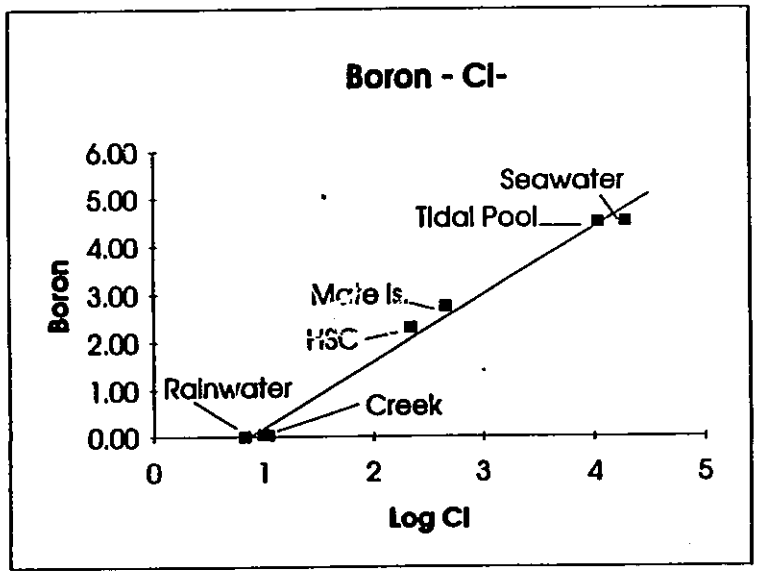

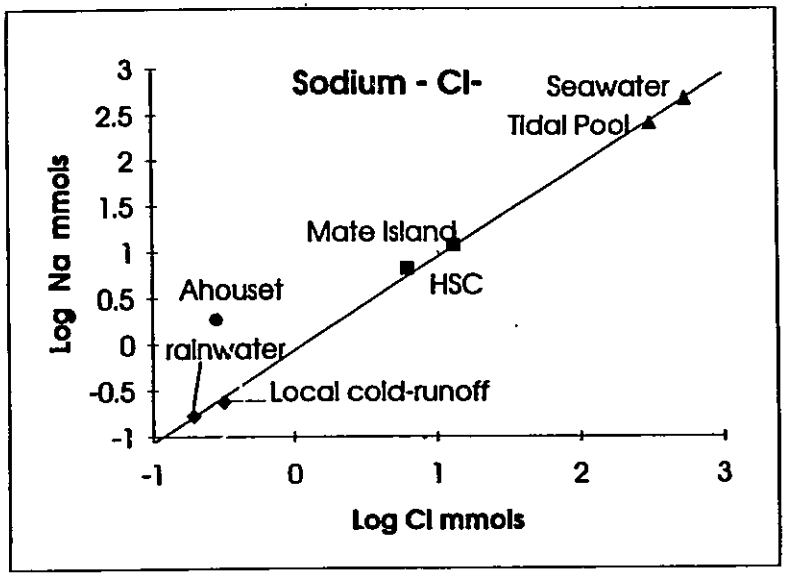

* all concentrations in ppm except where indicated

these waters to support so much bromide from seawater. The maximum amount of seawater mixing would be ~ 2% for HSC (2.8% - (30% x 2.8 %), and similiarly for Mate Island about 4%. These estimates however do not take into account the Cl- concentration in local shallow non-thermal run-off (~10 ppm, see Table 2.3.6a), nor do they make any allowances for chloride input from geothermal water-rock interaction, a major factor considering estimated mean residence times for HSC in the order of thousands of years.

Groundwater bromide/chloride ratios in excess of the 0.0034 value typical of seawater are not uncommon in brines and saline groundwaters of crystalline rocks of the Canadian Shield (Fritz & Frape 1982). Additionally bromide, the most conservative ion, has been found to increase in concentration over time in saline water of sedimentary basins (Fritz and Fontes, 1980). Edmunds (1987), in his description of deeply circulating thermal waters of meteoric origin found in the Carnmenellis Granites of southwest England, rules out a seawater origin for the bromide found in certain waters. Instead, mineral weathering of igneous biotites is purported to be the source of bromide. If the long mean residence time for the HSC waters is considered (Section 2.4.4) increased bromide concentration due to water-rock interaction and mineral weathering seems reasonable, and the bromide ratio in excess of that of seawater may indeed be attributable to such reactions.

Regardless of the precise mechanism for raising the bromide concentration, we can assume that such a process occurred prior to the input of a seawater component. We can model the potential bromide input from seawater mixing by varying the bromide portion associated with marine chloride and attributable to seawater mixing near the discharge zone.

Accordingly, an approximate geochemical profile can be proposed using different mixing ratios as shown in Table 2.3.6b. Naturally, all ions found in oceanic water in high concentrations will diminish markedly when the seawater component is subtracted.

If we start with 70% of the bromide (i.e. 70% Br- and all Cl- due to seawater mixing) two things are immediately apparent. Firstly, the Br/Cl ratio is almost an order of magnitude higher (0.04 versus .0049) supportive of bromide contributions from sources other than seawater mixing near discharge. The second major effect which removal of the seawater-mixing portion has, is to throw "off-balance" the anionic concentrations of magnesium, potassium, and in the case of Mate Island, sulphate.

Magnesium and potassium which should be present if the purported mixing ratios are accurate, are missing from the system. Mg and K deficiencies have been reported elsewhere in the literature however, and may be attributed to uptake by clay mineral assemblages such as chlorite, sericite or kaolinite, which frequently line fracture systems in crystalline rock and provide sinks for both potassium and magnesium (Fritz and Frape 1982; Gieskes and Lawrence 1981). Mineral saturation indices, some of which are shown in Table 2.3.4a, are in agreement with the hypothesis that species with these elements present are supersaturated and thus are subject to removal from solution.

Incorporation of seawater would most likely occur near the discharge zone as evidenced by the small amounts of tritium in the thermal waters of HSC, and the tidewater location of both the HSC hotspring and Mate Island warm seep. The offshore gas vent

Table 2.3.6b

Subtraction of Estimated Seawater Component

Ion	HSC	Mate Island	Seawater (sw)	Local sw	HSC -sw mix 1 (70% Br- from sw mix) ~ 2%sw	Mate Is. -sw mix 1 (~4.1% sw)	HSC -sw mix 2 (53.57% Br- from sw) -1.5%sw	Mate Is. -sw mix 2	HSC -sw mix 2 (35.7% Br- from sw) ~1%sw	Mate Is. -sw mix 2	HSC -sw mix 2 (17.9% Br- from sw) ~0.5%sw	Mate Is. -sw mix 2
Ca++	22.70	25.91	411	233.6	18.12	16.42	19.20	17.78	20.36	21.07	21.53	23.49
Mg++	0.08	12.18	1290	733.3	-14.29	-17.59	-12.24	-13.34	-7.25	-3.00	-3.59	4.58
Fe++	0.12	0.18	0	0.0	0.12	0.18	0.12	0.18	0.12	0.18	0.12	0.18
Ba++	0.004	0.00	0	0.0	0.00	0.00	0.00	0.00	0.00	0.00	0.00	0.00
Sr++	0.15	0.27	8	4.5	0.06	0.08	0.07	0.11	0.10	0.17	0.13	0.22
K+	2.00	7.80	399	226.8	-2.45	-1.41	-1.81	-0.09	-0.27	3.10	0.87	5.45
Na+	149.00	272.00	10760	6116.8	29.11	23.66	46.24	59.14	87.9	145.3	118.42	208.6
Li+	0.05	0.08	0.18	0.1	0.05	0.07	0.05	0.07	0.05	0.07	0.05	0.08
Al+++	0.02	0.04	0.00	0.0	0.02	0.04	0.02	0.04	0.02	0.04	0.02	0.04
Boron	2.29	2.74	5	2.6	2.24	2.64	2.25	2.65	2.26	2.69	2.28	2.71
Cl-	224.00	465.00	19350	11000.0	8.40	18.40	39.20	82.20	114.0	237.2	169.00	351.1
F-	1.55	1.94	1.3	0.7	1.54	1.90	1.54	1.91	1.54	1.92	1.55	1.93
Br-	1.10	2.27	67	38.1	0.3515	0.7226	0.46	0.94	0.72	1.48	0.91	1.87
SO4 --	31.05	42.80	2710	1363.0	4.34	-12.54	8.15	-4.63	17.43	14.58	24.24	28.68
HCO3 -	38.60	60.40	142	80.7	37.02	57.12	37.24	57.59	37.79	58.73	38.20	59.56
CO3 --	1.30	48.60	na	na	na	na	na	na	na	na	na	na
SiO2	50.10	16.80	5	2.8	50.04	16.68	50.05	16.70	50.07	16.74	50.09	16.77
Br/Cl	0.0049	0.0049	0.0035	0.0035	0.0418	0.0393	0.0117	0.0115	0.0063	0.0062	0.0054	0.0053

showed a similar gas chemistry to both Mate Island and HSC (N.S.B.G., 1988) and may be considered as a potential infiltration site for local seawater, which could then permeate along the fault zone and mix with upwelling geothermal fluids prior to discharge.

Seawater mixing summary

The Br/Cl ratios and conservative-ion mixing lines are strong evidence that Mate Island and HSC are part of the same geothermal system. The Mate Island vent's tidal flat location, temperature, and geochemical profile point conclusively to marine water mixing near discharge; an approximate maximum component of seawater likely to be 3 - 4%. Although seawater mixing at the main geothermal discharge vent at HSC remains unproven, possible seawater influx or mixing near discharge has a maximum of only about 1% the volume of the thermal waters.

2.4 Isotope Hydrogeology

2.4.1 Introduction

Groundwater studies have commonly included, since the 1960's, the use of isotopes [2] such as the radioactive isotopes of carbon (^{14}C), and hydrogen (^{3}H, or tritium T). These naturally-occurring radioisotopes, whose occurrence has been augmented this century through anthropogenic input from thermonuclear testing and the nuclear industry, can be used for estimation of a groundwater flow-system mean-residence time, or "age". Other non-radioactive or stable isotopes, such as ^{18}O and deuterium (^{2}H or D) have been used as indicators of source or provenance of recharge waters and, in geothermal systems, as a measure maximum reservoir temperature through water-rock interaction.

In this study carbon and tritium isotopes are employed as dating tools to estimate mean residence time, and ^{13}C data are also used as a provenence guide for dissolved inorganic carbon. Sulphur isotopes are utilized to determine the source of dissolved sulphide and sulphate species through calculation of a weighted average for ^{34}S, while the ^{18}O component of dissolved sulphate is employed in calculating sulphate-water geothermometer estimates. $^{18}O_{water}$ and deuterium are used together to estimate local meteoric water lines, predict potential recharge elevations, and to verify the range of maximum subsurface temperatures. Additionally, in this study, helium isotopes are used in conjunction with neon to investigate potential sources of geothermal gases.

---

[2] -isotopes of any given element are atoms which have the standard number of protons and electrons, but have a different number of neutrons.

2.4.2 ^{18}O - *Deuterium*

The first documentation of Oxygen-18 (^{18}O) and deuterium (D) for global precipitation resulted in establishment of the global meteoric water line (GMWL), a linear relationship between these two components of water molecules (Craig 1961). The linear relationship between ^{18}O and deuterium in meteoric waters may then allow the origin of recharge waters to be traced for flow systems discharging at lower elevations. (Gat, 1980).In high-temperature geothermal areas the ^{18}O signature of the recharge waters may be altered through underground exchange with the reservoir rocks, most of which contain ^{18}O-enriched silicate minerals (Fig. 2.4.2a). As hydrogen is not a primary rock-forming element, prolonged water-rock interaction at high temperatures can result in a "geothermal shift" whereby thermal waters plot to the right of the meteoric water line due to ^{18}O enrichment (Truesdell & Hulston 1980). The extent of the shift often represents the magnitude of the geothermal resource.

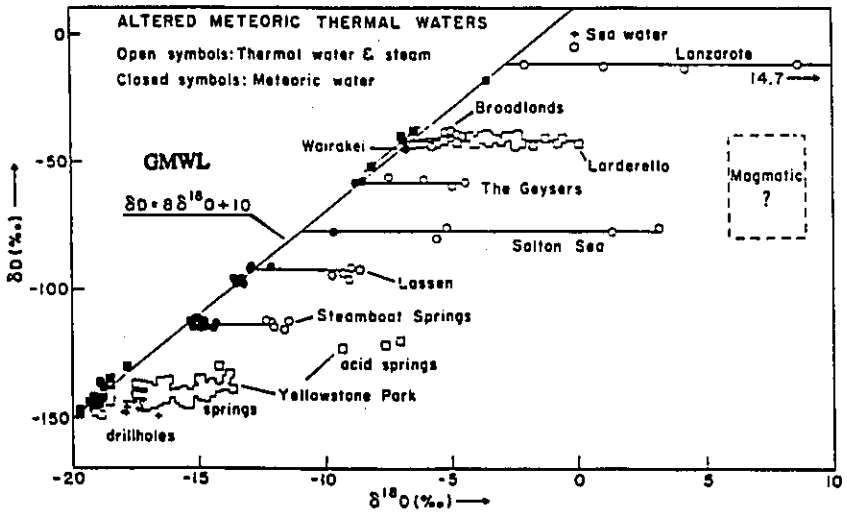

Fig. 2.4.2a ^{18}O-D plot of meteoric and thermal waters showing geothermal shiftdue to ^{18}O exchange with silicate reservoir rocks at temperatures in excess of 150° C. GMWL = Global Meteoric Water Line (after Truesdell and Hulston, 1980).

In this study, cold runoff waters were used to represent meteoric waters. The abundant annual precipitation in the area (~ 3300 mm annually) feeds a multitude of streams and creeks with fresh rainwater, so that samples taken from these runoff sources may be considered as a good approximation of local meteoric precipitation. Sample locations are shown in Fig. 2.4.2b.

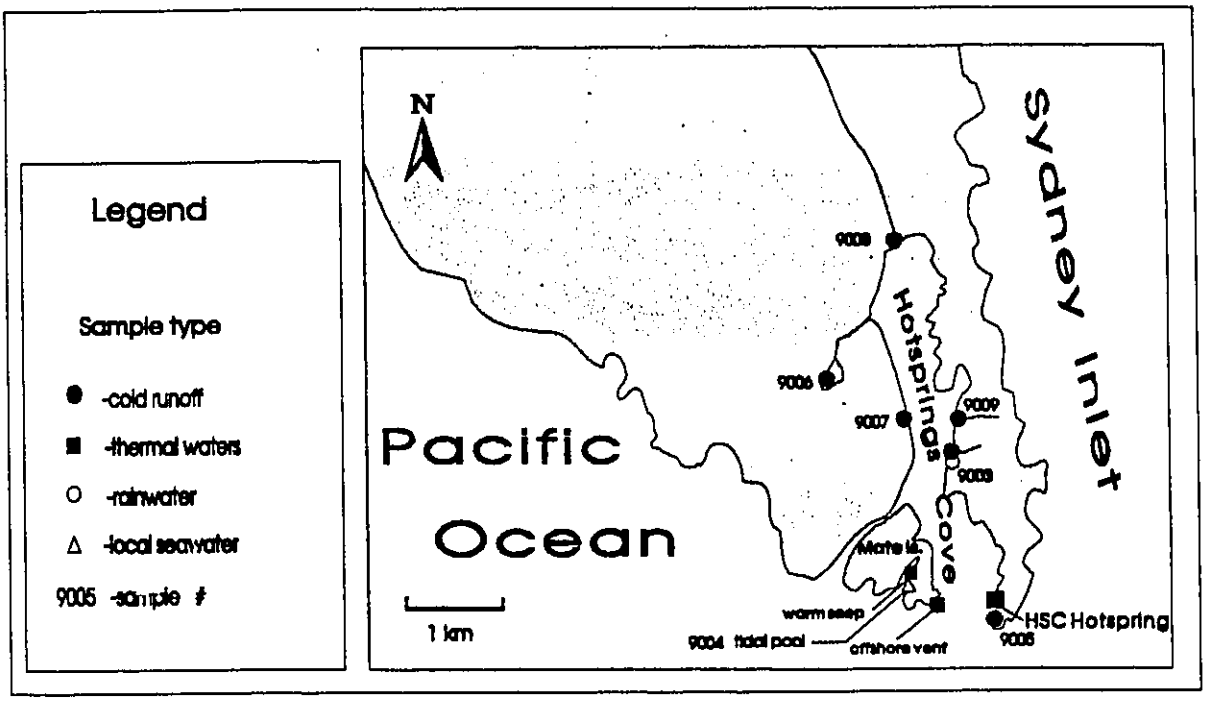

Fig. 2.4.2b Location of Hotsprings Cove area water samples

This approximation is substantiated when a least squares regression line of these waters is plotted for ^{18}O and deuterium. The local meteoric water line (LMWL) for Victoria, B.C. is very similiar to the regression plot for cold-runoff waters of the HSC area sampled in this study shown in Fig. 2.4.2c. Both have a slope of 7.7; only the intercept value differs from the Victoria line.

Table 2.4.2a; Fig. 2.4.2c

	18O	D
HSC HS	-10.17	-66.30
HSC HSB	-9.99	-63.80
HSC HSC	-10.06	-71.50
Ahouset tub	-8.38	-57.24
Mate Is. warmseep	-9.64	-68.50
Ahouset hotspring	-8.87	-58.00
Ahouset cro 10	-7.87	-49.40
hsccro5 (9005)	-8.49	-50.40
hsccrolodge (9006)	-8.94	-58.90
hsccro7 (9007)	-7.69	-47.00
hsccro8 (9008)	-9.97	-66.60
hsccro9 (9009)	-9.47	-64.90
hscro normas (9003)	-7.67	-49.23
Ahouset store (9011	-8.09	-51.70
tapwater (9002)	-7.90	-49.20
Cathedralgrove(90(	-11.30	-76.80
tidal pool (9004)	-4.83	-29.30

Regression Statistics

Multiple R	*0.977*
R Square	*0.954*
Adjusted R Sq	*0.951*
Standard Erro	*2.560*
Observations	*17*

Analysis of Variance

	df	*Sum of Square*	*Mean Square*	*F*	*Significance F*
Regression	*1*	*2041*	*2041*	*311.4*	*0.000000*
Residual	*15*	*98.3*	*6.6*		
Total	*16*	*2139*			

	Coefficients	*Standard Erro*	*t Statistic*	*P-value*	*Lower 95%*	*Upper 95%*
Intercept	*10.083*	*3.884*	*2.596*	*0.019*	*1.805*	*18.361*
x1	*7.702*	*0.436*	*17.647*	*0.000*	*6.772*	*8.633*

		y=mx+b	*x*
Intercept	*10.08*	*-77.72*	*-11.4*
x1	*7.70*	*-27.66*	*-4.9*

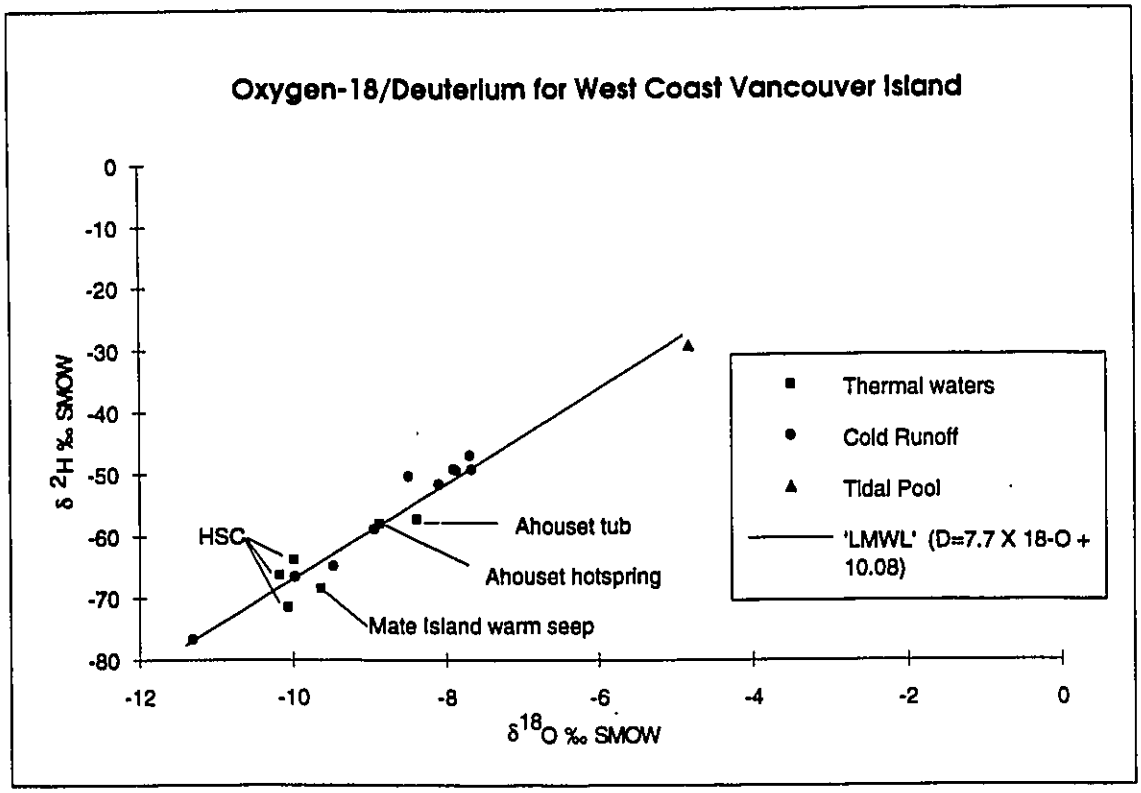

One other effect which may have significance for the ^{18}O-D signature of local cold runoff waters occurs due to seasonal variation in average air temperature. Because the samples in this study were collected in December, they would tend to represent minimum values as cooler temperatures increase fractionation effects resulting in more depleted ^{18}O-deuterium values relative to summer or mean annual precipitation. The thermal waters ^{18}O-D values plot on or very near to the local line, with no geothermal shift evident, hence maximum reservoir temperatures appear to be below 150°C.

The Mate Island warm seep has a value very similar to HSC pointing to a common origin and history (see also Section 2.3). Values for the Ahouset hotspring are less depleted, possibly indicative of a different origin, geothermal history, or mixing with shallow local meteoric waters. The "LMWL" reveals a difference of about 2.3 ‰ for $\delta^{18}O$ values taken from local runoff and HSC thermal waters. An ^{18}O depletion of approximately -1.5 to -5.0 ‰ per kilometre rise in elevation has been documented for precipitation in alpine areas (Gat, 1980). At Mount Meager, British Columbia about 225 km ENE of HSC, the depletion value determined was about -2.5 ‰ per km (Clark, 1982). If we use the -2‰ value for the present study we would then have an approximate recharge elevation for the HSC thermal waters of:

$$2.3/2.5 \times 1000 \text{ m} = 920 \text{ metres or about } 2800 \text{ ft.}$$

A local topographic high occurs near Stewardson Inlet about 7.5 km north of Hotspring Cove. Proximity to a major fault, which continues southward through HSC as the

Refuge Cove Fault, makes this area a probable location for recharge waters when considered along with its elevation of 2782 feet (see Fig. 2.2.1c).

The Ahouset hotspring plots on the local line and shows about a ‰ depletion with respect to local waters. Using the same formula for recharge elevation as above yields:

1/2.5 X 1000 m = 400 m or about 1300 feet.

Elevations in this range are found toward the centre of Flores Island near Mt. Flores, again in close proximity to a local fault which passes through the hotspring discharge area.

2.4.3 Sulphur Isotopes

Sulphur is widely distributed throughout the geosphere and prevalent in environments such as marine evaporites, metallic mineral deposits, volcanic rocks, and seawater sulphates. The two principle isotopes of sulphur are ^{32}S and ^{34}S, comprising 95.02% and 4.21% respectively of the total planetary budget (Faure, 1987). A wide variation in isotopic distribution exists between different reservoirs of sulphur, due in many cases to the discriminating fractionation effects of the sulphate-reducing bacteria *Desulfovibrio desulphuricans* (Krouse, 1980). Because more energy is required to strip oxygen atoms from the heavier $^{34}SO_4^{2-}$ ion than the $^{32}SO_4^{2-}$ ion, the heavier sulphate molecule is more frequently left behind in favour of the more-easily stripped, lighter ^{32}S-sulphate. This concentrates the ^{34}S in the sulphate fraction resulting in depleted ^{34}S values in the sulphide. The standard against which these variations in isotopic distribution are measured is the Canon Diablo Troilite meteorite (CDT) whose sulphur isotope distribution is set at delta sulphur-34 zero permil ($\delta^{34}S$ 0‰ CDT). Fig. 2.4.3a shows the CDT standard and the range and distribution ^{34}S values for a variety of sulphurous materials and environments.

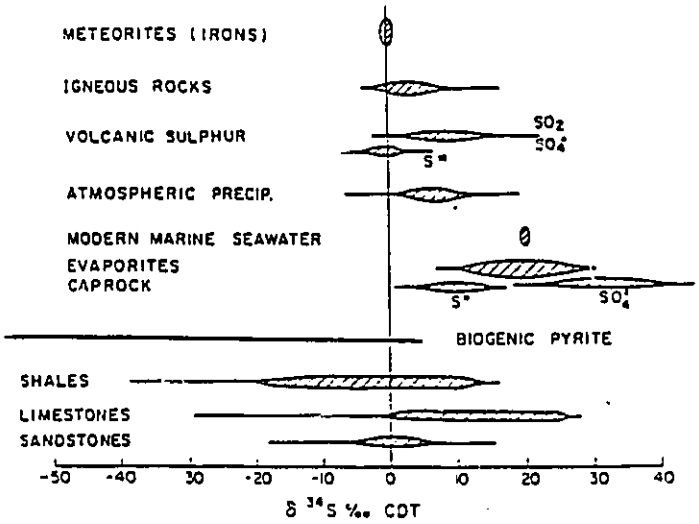

Fig. 2.4.3a Ranges in ^{34}S content for various sources of sulphur (after Krouse, 1980)

The concentration and ^{34}S signature of dissolved sulphur species can reveal valuable information about the redox conditions, recharge environments and geochemical evolution of groundwater within an aquifer or geothermal reservoir. Although (with only rare exception) marine waters are virtually devoid of dissolved sulphide (Krouse, 1980), modern oceans are the largest planetary reservoir of dissolved sulphate (Faure, 1987) and have a very constant $\delta^{34}S$ signature near +20 ‰ CDT (Krouse, 1980). Sulphur isotopes have particular relevance to the geochemical history of these west coast Vancouver Island Insular Belt hotsprings. It is interesting to note that Clapp (1913) made mention of the presence of hydrogen sulphide at the HSC site, yet by the time samples were shipped to, and analysed at, the Geological Survey of Canada laboratory in Ottawa, the only sulphur species detected was sulphate.

Present-day isotopic sampling techniques now enable both the sulphide and sulphate fractions to be collected and weighed from the same water sample, complete with their respective (and often very different) isotopic signatures. This must be done at the time of sampling, before any sulphide present oxidizes or degasses (Section 1.4.1). Following this the molar concentrations of the two species, when multiplied by their respective $\delta^{34}S$ signatures, can be added together and the resulting sum divided by the total number of moles of sulphur. This calculation provides a weighted average of the ^{34}S value for both sulphur species, and can be used to approximate the sulphate isotopic signature prior to reduction:

$$\delta^{34}S_{(initial)} = [\{\delta^{34}S_{(sulphate)} \times (SO_4^{2-})\} + \{\delta^{34}S_{(sulphide)} \times (HS^-)\}] / [(SO_4^{2-}) + (HS^-)]$$

where; round brackets denote molarity, and $\delta^{34}S$ values are as %CDT.

This calculation assumes no mixing of sulphate sources during or following sulphate reduction and that there are no other sources of dissolved sulphide.

Table 2.4.3a shows the different weight fractions of sulphide and sulphate present in the HSC and Ahouset thermal waters along with their respective isotopic signatures. For completeness the table shows the initial concentrations of CdS and $BaSO_4$ as well as their conversion into molar sulphur species and calculation of weighted isotopic fractions.

Table 2.4.3a* ***Sulphur Isotopes***

	SULPHIDE					SULPHATE			
						(Calculated from BaCl2 ppt.)			
	mg/l CdS (diss.HS-)	S mg/l	mg/l HS-	HS- mmols/l	delta S-34 sulphide	delta S-34 sulphate	mg/l BaSO4	mg/l SO4--	mmols SO4--
HSC	30	6.63	6.83	0.21	3.12	30.3	55	22.7	0.24
Ahouset	88	19.45	20.03	0.61	nd	9.66	14	5.77	0.06

	Weighted delta S-34 (both HS-& SO4--)	mg/l SO4 if all HS- oxidizes	mg/l SO4 from BaSO4	Potential Total Sulphate	Analyzed mg/l SO4 Dionex
HSC	17.62	20.46	22.7	43.12	31.05
Ahouset	nd	60.01	5.77	65.78	11.72

* all S values as CDT ‰

Seawater sulphate has a delta S-34 value of ~ +20 permil CDT
Average world-wide (Fritz & Fontes, Vol 3,1980)

The result of ^{34}S isotopic analysis for HSC reveals a fractionation effect amounting to more than a +27 ‰ CDT enrichment in the sulphate phase as compared to the sulphide phase. Such fractionation effects are quite common with sulphur, in fact bacterially-mediated fractionation differences between S-species of 75 ‰ are not rare (Faure,1987). Fig. 2.4.3b below shows schematically this fractionation effect away from the source sulphate toward the final $\delta\ ^{34}S$ signatures found in the sulpide and sulphate species. Data points are shown with schematic representation of the relative portions from each of the contributing species (size of shaded areas).

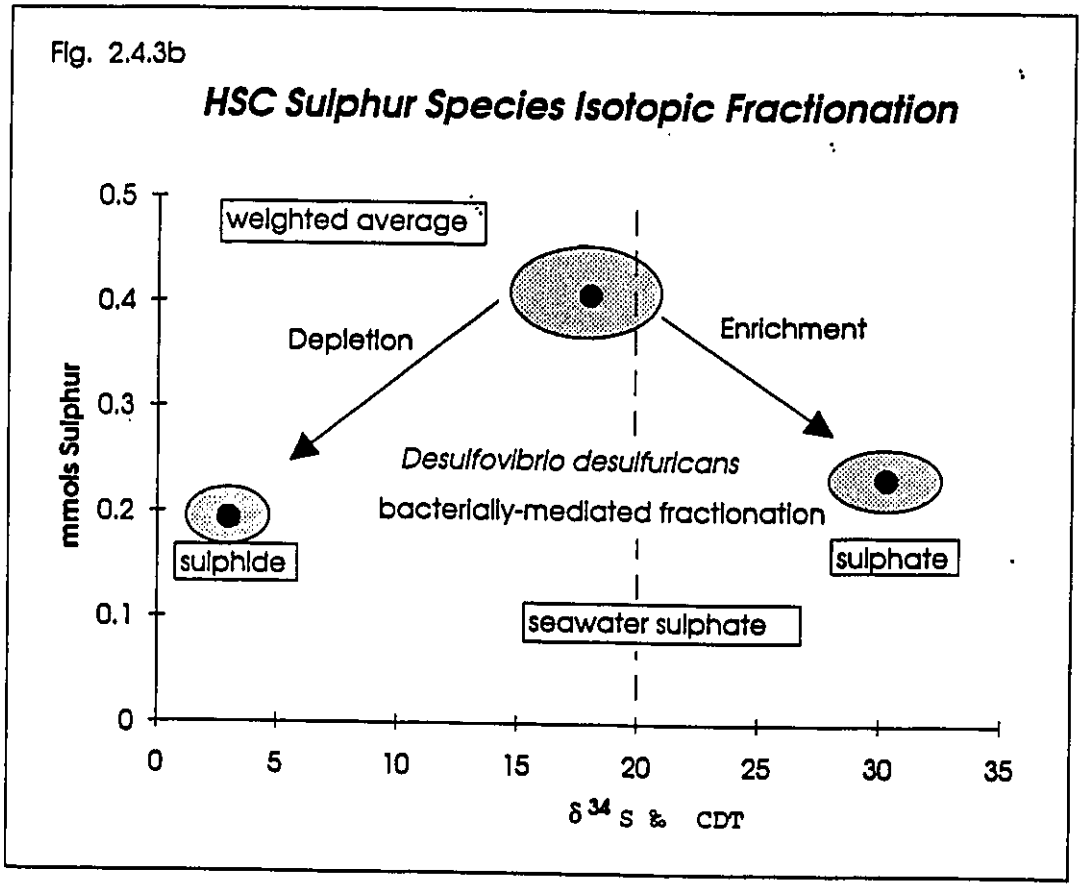

What is interesting here is that the weighted average points to an initial source of sulphate with a $\delta\ ^{34}S$ signature of 17.62 quite near the value of +20 ‰ found in oceanic sulphate (see Fig.2.4.3a). Although aerosol deposition of seawater sulphate in coastal recharge areas could contribute sulphate with this signature, the concentrations would be inadequate to account for the 0.45 mmols/l dissolved sulphate. Thus there must be another source of this sulphate with a seawater signature. Other potential sources for a small portion of ^{34}S-depleted sulphate include oxidation of pyrite minerals (incorporated early on in the geothermal system flow history) from porphyry copper deposits present in the study area north of Hotsprings Cove and near Mount Flores (Muller, 1981). Nonetheless, the $\delta^{34}S_{sulphate}$ value slightly lower than ocean water may in fact be supportive of *local* seawater as a source. The local seawater defined in Section 2.3.6 was shown to consist of approximately 43% non-marine coastal runoff. Surface waters have a range of $^{34}S_{sulphate}$ values lower than seawater, often in the range of +10 ‰ CDT (Krouse, 1980) so freshwater dilution would lower the $\delta^{34}S_{sulphate}$ signature. However sulphate concentration in the local runoff and rainwater samples was only about 1.2 ppm, thus the weight of this effect is minor. Unquantified carbonate impurities in the sulphide sample are a more likely cause of a lower weighted average value for the $\delta^{34}S_{sulphate}$ signature.

The seismically-active, highly-fractured and faulted geology of the HSC study area may facilitate seawater intrusion into coastal aquifers. Marine waters could penetrate deeply along regional faults such as the Refuge Cove Fault (RCF). Fluctuations in marine tides would aid in creating a zone of mixing, but denser saline waters would tend to gravitate

downwards, creating a deeper, more evolved saline groundwater with dissolved components of marine origin. Upwelling geothermal waters, driven by the difference in hydraulic head from the highland recharge area to the north, would be lighter and therefore more bouyant, confining the more saline waters while discharging. The elevated 0.0049 Br/Cl ratio of the HSC and Mate Island geothermal waters (Section 2.3.6) may be a reflection of a more evolved saline groundwater component of marine origin mixing with the discharging geothermal waters.

2.4.4 Tritium and Carbon Isotopes

Introduction

Tritium and carbon isotopes are used together in this study to estimate the mean residence time of the geothermal waters. ^{13}C data from dissolved inorganic carbon (DIC) are used to verify the source of carbon and check on possible modification processes occurring to the $^{14}C_{DIC}$. Radioactive isotopes of carbon (carbon-14 or ^{14}C) are produced naturally in the upper- atmosphere through the bombardment of nitrogen atoms by cosmic rays:

$$^{14}_{7}N + {}^{1}_{0}n \rightarrow {}^{14}_{6}C + {}^{1}_{1}p \qquad \text{Eqn. 2.4.3a}$$

where; n = neutron and p = proton

Thermal waters, present underground where closed system conditions prevail, are no longer in contact with atmospheric carbon dioxide sources and have also infiltrated beyond biological sources of modern carbon present in the soil zone. Under these conditions the percent modern carbon (pmc) will decline through radioactive decay of ^{14}C according to the radioactive decay equation:

$$A_t = A_o \bullet \exp(\ln 2 / t_{1/2} \bullet t) \qquad \text{Eqn 2.4.3c}$$

where; A_t = measured activity (or concentration), A_0 = the initial activity, $t_{1/2}$ = the half-life of the radioisotope, and t = time elapsed since commencement of decay

When the ^{14}C half-life of 5730 years is used in eqn. 2.4.3c the following radiocarbon decay formula results:

$$\text{mean residence time (t)} = -8267 \ln (A_t / A_0) \qquad \text{Eqn.2.4.3d}$$

As an example, a groundwater sample found to have a total dissolved carbon (TDC) component with 50 pmc would be 5730 years old, assuming no additional input from other subsurface carbon sources such as "dead" carbonate rocks or volcanic gases (where all modern carbon has long since decayed). Fortunately, carbon-13 (^{13}C) measurements can provide a check on these types of carbonate sources which can modify ^{14}C mean residence times and "artificially age" waters. Most types of vegetation in northern climates generally have $\delta^{13}C$ values between -22 and -35 %PDB for CO_2 (Gat, 1980) but are most frequently near-25‰ PDB. Thus, decaying organic matter in the soil root zone will often leave this ^{13}C isotopic fingerprint on infiltrating recharge waters. Any subsequent modification of the dissolved carbon component would then alter these ^{13}C and ^{14}C "signatures".

Radioactive isotopes of hydrogen, called tritium (T or ^3H), are also produced naturally in the upper- atmosphere through the bombardment of nitrogen atoms by cosmic rays:

$$^{14}_{7}N + {}^{1}_{0}n \rightarrow {}^{12}_{6}C + {}^{3}_{1}H \qquad \text{Eqn. 2.4.3b}$$

Like ^{14}C, tritium isotopes are useful indicators of mean residence time, although the half-life of this radioactive isotope is much shorter, only 12.43 years. While the natural abundance of ^3H is likely between 5 and 20 Tritium Units[3] (T.U.) (Brown, 1961) anthropogenic input this century has augmented tritium concentration. For example, values as high as 5000 T.U. were recorded in Ottawa area precipitation during the 1960's (Egboka, 1980). The primary usefulness of tritium as a dating tool relates both to it's rapid radioactive-decay and the

[3] - one tritium unit is equal to one ^3H atom per 10^{18} H-atoms

anthropogenic "spike" introduced in the twentieth century. Additionally, tritium is conservative and not affected by physiochemical or biochemical reactions. Zero tritium content in a given water sample in 1993 implies that the sample has been out of contact with the atmosphere for a minumum of about 40 years, while a sample with a high ^{3}H concentration was likely recharged during the 1960's.

Results and discussion

Tables 2.4.3a and b show mean residence time data from carbon and tritium isotopes for Hotsprings Cove and Ahouset. A direct calculation using ^{14}C is shown in Table 2.4.4a, while Table 2.4.4b shows corrected "ages" using two different calculation techniques.

Ahouset

The very high ^{3}H content in these waters suggests either substantial mixing or rapid circulation of the thermal waters. Direct calculation, shown in Table 2.4.4a, does not apply for the ^{14}C value at the Ahouset hotspring. Modified Pearson calculations (Pearson, 1980) which consider $\delta^{13}C$ values different from soil zone signatures, give values for Ahouset of ~2300 years if we use a soil zone correction, and ~ 11,000 if we apply a standard "q" value of 0.9 for crystalline terrain (Table 2.4.4b). However, for such modelling, the very high $\delta^{13}C$ value is problematic, and may reflect deep crustal or mantle CO_2 (see also Section 2.6). .As no sulphide was detected in solution at Ahouset, sulphide-based corrections outlined in this section do not apply. The presence of ~13 T.U. in these thermal waters, along with a low pmc value, however is evidence of substantial mixing (Mazor, 1991) likely with tritiated modern groundwaters. Thus radiocarbon modelling may be invalid for Ahouset.

HSC-Ahouset Mean Residence Time Estimates

Table 2.4.4a ***Direct Application of C-14 Decay Equation***

Hotspring	*HCO3- (mg/l)*	*CO3 -- (mg/l)*	*dI3C‰ (PDB)*	*C-14 (pmc)*	*Mean Residence time (years) t=-8270 ln (pmc)*	*Tritium (T.U.)*
HSC	38.80	1.30	-24.0 +/-0.1	18.4 +/- 0.22	13991 +/- ~ 100 years	1.0 +/-0.8
Ahouset	35.70	33.60	-2.83 +/-0.1	22.6 +/- 0.25	12314 +/- ~ 100 years	12.5 +/-1.1

Table 2.4.4b ***Corrected Mean Residence Times***

Hotspring	*HCO3- (mg/l)*	*CO3 -- (mg/l)*	*dI3C‰ (PDB)*	*C-14 (pmc)*	*"q" factor*	*Modified Pearson "Age"*	*"Desulfovibrio desulfuricans Sulphide" Corrected "pmc"*	*Sulphide Corrected "Age"*
HSC 1	38.80	1.30	-24.0 +/-0.1	18.4 +/- 0.22	*na*	*na*	0.493	5845
HSC 2	38.80	1.30	-24.0 +/-0.1	18.4 +/- 0.22	*na*	*na*	0.264	11029
Ahouset 1	35.70	33.60	-2.83 +/-0.1	22.6 +/- 0.25	0.186	2288	*na*	*na*
Ahouset 2	35.70	33.60	-2.83 +/-0.1	22.6 +/- 0.25	0.9	11083	*na*	*na*

HSC 1 - 0.21 mmols HS- produced from sulphate reduction, so 0.42 mmols of "dead" C-14 are introduced (see Section 2.4.4 in text). To correct for this, (0.001pmc x .42 mmols) was subtracted from (.184 x .66 mmols). This then used as the numerator and placed over the denominator of (0.66 - 0.42 mmols) to give corrected amount of DIC for "18.4 pmc". Thus pmc = ~ 50.

HSC 2 - 0.21 mmols/l HS- produced from sulphate reduction, so 0.21 mmols/l of "dead" C-14 are introduced (Section 2.4.4 in text). To correct for this, (0.001pmc x .42 mmols) was subtracted from (.184 x .66 mmols). This then used as the numerator and placed over the denominator of (0.66 - 0.42 mmols) to give corrected amount of DIC for "18.4 pmc". Thus pmc = ~ 50.

Ahouset 1: q=(-2.83 ~~+2)/(-24-2) Ahouset 2: q= 0.9 (crystalline rocks)

Table 2.4.4 a & b HSC and Ahouset estimated mean residence times

Hotsprings Cove

For Hotsprings Cove, the $\delta^{13}C$ value of -24 ‰PDB appears to indicate an input of biogenic $CO_2$from the soil zone. The low Eh value and redox conditions indicative of sulphate reduction support this interpretation, as does the very low DIC content and general lack of carbonate lithologies in this area of the Insular Belt dominated by silicate rock-types (Section 2.2). The minimal value of 1 T.U. for HSC is consistent with the ^{14}C data, particularly if the precision of +/- 0.8 T.U. is considered. This minimal tritium content could result from loss of analytical precision at these very low values, or may be partly due to spontaneous production of ^{3}H from ^{3}He (Andrews, 1985). The other potential source for the minimal tritium input could be local seawater, infiltrating near the discharge zone (see Section 2.3.6).

If we assume that $\delta^{13}C_{DIC}$ signature of -24 ‰ PDB is indicative of an unmodified soil zone signature, then the HSC DIC content has not been affected by subsurface processes such as exchange with carbonate rocks or deep crustal/mantle inputs. A direct application of Eqn. 2.4.3d gives a mean residence time for these waters of near 14,000 years, indicative of recharge during the last period of Pleistocene glaciation. It should be emphasized however, that even where a direct calculation of a ^{14}C "age" appears applicable as in the case of HSC, there may be other factors affecting both the ^{13}C and ^{14}C values, and serving to artificially "age" the waters. Consider for example the sulphate-reduction process outlined in Section 2.4.3. The full equation for sulphate reduction includes the organic matter neccessary to provide the electron source for the reduction of sulphate (S valence of +6) to a sulphide (S valence of -2). We may consider the posssibility of two different sources of organic carbon:

In both cases a source of "dead" carbon (~ 0 pmc) would be required to artificially age the waters.

1) DIC incorporation of CH_2O from sulphate reduction

Two moles of organic carbon, consumed by *Desulfovibrio desulphuricans* as an energy source, are required for each mole of HS- produced in the reaction (Pierre, 1980):

$$2\ CH_2O + SO_4^{2-} \rightarrow 2\ HCO_3^- + H_2S \quad \text{Eqn.2.4.4a}$$

In the case of HSC any hydrogen sulphide gas produced would convert to HS^-, releasing a proton, due to pH and Eh conditions (see stability field diagram, Fig. 2.3.4b). As well, 2 moles of bicarbonate are produced for each mole of H_2S produced. Fig. 2.4.4a suggests that the ^{13}C signature of much of the organic matter consumed under reducing conditions has $\delta^{13}C$ equal to ~ -25‰PDB (Irwin etal.,1977). These values were found in reducing marine sediments in Saanich Bay, Vancouver Island.

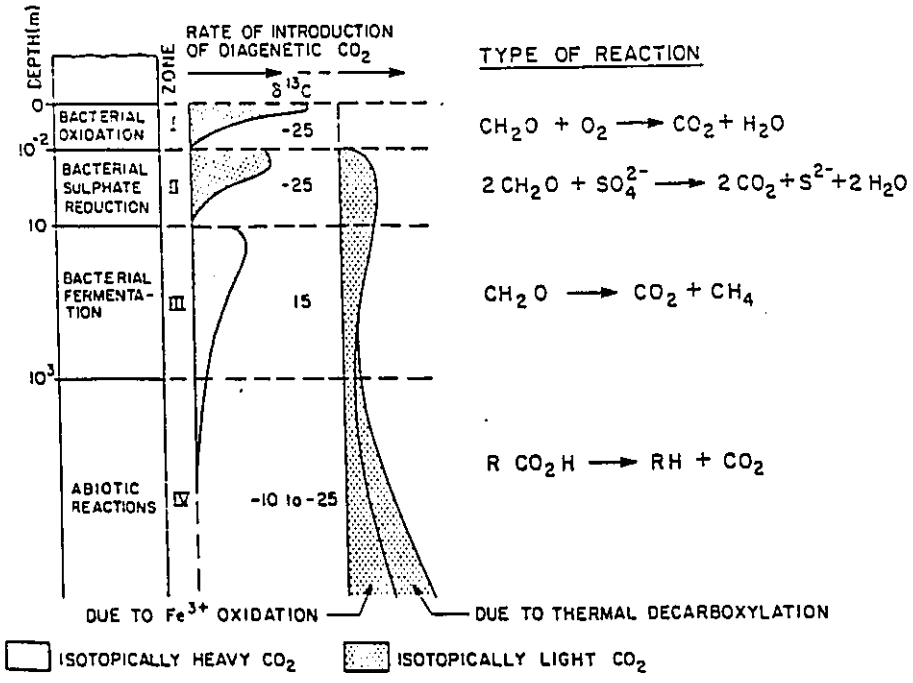

Fig. 2.4.4a ^{13}C in organic matter during diagenesis in reducing sediments (from Irwin etal.1977)

For the same reasons as those described above for the bacterially-mediated fractionation of $\delta\ ^{34}S$, the $\delta^{13}C$ value of the organic matter used as an energy source in the sulphate-reduction reaction will be weighted in favour of the lighter ^{12}C-dominated organics rather than those with ^{13}C. Bottom-sediments in contact with the saline groundwaters proposed in Section 2.4.3 may include dead marine organic material which is no longer ^{14}C-active. If mixed with thermal waters, this process would introduce for each mole of HS^- produced, 2 moles of virtually "dead" bicarbonate with a ^{13}C signature near ~ -25‰ PDB; the same value as that recorded at HSC.

For HSC, a sulphide-corrected mean residence time is calculated using the procedure outlined above and shown as HSC 1 in Table 2.4.4b. The change in estimated mean residence time is significant, approximately 1/3 the estimated age using direct ^{14}C calculation.

2) DIC incorporation of methane; CH_4

The presence of ~0.25% volume CH_4 in the gas phase of the thermal waters of HSC (Section 2.3.3) suggests that methane may be the carbon source for sulphate reduction. Isotopically light, radiogenically "dead' methane (very negative $\delta^{13}C$ and zero *pmc*), incorporated along the flowpath could be converted into DIC as shown in Eqn.2.4.4a:

$$CH_4 + SO_4^{2-} \rightarrow HCO_3^- + HS^- + H_2O \qquad \text{Eqn.2.4.4a}$$

Note that in this case the stoichiometric ratio of contributing carbon species is 1:1; 1 mole of bicarbonate is produced for each mole of HS^- produced. Thus, if we take the known value for the number of moles sulphide present at HSC (0.21 mmols/l) and subtract the same

number of moles of sulphide-related "dead" carbon from the total DIC, we will have a methane-corrected ^{14}C "age" for HSC. This calculation is shown as HSC 2 in Table 2.4.4b.

It is also possible that input of subduction-related "dead" carbon is occurring, either from CO_2 or CH_4, or both. Gas hydrates, largely methane gas, are present in large volumes in the continental slope Cresent Terrain accretionary wedge adjacent to the Pacific Rim Formation (pers.comm. Roy Hyndman, 1993). Any influx of this "dead" methane gas from the accretionary wedge, regardless of its precise input path could serve to artificially "age" the thermal waters. Both HSC and Mate Island thermal waters contain CH_4 gas although much of the methane at Mate Island is likely to come from decomposing tidal flat organics. The Ahouset hotspring $\delta^{13}C_{DIC}$ signature of -2.83‰ CDT suggests possible input of CO2 from such deep-seated sources. Also, calculations demonstrating addition of helium gas, from subducted Juan de Fuca basalt, are part of Section 2.6.

Summary of $14C_{DIC}$ modification processes and corrected mean residence time estimates

Thus, while it is quite feasible that the HSC thermal waters are thousands of years old, there are a number of potential modifying influences on its ^{13}C and ^{14}C signatures, including sulphate-reduction, and/or influx of dead carbon from CO_2 or methane gas. These modificatons would serve to artificially age the waters. Corrected ages for HSC fall between ~ 6000 and 11,000 years, while a direct application of the ^{14}C decay equation yields ~14,000 years. Helium gas volume measurements from HSC are qualitatively consistent with a relatively long mean residence time. The Ahouset Hotspring shows evidence of substantial mixing of an older thermal component with young meteoric water, the source of DIC is highly modified and "age" estimates should be treated with caution.

2.5 Geothermometry, Heat Flow and Depth of Circulation

2.5.1 Geothermometry; Introduction

One of the primary factors in assessing a geothermal resource for any particular application or exploitation is the maximum temperature of the thermal reservoir. While boreholes provide direct means for measuring temperature and other parameters at depth, the cost of drilling operations can be prohibitive. Additionally, drillholes can miss the prime location in a geothermal anomaly and thus give a misleading representation of the potential resource. Obviously then, even exploratory drilling is one of the later steps to be taken when evaluating a geothermal resource, initiated when all other less expensive assessment techniques have been applied. One such preliminary cost-effective technique involves the analysis and interpretation of aqueous geochemical and isotopic data. Since the 1960's, a number geochemical "thermometers" or geothermometers, have been developed to estimate maximum fluid temperatures at depth.

Recharge waters, regardless of origin, will undergo changes in chemistry once underground due to effects of temperature, pressure, and water-rock interaction with the host rock (Freeze and Cherry, 1979). Given sufficient time, thermal waters can reach chemical and isotopic equilibrium with the reservoir wall-rock. Thus the geochemistry of the waters which eventually discharge at the surface is a reflection of both their origin and thermal history.

In high-temperature reservoirs, where mean residence times are hundreds or thousands of years, the ratios of cations in solution are controlled by temperature-dependent equilibrium reactions between the fluid and the host-rock reservoir (Fournier, 1981). For example:

$$NaAlSi_3O_8 + K^+ \longrightarrow KAlSi_3O_8 + Na^+ \qquad \text{Eqn. 2.5.1a}$$

Albite $\longrightarrow$ K-feldspar where: $K_{eq} = [Na^+]/[K^+]$

is one reaction influencing alkali metal concentrations in solution. Alkali metal concentrations and pH is in turn influenced by reactions such as:

$$3\ KAlSi_3O_8 + 2H^+ \longrightarrow KAl_3Si_3O_{10}(OH)_2 + 6\ SiO_2 + 2\ K^+ \qquad \text{Eqn. 2.5.1b}$$

3 K-feldspar $\longrightarrow$ K-Mica + 6 Quartz where; $K_{eq} = [K^+]/[H^+]$.

It is noteworthy here that alteration to K-mica not only raises the pH (by consuming H^+ ions) but also produces 6 moles of silica and 2 of potassium for each mole of altered potassium feldspar. Reactions like the above are important in determining the composition of geothermal solutions, in fact, the silica and Na-K geothermometers are still among the most studied and oft-cited in the literature. The following subsections of Section 2.5 detail the application of silica, $\delta\ ^{18}O$ in sulphate-water, sodium-lithium, and other geothermometers.

2.5.2 Silica Geothermometer

Considering the ubiquity of silicate minerals throughout the geosphere it is little wonder that the content of dissolved silica in natural waters has long been a subject of interest. In fact, analyses of SiO_2 in hotsprings in North America dates back to 1885 (Fournier and Rowe, 1966), and in Canada, at Hotsprings Cove, to 1898 (Clapp 1913).

It was not however, until the latter half of this century that detailed analysis of quartz

solubility was reported, along with its variation with temperature and pressure (see for example Kennedy 1950; Bodvarsson 1960). More recently other quartz polymorphs including chalcedony, cristobalite and amorphous silica (opal) have also been discussed (Fournier and Rowe 1966; Arnorrson 1975).

Although quartz dissolution is rapid in fluids where temperatures are above ~150 ° C, silica's ability to precipitate out as the solution cools is kinetically inhibited. This is due in part to the tendency for monomeric H_4SiO_4 to polymerize as temperatures decrease. This polymerization in turn slows the rate of precipitation. Even so, the silica geothermometer is best applied at hotsprings where flow rates are high as this lessens the chance for re-equilibration with amorphous silica near the discharge zone. Other factors to be considered when applying silica geothermometers are:

1) possible steam separation, which will concentrate SiO_2 in the residual fluid phase
2) dilution

and 3) pH effects.

Steam separation effects are unlikely in these thermal waters as predicted maximum temperatures are far below those required to produce the significant steam fractionation and associated increased silica concentration described by Fournier and Rowe (1966). The Hotsprings Cove silica content of ~ 50 ppm would not be greatly affected by dilution due to the < 2.8% seawater mixing, as the premixed SiO_2 content would be only about 1 ppm higher. The elevated pH level of both springs however could have an effect on geothermometer

estimates. Fig.2.5.2a reveals that, at 50° C and pH 8.7 (same pH as HSC) quartz solubility would increase by 10% compared with pH 7 waters. Hence silica geothermometer estimates would overestimate the last temperature of equilibrium by about 7°C for quartz and chalcedony.

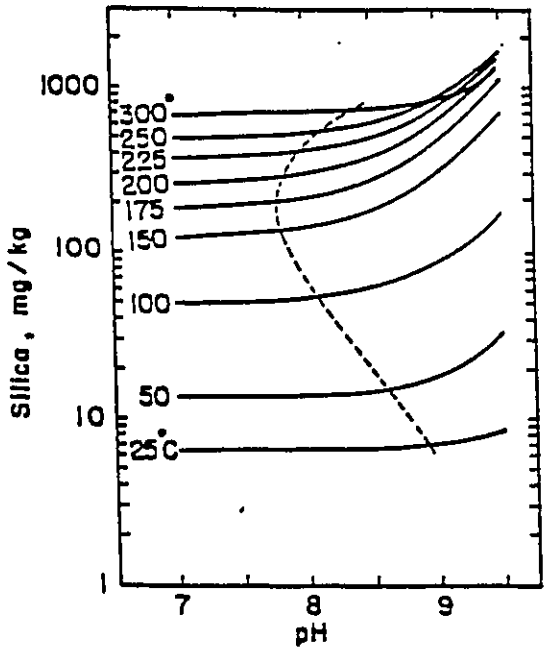

Fig. 2.5.2a

Effect of pH on quartz solubility at various temperatures. Dashed line indicates pH necessary for a 10% increase in solubility compared to pH 7 (from Fournier, 1981).

At 100° C these effects are even more pronounced and a pH of only 8.2 yields a 10% silica increase, while at pH 8.7 the excess silica in solution would approach 40%. Thus application of silica geothermometers in high pH waters are likely to overestimate reservoir temperatures.

Table 2.5.2b shows calculated quartz equilibrium solubilities for different polymorph types over a range of temperatures. Discharge temperatures for hotsprings in this study are shown with equivalent silica geothermometer temperatures. For amorphous silica all hotsprings show discharge at temperatures exceeding the predicted reservoir temperature. Additionally,

no amorphous silica was observed precipitating out at any of the hotspring vents so it is unlikely that any of the thermal waters are in equilibrium with opal. If equilibrium conditions exist for silica, then they must be with quartz or the other quartz polymorphs; chalcedony or cristobalite.

Table 2.5.2b ***Silica Geothermometer Temperature Estimates (°C)***

	SiO2 (ppm)	Quartz*	Chalcedony**	Cristobalite***	Opal****
HSC	50.1	102	72	52	18
Mate Island	16.8	57	25	8	-9
Ahouset	18.9	61	29	12	-6

*T (°C) =(1309/(5.19-Log(ppm Silica))) - 273.15 *(All formulae from Fournier, 1981)*
**T (°C) =(1032/(4.69-Log(ppm Silica))) - 273.15
***T (°C) =(1000/(4.78-Log(ppm Silica))) - 273.15
****T (°C) =(731/(4.52-Log(ppm Silica))) - 273.15

Arnorsson (1975) has described how chalcedony usually controls aqueous silica in the basaltic terrain of Iceland when temperatures are below 110° C, while certain granitic terrains tend to be in equilibrium with chalcedony below 90° C and with quartz when temperatures exceed 90° C. If the apparent long mean residence time of HSC hotspring waters is considered along with the regions predominantly granitic rock-type, then silicate equilibrium with chalcedony may be deemed reasonable if the maximum reservoir temperature is approaching 90° C. The same case can be made for equilibrium with quartz as, at the predicted quartz maximum reservoir temperature of 102° C, equilibrium conditions would likely have sufficient time to be established.

Silica geothermometer estimates for Ahouset range from 12° to 61° C. However its

low discharge rate, and pH of 10.05 may both have an effect on accuracy. The discharge temperature of 22.7° C closely approximates the 25° C curve of Fig. 2.5.2a where a pH 9 value yields a ~10% increase in quartz solubility, and pH 10 increases are offscale.

2.5.3 Sodium-lithium Geothermometer

Elevated concentrations of lithium in hotsprings are common and have in fact long been considered to contribute to the value of health spa hydrotherapy (Elworthy, 1925). From a geothermal prospecting perspective, distinct correlations between Li+ concentration and reservoir temperature have been observed. Increased concentration may be due, in part, to the small atomic radius of lithium (0.78 Å) which could, for example, retard its co-precipitation with other alkali metals in near surface clays (Mahon, 1976).

Regardless of the precise physicochemical mechanism, Li acts, in thermal waters, as a soluble element. Furthermore, the mean lithium concentration in most igneous and sedimentary rocks falls within a narrow range; 10-70 ppm (Heier & Billings 1969), explaining its presence in thermal waters from a wide variety of geological settings. A direct empirical relationship between sodium and lithium concentration, plotting log Na/Li as an inverse function of temperature and absolute temperature has been developed where:

$$\log Na/Li = 1000\ K^\circ - 0.38 \quad \text{[for waters where Cl- conc} < 0.3\ M] \qquad \text{Eqn. 2.5.3a}$$

Table 2.5.3a shows calculated maximum reservoir temperatures for HSC, Ahouset, and Mate Island thermal waters.

Table 2.5.3a ***Na-Li Geothermometer*** (after Fouillac and Michard, 1981)

Log Na/Li=1000T-0.38 (where Cl concentration < 0.3M)

	Na (ppm)	mmolsNa	Li (ppm)	mmolsLi	log na/li	°K	°C
HSC 1	149.0	6.481	0.054	0.008	2.921	303	30
Ahouset	42.5	1.849	0.008	0.001	3.205	279	6
Mate Island	272.0	11.831	0.077	0.011	3.028	293	20

Recalculated West Coast Na-Li Geothermometer*

	Na (ppm)	mmols Na	Li	mmols Li	log(Na/Li)	°K	°C
HSC-sw	46.24	2.011	0.050	0.007	2.446	354	81
Mate Is. -sw	59.14	2.572	0.070	0.010	2.407	359	86

* -a component of seawater equivalent to 0.6 x the maximum 2.8% and 5.8% local seawater was subtracted from HSC and Mate Is. respectively; (see 60% seawater Br- column in Table 2.3.6b)

A major disadvantage of the Na-Li geothermometer is that the Na/Li ratio is greatly affected by Na input occurring during any mixing with marine waters. One of its major advantages, aside from the wide applicability previously mentioned, is that it is not strongly influenced by chemical re-equilibration processes occurring during ascent of thermal fluids. This again is largely due to the consistent solubility of lithium (Fouillac, 1981).

The reliability of Eqn. 2.5.3a falls immediately into question when applied to this study, as the HSC and Mate Island log Na/Li calculated subsurface temperatures are below their actual discharge temperatures. Subtraction however, of the seawater mixing component (1.5% for HSC) outlined in Section 2.3.6 yields more plausible Na-Li geothermometer estimates for HSC and Mate Island. The predicted reservoir temperatures are in fact quite consistent for both springs, ~81° C and 86° C respectively. These geothermometer predictions are similar to

silica-based estimates and are consistent with the hypothesis that a minor component of seawater is mixing with these thermal waters and that Mate Island and HSC are discharges from the same parent reservoir, irrespective of its precise maximum temperature. Li+ concentrations were near detection in the low T.D.S. waters of Ahouset warm spring (detection limit 0.005 ppm) and geothermometer estimates are below discharge temperature, hence lithium-based geothermometers are not applicable there.

2.5.4 Sulphate-water Geothermometer

The equilibrium distribution of ^{18}O in water and ^{18}O in dissolved sulphate species in a geothermal system is dependent upon the temperature at which equilibrium conditions are established. Various authors have documented how the $\delta\,^{18}O$ values in sulphate become less positive with increasing temperature (Mitzutani and Rafter, 1969; Mitzutani 1972). The following equation defines one representation of this isotopic exchange reaction:

$$1000 \ln \alpha_{\text{sulphate-water}} = 3.251\,(10^6/T^2) - 5.1 \quad \text{(Mitzutani and Rafter, 1969)} \qquad \text{Eqn. 2.5.4a}$$

$$\text{where; } T = {}^{\circ}K, \text{ and } \alpha = (\delta\,^{18}O_{\text{sulphate}} + 1000) / (\delta\,^{18}O_{\text{water}} + 1000)$$

While nearly 100% isotopic equilibrium can be attained in about 18 years for 200°C water at pH 7 (McKenzie and Truesdell, 1977), the exchange reaction is slower for lower temperature geothermal systems (Chiba and Sakai, 1985). This, however, can be considered advantageous once equilibrium conditions are attained in a reservoir at depth, because the $\delta\,^{18}O$ signatures would tend to be preserved during the shorter-term ascent and discharge to surface

(Fournier, 1981). It is also part of the reason why the sulphate-water geothermometer is considered to be among the most reliable of the various geochemical tools used to estimate geothermal reservoir temperatures. There are however a number of possible complicating factors for this geothermometer including:

1) steam separation, which can affect the $\delta\,^{18}O_{water}$ signature

2) oxidization to sulphate of isotopically depleted H_2S

and 3) mixing with non-thermal waters.

For HSC, steam separation is unlikely to affect the system as most geothermometer estimates are below 100° C and $\delta\,^{18}$O-D plots show no geothermal shift. With regard to incorporation of isotopically-depleted H_2S, the lack of oxygen, negative Eh, and redox conditions all point to sulphate reduction rather than sulphide oxidation. Seawater mixing could have a minor effect however, by lowering the $\delta\,^{18}O_{sulphate}$ value.[4] If the seawater mixing component is removed (using the 1.5% seawater model, Table 2.3.6b) the seawater-mixing corrected $\delta\,^{18}O_{sulphate}$ value changes from 9.89 ‰to 10.93 ‰:

$$\delta\ 9.84\ ‰ = \frac{(\delta\ 9.45\ ‰ \times 22.9\ ppm)^5 + (\delta\ ^{18}O_{sulphate}(premixed) \times 8.15\ ppm)}{(31.05\ ppm)} \qquad \text{Eqn. 2.5.3b}$$

$$\delta\ ^{18}O_{sulphate}(premixed) = +\ 10.93.$$

The seawater-corrected sulphate-water geothermometer estimate for HSC and unmodified sulphate-water geothemometric calculations for HSC and Ahouset are shown in Table 2.5.4a.

---

[4] seawater sulphate has a narrow range of $\delta\,^{18}$O values near +9.45 ‰ SMOW (Krouse, 1980)

[5] δ^{18}O signature x weight fraction of seawater sulphate attributed to mixing

Table 2.5.4a ***Sulphate Water Geothermometer*** (after Mitzutani and Rafter, 1969)

1000 ln alpha (SO4 - H2O)= 3.251(1million/°K X°K)-5.1

Where alpha = d 18O (SO4)+ 1000/ d 18O (H2O)+1000

	delta O-18 water	delta O-18 sulphate	Alpha (@)	1000 ln@	1000 ln@ plus 5.1	3.251/ 1000 ln@+5.1	X 1million	°K= sqrt	°C
HSC	-10.06	9.84	1.0201	19.9028	25.0028	0.1300	130025	361	87
Ahouset	-8.87	7.89	1.0169	16.7686	21.8686	0.1487	148661	386	112
HSC-sw SO4	-10.06	10.93	1.0212	20.9816	26.0816	0.1246	124647	353	80

The corrected maximum reservoir temperature estimate for Hotsprings Cove changes slightly, from 87°C to 80°C. The value for Ahouset, interestingly, is above boiling. This may be an over estimation, due to two separate effects, both of which are a result of mixing with local, non-thermal meteoric groundwaters. These two modifying effects are:

1) less depleted $\delta\ ^{18}O_{water}$ values

and 2) oxidation to sulphate of a depleted H_2S component which was present before mixing.

Both effects reduce the difference between the $\delta\ ^{18}O_{sulphate}$ and $\delta\ ^{18}O_{water}$ values, which increases the estimated reservoir temperature. No dissolved sulphide was detected in the Ahouset thermal waters, consistent with the possibility of the addition of an oxidized H_2S component to the sulphate fraction.

2.5.4 Na-K-Ca and Log (√Mg/Li) Geothermometers

There are two other cation-based techniques which have a limited applicability in this study; the Na-K-Ca and log (√Mg/Ca) geothermometers. The Na-K-Ca-based technique

shown below was developed due to inaccuracies in the Na-K geothermometer for calcium-rich waters, and for reservoirs where temperatures are below 150°C (Fournier and Truesdell, 1973).

$$K^\circ = \frac{1647}{\log (Na/K) + \beta [\log (\sqrt{Ca}/Na) + 2.06] + 2.47} \qquad \text{Eqn. 2.5.4a}$$

Dilution of thermal waters by more saline waters which are cooler can have an effect on the Na-K-Ca technique (Fournier, 1981). This effect is seen in calculations using this formula for Mate Island where more significant seawater mixing occurs. Predicted reservoir temperatures are below the discharge temperature. The estimated maximum temperature for HSC however matches the discharge temperature near 50° C which could be indicative of conditions approaching equilibrium for a near-surface reservoir.

On the other hand, Na-K-Ca calculations using the seawater mixing models are inapplicable as they give negative temperatures for both Mate Island and HSC, a reflection possibly of non-equilibrium, supersaturated conditions for sodium, calcium and potassium involving minerals such as the smectites shown in Table 2.3.2d. This would affect the concentrations of these cations in the near-surface environment, causing inaccuracies in estimated maximum reservoir temperatures. The Mg-corrected Na-K-Ca geothermometer is inapplicable here as predicted temperatures were below discharge temperatures. The log ($\sqrt{Mg}/Li$)-based geothermometer was calculated by the Solmineq geothermal modelling program (Kharaka and Mariner, 1988). Predicted reservoir temperatures are similiar to the silica, sodium-lithium and sulphate water geothermometer estimates, and are shown along with the Na-K-Ca geothermometer estimates in Table 2.5.5a.

2.5.5 *Geothermometer Summary*

Table 2.5.5a **Summary**
Geothermometry Maximum Temperature Estimates (°C)

Note: any geothermometer estimate below discharge temperature is not included in calculating the mean. The sulphate-water geothermometer is excluded for Ahouset due to possible oxidation of a depleted sulphide fraction.

		Geothermometer						
	Discharge Temp	Sulphate - Water	Chalcedony	Quartz	Log (sqrtMg/Li)	Na-K-Ca	Log (Na/Li)	Mean
HSC	50.3	89	72	102	80	50	na	86
HSC -sw	50.3	81	72	102	na	na	75	83
Ahouset	22.7	115?	29	61	36	na	6	42
Mate Island	25.4	na	25	57	36	97	20	63
Mate Is. - sw.	25.4	na	26	59	na	na	76	68

Although a mean value for geothermometers incorporates all the assumptions and weaknesses inherent for each geothermometer temperature estimate, it may be considered useful as a general approximation of reservoir temperature. Geothermometer estimates for HSC are in the 70° - 100°C range with a mean value of 86° C, similiar to estimates which include subtraction of seawater. Mate Island geothermometric calculations have been included for completeness. However, if we consider Mate Island to be part of the HSC system then the geothermometer estimates for the latter may be considered more reliable. No geothermometer estimates are significantly above 100° C, and since it is unlikely that *all* have re-equilibrated to lower discharge temperatures, a significant reservoir of high temperature geothermal water is probably not present.

Temperature estimates for Ahouset are not much higher than discharge temperatures with the exception of the sulphate-water and quartz geothermometers. Possible explanations for

the high sulphate-water estimate may be related to mixing with non-thermal groundwaters (Section 2.5.3) whereas the quartz geothermometer estimate (61° C) may be due to weathering reactions, such as Eqn. 2.5.1a which can raise the pH while adding silica. Given the limited amount of data collected in this study for Ahouset it is difficult to predict accurately the effects of an unknown amount of mixing on geothermometer estimates.

2.5.6 Geothermal Gradient and Depth of Circulation

No precise downhole measurements of the geothermal gradient exist for the study area. Heat flow measurements for the southern half of the west coast of Vancouver Island are low; heat flux ~31 mW/m^2 (Bentkowski and Lewis, 1989) and may be attributed to two principal factors:

1) the thickened crust (up to ~ 45 km maximum thickness) resulting from subduction of the Juan de Fuca plate beneath the western margin of the continent (see for example Lewis, 1988, and Fig.2.2.1d).

2) the coolness of the relatively young subducting oceanic slab, which acts as a heat sink and depresses isotherms (pers.comm. Roy Hyndman).

Consequently, the geothermal gradient in the area of HSC is quite low, likely about 22°C/km (pers.comm. Trevor Lewis). Using this geothermal gradient, and an estimated maximum subsurface temperature near 90°C, the depth of circulation of the HSC thermal waters would be about 4 km. However topographic effects tend to pull isotherms upwards to mimic, to some extent, surface topography, thus depth of circulation may be slightly less, perhaps in the range of 3-4 km.

2.6 Noble gas Isotopes; Helium and Neon

Helium isotopes, employed as an interpretational tool for regional tectonics in Section 4 are an integral part of this thesis study. Much of the data gathered and interpretations reached pertain to the active subduction zone of the Insular Belt beneath HSC and Ahouset. Hence, it is also important to include findings relative to these west coast Vancouver Island hotsprings in this section. The reader may wish however, before proceeding with this section, to first read the introductory background section on helium and the noble gases in Section 4.2.1 and Appendix He.

2.6.1 Verification of Noble Gas Sample Purity

Introduction

Three checks on the purity of noble gas samples collected involve consideration of:

1) neon excess

2) helium volume

3) neon solubility at assumed recharge elevation.

1) Neon excess

Although the crustal production of helium resulting from alpha decay of uranium and thorium is significant, subsurface production of neon is considered to be relatively insignificant (Bottomley et al., 1984). Hence, whereas the atmospheric ratio of He/Ne is 0.29, ratios from primordial and crustal sources are usually >100. This facilitates use of neon concentration as a check against atmospheric contamination during sampling, as shown below (Craig et al. 1978a, Torgersen and Jenkins 1982).

$$(R/R_{air})_{corrected} = [(R/R_{air})\ X] - 1 / X - 1 \qquad \text{Eqn. 2.6.1a}$$

where $X = (He/Ne)/(He/Ne)_{air}$; $R/R_{air} = {}^3He/{}^4He_{sample} / {}^3He/{}^4He_{air}$

The correction assumes that samples are mixtures of atmospheric helium and neon with an additional pure helium component added from radiogenic and/or mantle sources. If Ne values are not available the *volume* of He can be used as a gauge of the amount of air contamination. This is because the low atmospheric concentration (5.24 ppm He) and low solubility of helium in water (4.5×10^{-8} cc/g H_2O) at STP and 0% salinity) ensure that if greater than 5 times the atmospheric concentration is present (from radiogenic or mantle sources) then the effects of contamination are negligible (Torgersen and Jenkins, 1982). Table 2.6.1a shows the concentrations of both neon and helium in samples from Hotsprings Cove and Ahouset.

Table 2.6.1a Sample	*Helium R/R air*		*Total He Vol* cc STP/g x10-7		*He Vol.* R/Air	*Total Ne Vol* cc STP/g x10-7		X**	*(R/R air)* corrected*
Hotsprings Cove 1	0.27	+/- 1%	13.5	+/-.05	30.01	1.86	+/- 10%	25	0.24
Hotsprings Cove 2	0.27	+/- 1%	11.9	+/-.05	26.44	1.28	+/- 10%	32.1	0.25
Ahouset	0.28	+/- 1%	3.26	+/-.05	7.244	2.32	+/- 10%	4.85	0.09
Fresh water (air equilibrated s.l.)	1.00		0.45	n.a.	n.a.	1.8	n.a.	n.a.	n.a.

** **(R/Rair) corrected= ((R/R air) X) -1 / (X - 1)**

* *where; X = (He/Ne)/(He/Ne) air,*
and where; (He/Ne) air = 0.29; includes atmospheric and radiogenic sources (Craig etal,1978a).

He dissolved in water in equilibrium with atmospheric Helium (5.24 ppm), has a solubility of 4.5 X 10-8 cc/STP/gH20

Atmospheric Neon has a solubility of approximately 1.8 x10-7 @ STP and a solubility of approximately 1.7 @ 50 C

The calculation of neon excess, used as a helium isotope correction factor to account for the possible entrapment of air bubbles during sampling, is also shown in the table. This correction process is based on the stable concentrations of both noble gases in atmospheric air; 5.24 ppm He and 18.18 ppm Ne, (dry air volume at sea level and 1 atmosphere pressure). The last column in Table 2.6.1a shows the corrected values using the neon excess calculation. The change for the two HSC samples is within the limits of analytical error, thus the 0.27 values for R/R_{air} for helium will be considered valid as the analytical error given for neon is actually greater (+/- 10 %).

The Ahouset sample may have entrained a small portion of excess air. This is perhaps to be expected with this low flow spring, which shows evidence of mixing with non-thermal waters. This possibility of entrainment of a portion of excess air is further discussed below in part 3; neon gas solubility variation with temperature and pressure.

2) Helium volume

The volume of helium gas, as discussed above, can provide a qualitative check on sample contamination. In this regard all samples meet the volume criteria, ranging from 7 to 30 times atmospheric volume for these three Insular Belt samples.

3) Neon solubility at an assumed recharge elevation

A third check on the reliability of noble gas measurements involves solubility calculations described by Mazor (1991). The initial content of noble gases in a given fluid will be related to (Mazor, 1972):

1) temperature of the recharge waters

2) recharge elevation (^{18}O-D-derived elevation (Section 2.4.2) used as assumed values).

Although helium variation with temperature is minimal, neon gas solubility at sea level ranges from 2.3 x 10^{-7} (cc gas/cc distilled water) at 5° C, to ~ 1.8 x 10^{-7} for temperatures over 40° C (Mazor 1979). Where neon data are available, this relationship, combined with gas solubility variation with altitude, can be used to estimate the amount of noble gas incorporated at recharge (before closed-system conditions commence) provided no entrapment of excess air occurs in the unsaturated zone during recharge (Heaton and Vogel, 1981). The noble gas solubility for a given temperature at sea level is divided by a factor greater than unity to account for decreased solubility at altitude. For example, at a recharge elevation of ~ 900 m and recharge temperature of 7° C (average during 80% of Tofino area precipitation; see Fig. 2.1.2) the solubility of neon is:

$$2.1 \text{ X } 10^{-7}/1.15 = 1.85 \text{ X } 10^{-7} \text{ cc/g } H_2O \qquad \text{(from Fig.2.6.1a \& b)}$$

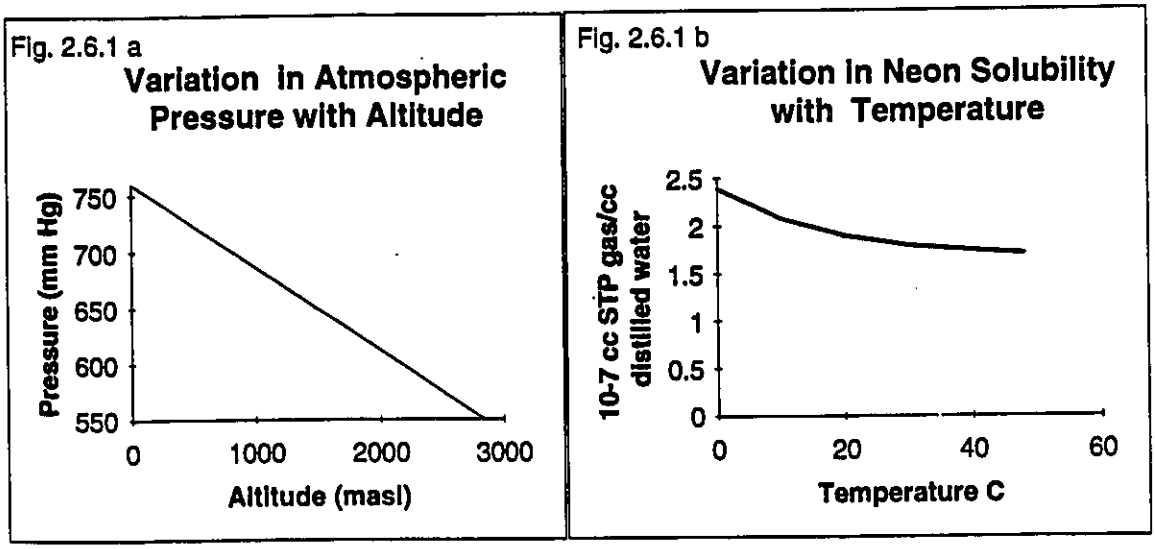

Fig. 2.6.1a & b Variation in pressure with altitude and neon gas solubility with temperature (after Mazor, 1991).

This approximation concurs with the measured concentration at the discharge vent for Hotsprings Cove (HSC 1) which is 1.86 x 10^{-7} cc/g H_2O. If a recharge elevation of ~400 m is assumed for Ahouset then the solubility of Ne in those thermal waters would be:

$$2.1 \times 10^{-7}/1.05 = 2.00 \times 10^{-7} \text{ cc/g } H_2O.$$

The measurement of neon content in the sample from Ahouset is 2.32×10^{-7} cc/g H_2O, so there remains a slight excess of Ne gas in this sample. Subtraction of the analytical error (+/-10%) gives a volume of 2.088×10^{-7} cc/g H_2O which equals approximately the solubility value for waters at ~ 8° C near sea level. This is consistent with indications of mixing of thermal waters with cool local meteoric waters for Ahouset, such as the presence of 13 T.U.with 18 pmc ^{14}C. Any other excess from this site may be due to entrapment of air in the aerated zone where these meteoric waters infiltrate (Heaton and Vogel, 1981).

In conclusion, all sample analyses are considered as valid using the neon excess, helium volume and recharge solubility calculations. Hotsprings Cove thermal waters are below saturation for atmospheric neon, indicative of good sample purity, whereas the Ahouset hotspring shows minor input from mixing with local meteoric waters in equilibrium with atmospheric neon gas near sealevel. Nonetheless, the Ahouset helium gas volume (>7 times the atmospheric concentration) and uncorrected R/R_{air} (which is statistically identical to HSC values) support the validity of the Ahouset R/R_{air} of 0.28.

2.6.2 Discussion and conclusions

The initial content of ^3He in a given fluid will be related to recharge elevation and temperature of the recharge waters (Mazor, 1972). Thus, without any additional ^3He input, the ratio of $^3He/^4He$ will decline in any geologic setting where input of radiogenically-produced ^4He occurs. Similarly, the R/R_{air} of $^3He/^4He$ will decline under the same circumstances.

Examination of the $^3He/^4He$ ratio alone then can be misleading, for, where radiogenic production of ^4He occurs, input of mantle-derived ^3He gas could be overlooked unless the **volume** of helium gas is considered along with its isotopic ratio. An example of this occurs at Hotsprings Cove and Ahouset where plutonic rocks of the West Coast Complex, Island Intrusions, and Catface Intrusions provide a source of radiogenic He through α-decay of uraniferous minerals (for equation see Appendix He). Geothermal reservoirs tend to act as a sink for helium, particularly in highly-fractured and seismically-active zones (Mazor and Bosch, 1989)

The helium R/R_{air} values (Table 2.6.1a) of 0.27, and 0.28 for HSC and Ahouset may at first glance simply reflect a local radiogenic helium signature with no sign of additional ^3He input. However, when the volume of helium gas present is also considered, a genuine contribution of ^3He from sources other than atmospheric is evident (pers. comm.John Andrews). The table reveals that, despite R/R_{air} values near 0.27, an excess of ^3He of ~ 7 and 8 times atmospheric is present for the two samples at HSC, and more than twice the atmospheric amount is present for Ahouset thermal waters. Furthermore, the ratio of excess $^4He/^3He$ is

precisely the same for all samples at 6.3. Thus radiogenic input of excess ^{4}He outstrips the mantle input of ^{3}He by a factor of ~ 6. This factor is orders of magnitude less than would be expected if the excess ^{3}He were produced entirely as a result of the spontaneous fission of ^{6}Li (see Appendix He), while the other source of ^{3}He, atmospheric contamination, has already been considered above. This leaves mantle-related processes as the remaining source.

The question of origin of the excess helium in these Insular Belt thermal waters must now be dealt with. Certainly a portion of the helium must come from radioactive decay as this is the only possible source of such an excess of ^{4}He. However, the excess ^{3}He, as shown above must come from a mantle-related source. The important qualifier in this question is whether or not the light isotopic contribution comes *directly* from the mantle. Indirect input from subducted oceanic crust is also possible in this region where the eastern margin of the Juan de Fuca Plate is being consumed.

Processes of hydrothermal circulation remove large quantities of ^{3}He from oceanic crust while radiogenic production of ^{4}He lowers the isotopic ratio even further so that the resultant R/Rair can have an absolute maximum of ~ 2 (Poreda and Craig 1989). Current production of new oceanic crust along the spreading centre of the Juan de Fuca ridge is typified by superheated fluid temperatures (up to 350°C) driving rapid, powerful circulation of seawater throughout the oceanic crust (Davis and Villager, 1992). Hence, retention of any ^{3}He which is extremely volatile is highly unlikely. However, if we use a R/R_{air} value of 2 for a subducted oceanic crust, we can then calculate its relative helium gas contribution to the hotspring waters by using different ratios for various crustal rock-types. The *actual* ^{3}He/^{4}He isotopic ratios for

most crustal rocks vary from 1 to 5 x 10^{-8} (Mamyrin and Tolstikhin, 1984).

For a ^{3}He rich basalt, where $R/R_{air} = 2$; $R_{actual} = 2 \times 1.38 \times 10^{-6} = 2.76 \times 10^{-6}$

Now, the actual helium isotopic ratio at a particular hotspring can be solved for contributing portions from both the basalt and the various crustal rocks, the latter having actual helium isotopic ratios ranging from 1 to 5 x 10^{-8}. If we use an average value of 3 x 10^{-6} for the crustal rock, and the maximum oceanic basalt value of 2.76 x 10^{-8} we then have:

^{3}He-rich Basalt (Portion) + Crustal Rock (1 - Portion) = Actual He ratio.

Substituting in the values for each of these components:

$$2.76 \times 10^{-6} (P) + 3 \times 10^{-8} (1-P) = 3.45 \times 10^{-7}$$

Multiplying both sides by 10^8 and solving for the respective crustal and subducted basaltic portions we have:

276P + 3 - 3P = 34.5. Thus, 273P = 31.5; or, P= 0.115.

Hence the portion of helium gas from subducted oceanic crust would be about 11.5%, with an 88.5% contribution from the local host rock.

If we lower the actual ratio of the contributing crustal rock to the lowest average crustal value of 1×10^{-8}, the resultant contributions calculated as above are 12.2% for the subducted basalt and 87.8% for the host rock. Raising the crustal ratio to its maximum only lowers the basaltic contribution to 10.9%. Hence, a figure of 11.5% is a good approximation of the contribution of ^{3}He released from the Juan de Fuca basalt during subduction beneath the continental margin.

Geophysically-derived indications of reflector zones present beneath the crust under the west coast of Vancouver Island were shown in Fig. 2.2.1d. Previously, this type of geophysical variation beneath the crust was generally interpreted as a change in the dominant rock-type (pers. comm. Trevor Lewis). Recent detailed geophysical work however indicates that changes in the geophysical signature may in fact be due to increased concentrations of volatiles in these zones (see for example Hyndman and Wang 1993, Lewis et al. 1988, Davis and Lewis 1984) and that these subduction zone volatiles include helium gas.

The volatile gases are then subject to upward migration along local thrust faults such as the Tofino and West Coast Faults, particularly during periods of seismic activity. Intersection with the Refuge Cove Fault (Section 2.2.1) would facilitate incorporation of these gases into HSC and Ahouset. Seismic events along the west coast of Vancouver Island appear to be related to the trend of the WCF-TF and the subduction front, with localized epicenters occurring also at or near the Refuge Cove Fault and HSC (Section 2.2.2).

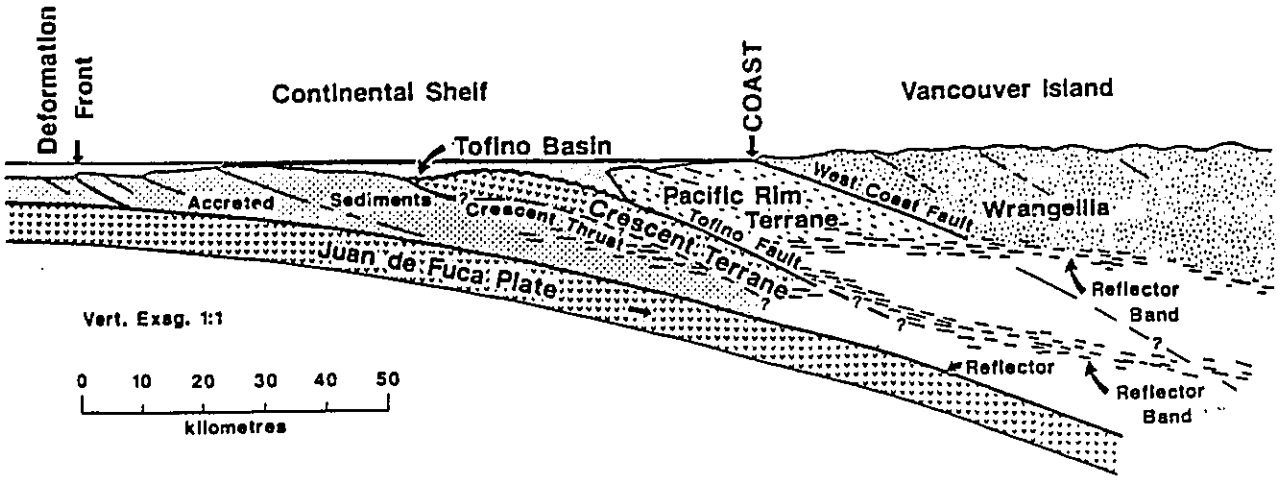

Fig. 2.6.2a **Volatile zones beneath the Tofino and West Coast Faults**

Reflector bands (Fig. 2.6.2a) are directly beneath extensions of the West Coast and Tofino Faults it is likely that such volatiles are permeating upwards along these major fault zones and being "captured" in the local geothermal reservoir. This process may be continuous, or episodic; larger volume expulsions coinciding with the seismic events which are so frequent along the subduction front (Section 2.2.2).

Interestingly, reports by native residents of gas expulsions at the offshore vent adjacent to Mate Island, near HSC, also support the hypothesis of periodic release of fault-related gases in the area. Further the extension of the Refuge Cove Fault (as in Fig. 2.2.1d) and intersection with the WCF occurs offshore of Flores Island which hosts the Ahouset Hotspring.

One of the most intriguing aspects of this area is that despite a subduction front length of hundreds of kilometres, the only thermal discharges found to date are the two being discussed. The offshore gas vent near Mate Island and the rare but seemingly linear series of pure gravel deposits on the continental shelf and slope (Conway et al., 1990) may be offshore analogs to the terrestrial geothermal expressions at HSC, Mate Island and Ahouset. This and other phenomena of these Insular Belt geothermal waters raise many questions about their relationship with the dynamic local and regional tectonic environment. Suggestions for future research are included at the end of Section 4.

2.7 Summary; Hotsprings Cove and Ahouset geothermal waters

The thermal waters of Hotsprings Cove reveal geochemical consistency dating back to 1898, which reflects evolution through interaction with crystalline host rock of the Insular Belt. The Mate Island tidal flat thermal seep and an associated offshore vent are likely part of the same geothermal system. Binary mixing models, with local recharge waters and local seawater as end-member components, indicate local seawater and contributions of 4-6% for Mate Island and minor mixing at HSC, up to ~ 1% local seawater.

^{18}O-D relationships point to local recharge at ~ 900 m for these thermal waters. Modification of ^{14}C by sulphate-reducing bacteria provide mean residence time estimates in the order of 6000 to 11,000 years. $\delta^{34}S$ values support the hypothesis that saline waters of marine origin may also be contributing to the geothermal flow system. Chemical and isotopic geothermometer estimates range from 70 to 120°C with the most reliable estimates near ~ 90°C.

The waters of Ahouset hotspring, located about 12 km south of HSC on Flores Island, have low total dissolved solids, a pH near 10, and show evidence of mixing with modern local non-thermal waters. It is likely part of a system separate from HSC.

Helium gas isotopes are consistent for all samples from these Insular Belt hotsprings; $R/R_{air} = \sim 0.28$. Calculations modelling crustal and mantle-associated sources indicate ~11.5 % helium gas volume contribution from the subducting Juan de Fuca plate.

3 Selkirk Range Hotsprings; Halcyon, St. Leon, and Nakusp

3.1 Introduction

Ice-cold mountain streams adjacent to scalding hot geothermal springs are set against the backdrop of spectacular mountain vistas in the Selkirk Mountains of the Omineca Crystalline Belt. Three hotsprings found on the eastern side of Upper Arrow Lake; Nakusp, St. Leon and Halcyon are studies in contrast.

At Nakusp, modern-day engineering, an aqueduct system, and paved parking facilities provide easy access to the indoor geothermal pool facilities, whereas at the St.Leon hotspring a narrow path down the thickly-wooded forest slope leads to a shallow, cement and stone tub. The Halcyon hotsprings (Plate 3.1a)., though developed in the late 1800's as one of the first mineral spring resorts in Canada, today consists of a pair of crudely-fashioned, plastic-lined log tubs (Plate 3.1b).

Despite the asthetique differences, these Omineca Belt geothermal springs, set on the western flank of the Kuskanax Batholith adjacent to the Columbia River Fault zone, have in common a number of geochemical and geological characteristics. Together they represent a geothermal flow system in a Cordilleran geologic setting to compare with the contrasting tectonic environment of the west coast Vancouver Island Insular Belt hotsprings.

Plate 3.1a (left) Halcyon hotspring sulpha-lithia waters main discharge vent

Plate 3.1b (right) Plastic-lined log tubs at the former site of a therapeutic spa for tuberculosis patients.

3.1.1 Location and Access

The study area, in southeastern British Columbia, extends north-south along the eastern side of Upper Arrow Lake, its northern limit located near Galena Bay about 40 km south of Revelstoke, British Columbia. All three of the thermal springs in this study can be accessed by automobile on secondary roads which connect with highway 23 (Fig. 3.1).

3.1.2 Climate, Physiography, and Hydrology

Mean annual air temperature in Revelstoke is about 7° C with the months of December through February below freezing (Fig. 3.1.2a). Mean annual precipitation is near 1100 mm, about half falling during the months of November through February (Environment Canada, 1980). The area is well treed with softwood timber and logging operations based in Nakusp continue in the region.

Mountain sides in the region can be steep to near vertical. Topography in the area of Halcyon hotspring increases rapidly from about 425 m (1400 ft.) at the shore of Upper Arrow Lake to ~760 m (2500 ft.) at the hotspring and ~2055 m (6750 ft) at Mt Halcyon ~1.5 km ENE of the hotspring (Fig. 3.1); a 1:4 ratio of elevation change per horizontal distance. Similiar topographic gradients occur near St. Leon and Nakusp hotsprings.

The Upper Arrow Lake area of the Columbia River Valley was flooded during the 1960's as a result of a hydroelectric agreement with the United States. The water level in

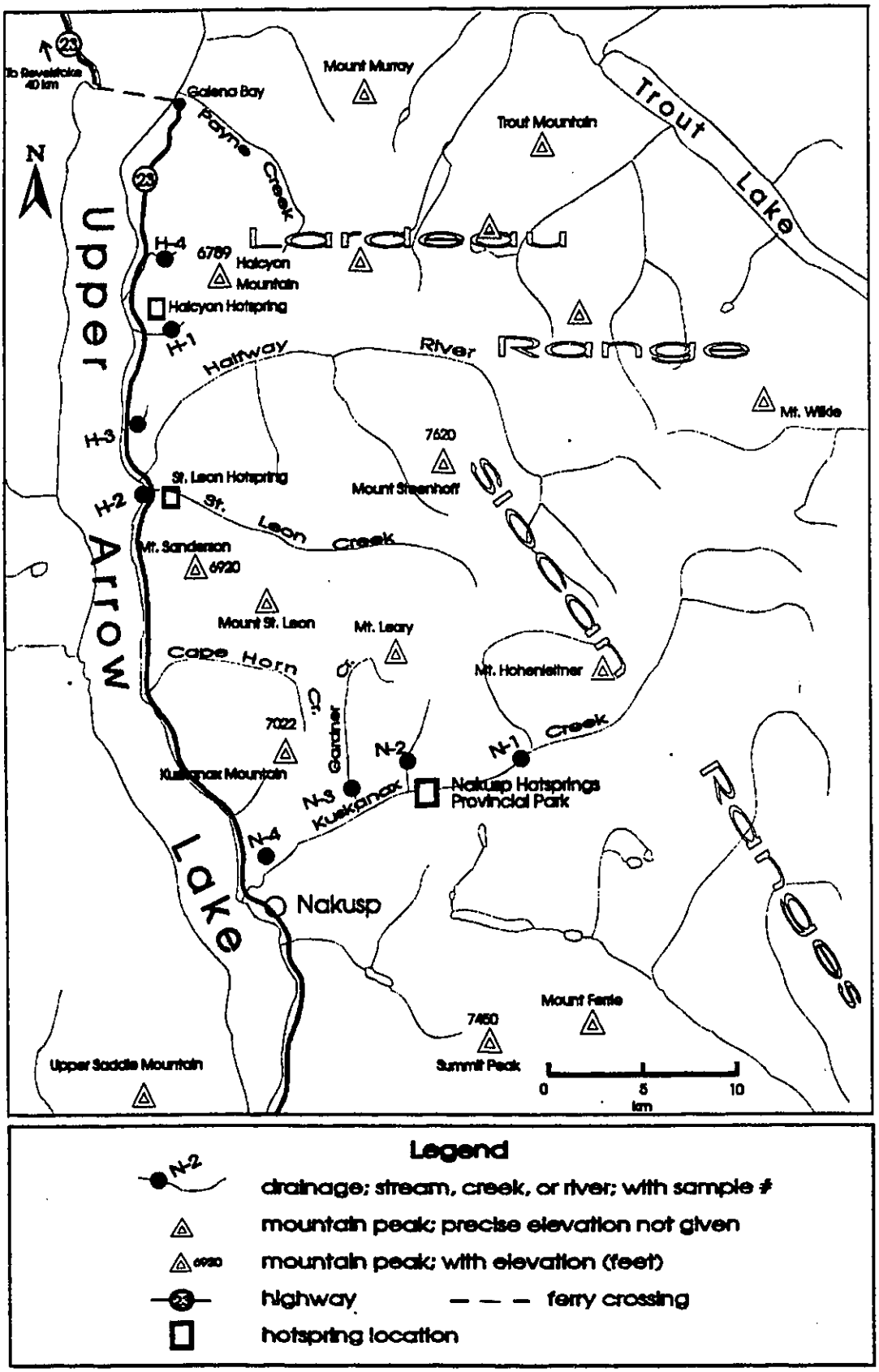

Fig. 3.1 Location, access, drainage, and topography; SelkirkRange hotsprings

Fig. 3.1.2a

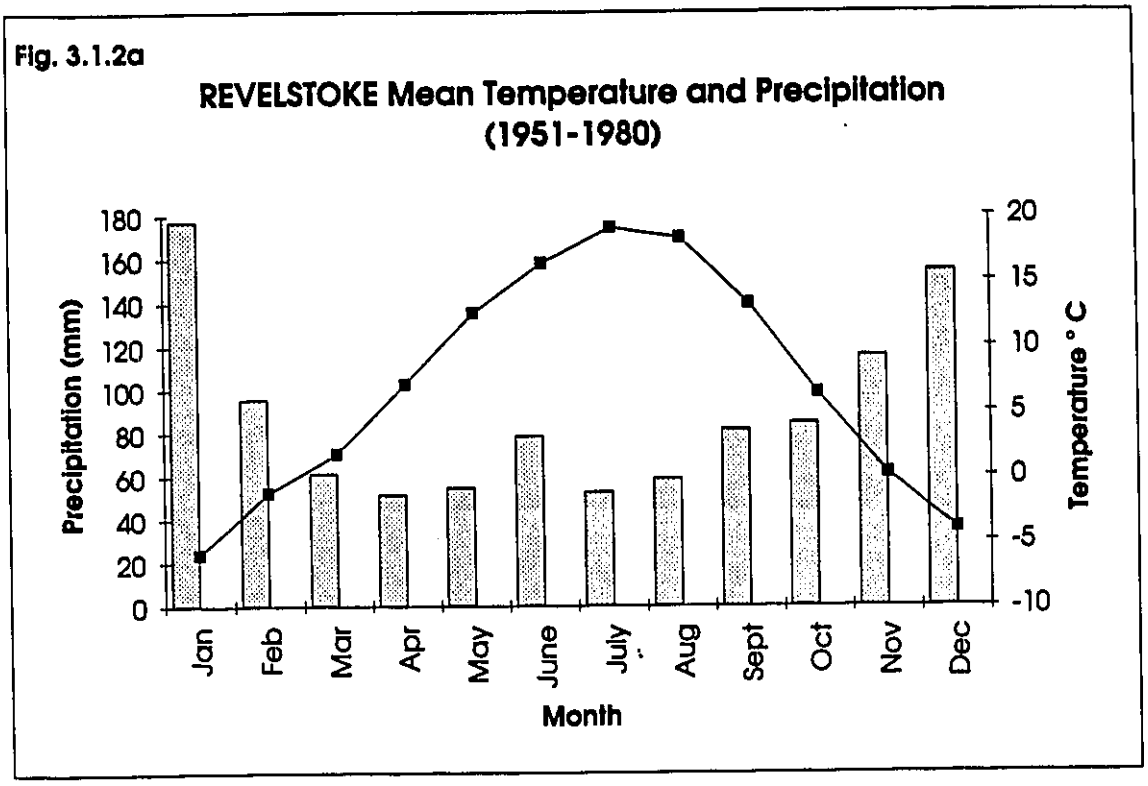

Upper Arrow Lake is now maintained at between ~425m (1395 ft) and 442 m (1450 ft) above sealevel (Read and Wheeler,1976). In addition to the Halfway River, Nakusp River and St. Leon Creek which drain the study area and empty into Upper Arrow Lake, there is an abundance of mountain streams and creeks which cascade down the western flank of the Kuskanax Batholith. The nearest alpine glacier melt-waters are on the eastern edge of the batholith and do not pass through the immediate study area.

3.1.3 Previous work

In 1889 Sir George Dawson examined Halcyon hotspring as part of a reconnaissance survey on the geology of the Kootenay region. Previous geochemical work on the Halcyon hotspring by Elworthy (1925) included analyses of chemical and

radioactive constituents and a comparison of his results with analyses from 1917. Souther and Halstead (1973) sampled and reported aqueous geochemical and gas analyses as part of their paper on mineral and thermal springs of Canada (see Section 3.3.1).

The Nakusp hotspring waters were mentioned by Elworthy (1925) who referred to the analyses reported by F.G. Wait (1898). Souther and Halstead (1973) also briefly mention the Nakusp spring, and refer to is major ionic constituents. No mention is made of St. Leon Hotspring in the scientific literature.

3.2 Geology

3.2.1 Physical and tectonic setting

The Selkirk Range Hotsprings examined in this study are located on the western edge of the Kuskanax Batholith in the southern portion of the Omineca Belt of the Canadian Cordillera (Fig. 3.2.1a). An area of extension and high heat-flow, intense deformation and uplift, the Omineca belt is underlain by metamorphic and granitic rocks, and has predominantly northwesterly-aligned structural features (Gabrielse et al.,1991) such as the Columbia River Fault Zone (CRFZ). The CRFZ and Upper Arrow Lake separate the Monashee Metamorphic Complex from the Kuskanax Batholith and define the western limit of the Kootenay arc (Parrish and Wheeler, 1983).

The first Geomagnetic Depth Sounding (GDS) surveys conducted in the Cordillera detected, at depth, a fundamental change between the cratonic rocks of ancestral North

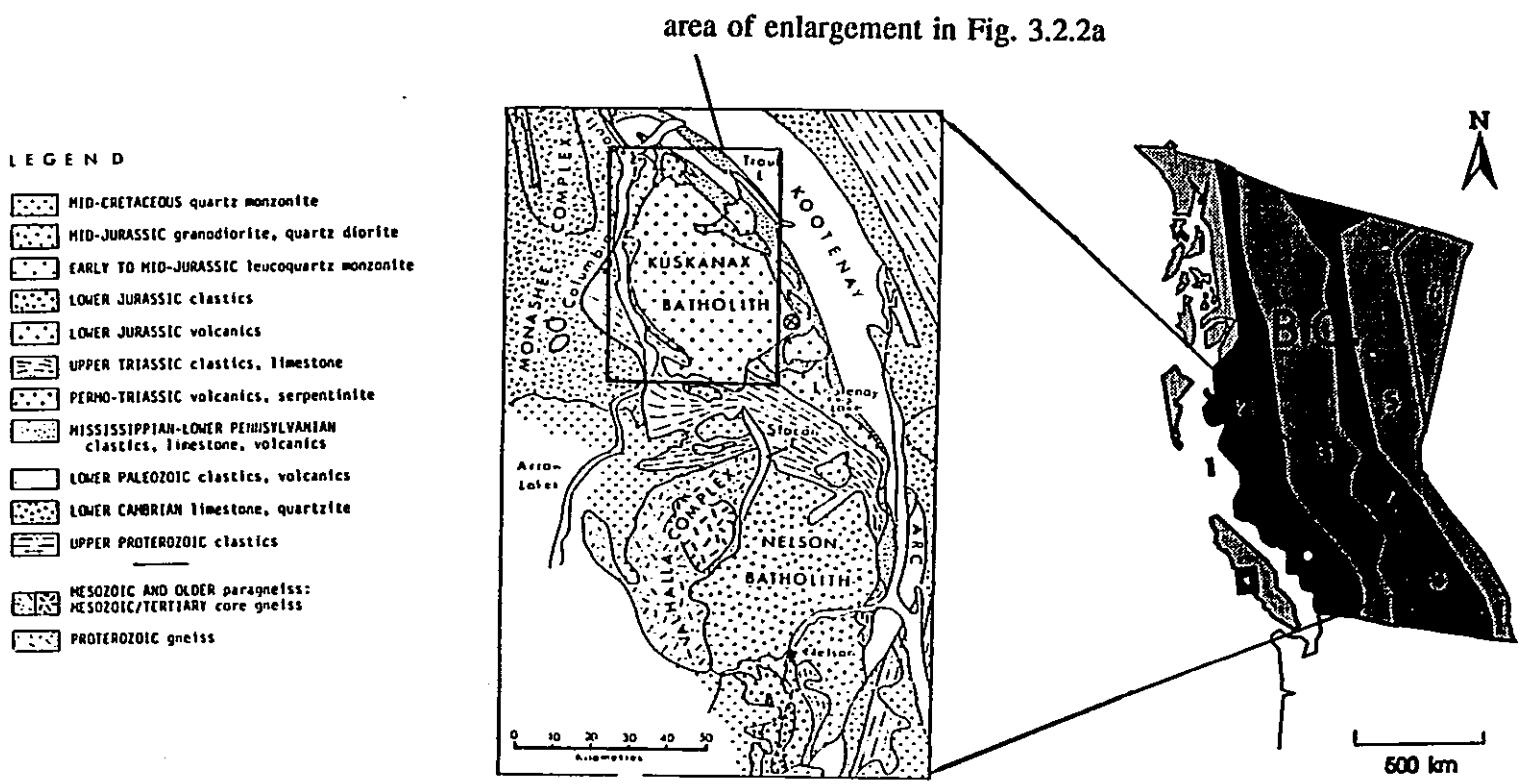

Fig. 3.2.1a Location and Geological Setting (after Parrish and Wheeler, 1983)

America and the accreted terrains to the west (Hyndman, 1963). The delineation follows the Rocky Mountain Trench southward through the northern Cordillera, then veers westward and follows the Columbia River and the CRFZ passing directly through the study area before veering east between the Kuskanax and Nelson Batholiths along the Slocan Lake Fault prior to rejoining the Rocky Mountain Trench (RMT) (Lajoie and Caner, 1970). This discrepancy may be of some importance when considering the potential for upward migration of deep-seated volatiles through the CRFZ (Section 3.6).The Slocan Lake Fault is a deeply-penetrating regional suture which dips northerly at < 25° beneath the Kuskanax Batholith and further east connects with the RMT (pers. comm. R.L. Brown). The CRFZ has a pronounced flexure adjacent to the Kuskanax, due possibly to emplacement of the pluton. This synformal feature in the eastward-dipping CRFZ, directly beneath Halcyon Hotspring may serve to "funnel" any mantle-derived volatiles migrating upward from the SLF or the RMT.

The Kuskanax Batholith, which intrudes the late Paleozoic-Triassic rocks of the Kootenay Arc (Read and Wheeler, 1976) and transects the structural trend of the region, is one of the oldest plutons in the southeastern Cordillera (Read, 1973). It most likely intruded the Kootenay arc prior to second-phase metamorphism (Parrish and Wheeler, 1983) and is an alkaline to peralkaline homogeneous quartz-monzonite body which outcrops over an area of approximately 1200 km^2. An intermittent band of metasediments and metavolcanics, some of which have reached the amphibolite stage of metamorphism define the perimeter of the batholith (Read and Wheeler, 1976).

3.2.2 Rock Types

The oldest outcrop in the immediate map area belongs to the Milford Group. These Misssissippian to Permian age rocks unconformably overlie the Paleozoic Lardeau Group in other regions adjacent to the Kuskanax Batholith; the unconformity commonly faulted (Read and Wheeler, 1976). Paragneiss and biotite schist of the Milford Group outcrop at Halcyon hotsprings in a narrow band of < 100 m width along with other Milford Group rocks mapped by Read et al. (1973) in close proximity to the discharge site (Fig. 3.2.2). A rock sample from the discharge vent, taken during the present study, consisted of > 95% quartz, and is assumed to be Milford metasandstone.

The Kaslo Group consists of amphibolites which fringe the Kuskanax Batholith and also occur on the west side of Upper Arrow Lake in the Thor-Odin gneiss complex (Reesor and Moore 1971). In other areas of the region the group occurs as lower-grade greenschist facies (Read and Wheeler, 1976).

Bottom breccia and conglomerate (Trscg) units of the Slocan Group unconformably overlie the Kaslo Group and grade into limestone and argillite (Trsc) , then phyllite and fine-grained quartzite (Trsp). The Slocan Group pelitic rocks are overlain by approximately 1200 m of volcanics which include meta-dacite and meta-andesite flows. South of the map-area, separating the Kuskanax and Nelson Batholiths, is a 15 km wide band of Slocan Group rocks which continues northwesterly through the Nakusp area to the west side of Upper Arrow Lake area and then terminates at the Columbia River Fault. Metamorphosed Slocan Group rocks "wrap-around" the batholith exterior to and, in the

Fig.3.2.2 Geology, Selkirk Range Hotsprings

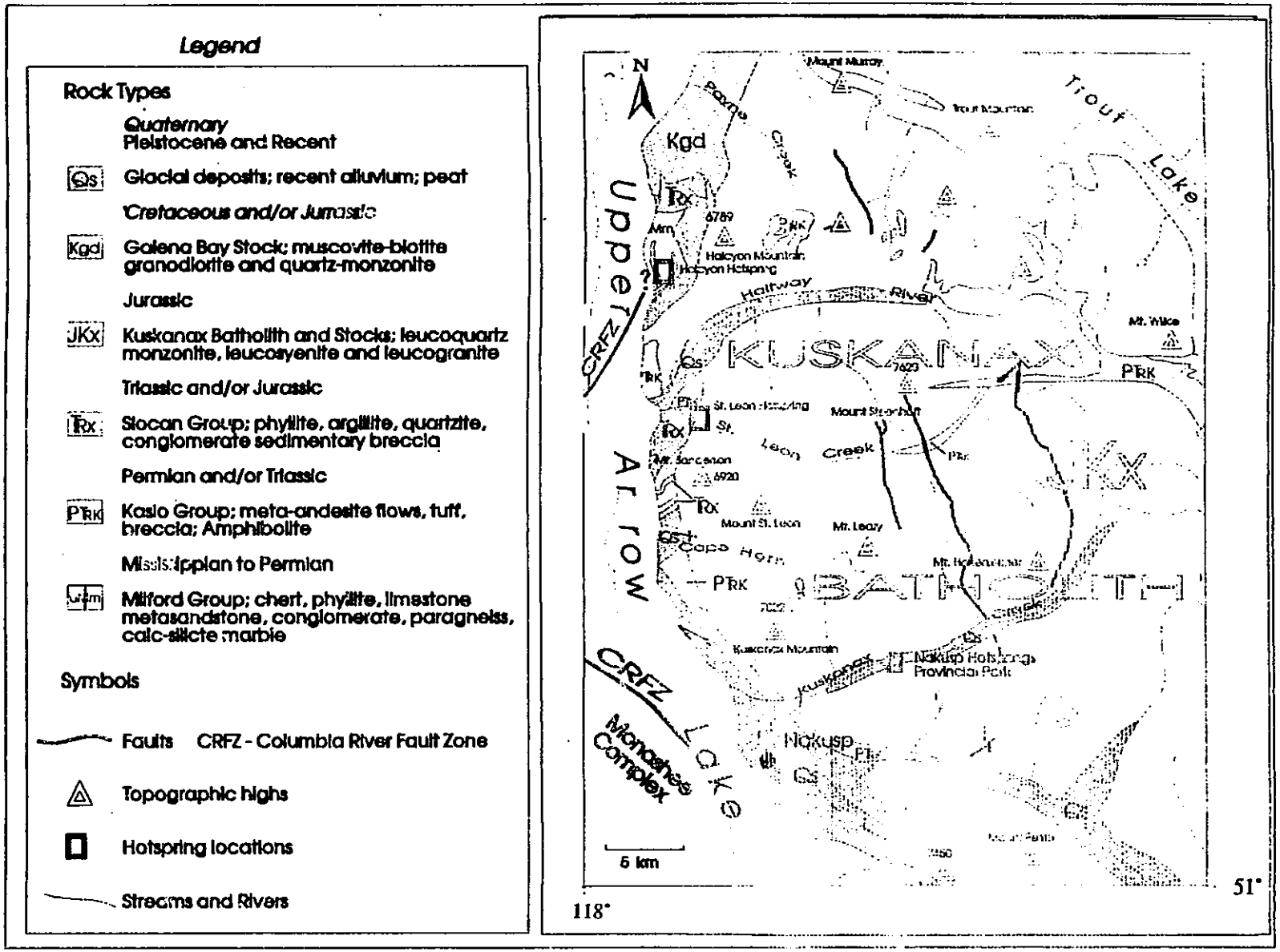

St. Leon hotspring area, interfingered with the Kaslo Group as shown on Fig 3.2.2 (see also regional map, Fig. 3.2.1a).

The outcrop of the 1200 km^2 Kuskanax Batholith is very homogeneous and can be characterized as a leucocratic, aegirine-augite-bearing quartz-monzonite body, predominantly alkaline to peralkaline (Parrish and Wheeler, 1983). Albite and microcline phenocrysts, with coatings of the same two minerals, make up the bulk of the mineralogy. At the margins of the batholith aegirine-augite and alkali amphiboles define lineations and foliations parallel to the fold axes of the intruded Slocan, Kaslo, and Milford Groups (Read and Wheeler, 1976). K-Ar and U-Pb dating techniques both imply an age of 175 (+/- 5) Ma for the Kuskanax (Read and Wheeler, 1976; Parrish, 1983).

The Jurrassic to Cretaceous Galena Bay Stock forms a 1.5 km wide band at the north end of Upper Arrow Lake adjacent to the Kuskanax Batholith and has a similiar mineralogy to the Kuskanax, predominantly a quartz monzonite (or quartz diorite) rock but more lineated with biotite and muscovite present as the accompanying mafic minerals (Read and Wheeler, 1976). The age estimates for this stock vary considerably, from micaceous K-Ar based estimates of 66 - 90 Ma (Read and Wheeler, 1976) to 150 Ma estimated from a Rb-Sr-based whole rock isochron (R.L. Armstrong pers. comm. in Read and Brown, 1981). More significant than a precise age is the relative time of emplacement of the Galena Bay Stock with respect to regional structures such as the Columbia River Fault Zone. Regional maps of Read and Brown (1981) show the Galena Bay Stock intruding the CRFZ north of Halcyon with the fault reappearing in the

Columbia R. to the north of Upper Arrow Lake. The regional map of Parrish and Wheeler (Fig.3.2.1a) has the assumed fault to the west of the stock along the lakeshore.

Major Quaternary deposits in the area are found along the Halfway River and Kuskanax Creek, the latter hosting the Nakusp Hotsprings which discharge about 30 m above the level of the creek in an unsorted cobble and boulder deposit. The town of Nakusp itself is situated on a Quaternary deposit which covers approximately 16 km^2. One other major occurrence of drift occurs just north of Cape Horn Cr. adjacent to Upper Arrow Lake. Near the lake, vegetation and drift frequently obscure the geology and geological boundaries such as the Milford and Kaslo Group boundaries north of Halcyon Hotspring and the CRFZ delineaton near the Galena Bay Stock (Read and Brown, 1981).

3.2.3 Occurrence of Hotsprings

Despite the common regional setting of the Kuskanax Batholith, these three Selkirk Range hotsprings discharge in different fashions from different geologic settings. The Halcyon hotspring occurs on the east side of Upper Arrow Lake, approximately 1100 ft above the lakeshore on a steeply inclined, wooded slope. The 50.5° C sulpha-lithia waters flow from fissures in the host quartzite bedrock (Plate 3.1a). Two main vents discharge about 2.5 litres/sec (Elworthy, 1925) into the small, sandy-bottomed, bedrock basins. The main pool is about $1m^2$ and 0.5 m deep and releases gas bubbles from continually-changing locations in its sandy bottom. Two 2" PVC pipes siphon the thermal waters about 20 m downslope to the plastic-lined log bathing pools (Plate 3.1b) which overlook the spectacular vista comprising Upper Arrow Lake and the Monashee

Mountains to the west. The hotspring locale is permeated with the smell of hydrogen sulphide gas. No travertine is deposited but rich algal growths clog the small streams which flow freely downslope from the springs across the rough access road.

In contrast, the three Nakusp hotspring vents discharge from an unsorted boulder and cobble Quaternary deposit, in a subhorizontal terrace adjacent to Kuskanax Creek (plate3.2b). Square cement engineered tanks funnel the 57.7° C waters into an aqueduct system which parallels and then crosses the Kuskanax Creek strapped to the underside of the foot-bridge which leads back along the north side of the creek to the indoor municipally-operated swimming pool. No gas discharge is evident at any of the vents.

The St. Leon hotspring, like Halcyon, is set in a bedrock location, however its 2 litre/sec flow at 48.3° C is free of sulphide and is precipitating calcite. The two discharge vents are about 10 m apart, the lower one depositing travertine in a 3 m wide cave-like enclosure (Plate 3.2a). The other vent discharges about 2 m higher up the forest slope into a 2x3 m bedrock-enclosed basin from which a plastic pipe leads into a rough in-ground, stone and cement pool. The flow includes periodic, small gas bubbles which percolate slowly upwards clinging to the wall of the the upper pool. The nearby St. Leon Creek, just downslope from the hotspring, is not visible due to the thick softwood forest cover which also keeps the site in perpetual shadow.

Plate 3.2a (top) St. Leon hotspring discharge in fractured quartzite

Plate 3.2b (left) Naskup hotspring discharging 57.7° C sodium sulphate waters from Quaternary boulder boulder and cobble deposit

3.3 Aqueous Geochemistry

3.3.1 Introduction

References in the literature to Nakusp and Halcyon hotsprings date back to 1888 and 1898, respectively. The earliest recorded quantitative geochemical analyses are reported by Elworthy (1925) who refers to the following qualitative analysis of Nakusp by F.G. Wait (1888).

> A qualitative analysis showed it to contain :
>
> Potassa.....trace.
> Soda.....very small quantity.
> Lime .....very small quantity.
> Magnesia.....very trifling quantity.
> Sulphuric acid.....small quantity.
> Carbonic acid.....trace.
> Chlorine.....very small quantity.
> Silica.....trace.
> Organic matter.....trace.
>
> Boiling produced a scarcely perceptible precipitate.

Table 3.3.1a Early "qualitative analysis" of Nakusp hotspring (from F.G. Wait, 1888)

Unfortunately the difference between trace and small, or trifling and very trifling was not defined! However, these historical references may be of use for qualitative comparison with more recent analyses.

A description of Halcyon by Sir George Dawson (1898) included no specific geochemical breakdown but did mention the presence of hydrogen sulphide, a lack of carbonate in the waters, as well as an appreciable gas discharge and alteration of host-rock feldspar to kaolin at the discharge vent. No mention was made of St. Leon hotspring

by any of these authors. Elworthy (1925) refers to the sulpha-lithia waters of Halcyon and their reputed therapeutic value, and compares chemical analyses from that year with those of the Inland Revenue Laboratory from 1917. Those analytical results, as well as those reported by Souther and Halstead (1973), are shown in Table 3.3.1b along with analyses from this study.

The hotsprings of this study were chosen as alternative sites to the string of Coast Plutonic Belt hotsprings south of Mt.Meager which were to be sampled during the first week of September 1, 1991. A landslide at that time forced road closure of all access highways in the Pemberton area. The Selkirk Range springs were then chosen as alternative sites and sampled on September 5 and 6. All techniques of sampling and analysis are as previously described for the west coast Vancouver Island hotsprings.

3.3.2 Ionic Constituents

The three Selkirk Range hotsprings appear to have a common geochemistry and can be characterized as sodium, calcium-sulphate waters with alkaline pH values. Table 3.3.2 shows the ionic constituents, first in weight fractions (ppm) and then as milli-equivalents per litre. Cationic-anionic mass balance calculations are shown in Table 3.3.2c. All waters are below or near the 5% mark with respect to balancing, within the range of acceptable analytical error.

The dominance of the sulphate anion over bicarbonate is most readily evidenced if milli-equivalents/litre are examined. Sulphate ion concentrations are, for all three springs,

Table 3.3.1 b

Halcyon Hotspring Geochemical Analyses 1917 - 1991

Year	*1917*	*1923*	*1975*	*1991*
Author	*McGill*	*Elworthy*	*Souther and Halstead*	*This study*
Temperature °C	nr	50.8	~ 51	50.3
pH	n.r.	n.r.	nr	8.71
Dissolved constituents (ppm)				
Na	5.71?	161	161	179
Ca	84	57	57	60
K	nr	8.1	nr	7.9
Mg	nr	trace	nr	0.66
Cl	8.14	9	nr	6.3
HCO3-	nr	48	48	49
SO4--	433	363	433	435
SiO2	nr	71.3	nr	37.1
TDS	nr	718	788	775

n.r. - not reported

Table 3.3.2a — ***Selkirk Range Hotsprings***

Aqueous Geochemistry

Anions (ppm)

	Temp	pH	Eh	NO3ppb	F-	Cl-	Br-	SO4--	HCO3-	CO3 --
% error					+/- 5%	+/- 5%	+/- 5%	+/- 5%	+/- 5%	
							ppb			
Halcyon	50.50	8.00	-0.185	b.d.	7.77	6.03	50.00	435.00	48.80	na
St.Leon	48.30	8.55	-0.181	b.d.	5.69	2.26	50.00	535.00	15.86	na
Nakusp	57.70	8.15	-0.212	b.d.	2.32	2.34	50.00	300.00	30.98	na

* - below detection

Cations ppm

	Ca++	Mg++	Fe++	Ba++	Sr++	K+	Na+	Li+	Al+++	B+++	SiO2
% error	+/- 5%	+/- 5%	+/- 5%	+/- 5%	+/- 5%	+/- 5%	+/- 5%	+/- 5%	+/- 5%	+/- 5%	+/- 5%
Halcyon	60.41	0.66	0.01	0.01	2.63	7.9	179	0.60	0.02	0.17	37.10
St.Leon	157.81	0.13	0.04	0.02	5.72	7.1	131	0.23	0.02	0.05	34.30
Nakusp	68.71	0.34	0.02	0.04	5.34	5.7	95	0.06	0.02	0.07	34.10

Table 3.3.2b — ***Anions (meq/l**)***

	Temp	pH	Eh	NO3ppb	F-	Cl-	Br-	SO4--	HCO3-	CO3 --	meq sum
Halcyon	50.50	8.00	-358.20	b.d.	0.41	0.17	0.001	9.06	0.80	na	10.44
St.Leon	48.30	8.55	-355.00	b.d.	0.30	0.06	0.001	11.14	0.52	na	12.02
Nakusp	57.70	8.15	-377.00	b.d.	0.12	0.07	0.001	6.25	0.51	na	6.94

**milliequivilants/litre

Cations (meq/l)

	Ca++	Mg++	Fe++	Ba++	Sr++	K+	Na+	Li+	Al+++	B+++	meq sum
Halcyon	3.01	0.05	0.0004	0.0001	0.0599	0.202	7.79	0.086	0.002	0.047	11.25
St.Leon	7.87	0.01	0.0013	0.0003	0.1305	0.182	5.70	0.033	0.002	0.014	13.95
Nakusp	3.43	0.03	0.0007	0.0006	0.1218	0.146	4.13	0.009	0.002	0.019	7.88

Table 3.3.1c — ***Cation anion mass balances***

((cations -anions)/(cations + anions))

				% difference
Halcyon	(8.32 -7.74)/(8.32+7.74)	→	0.0377	3.77%
St.Leon	similarly	→	0.0741	7.41%
Nakusp	" "	→	0.0635	6.35%

at least an order of magnitude higher than the bicarbonate concentrations, a clear reflection of the lack of carbonate terrain in the area. The sulphate concentration is highest in the St. Leon hotspring, the only spring where no sulphide was detected. Sulphur species and sulphur isotopes are discussed in Section 3.4.3.

For cations, the sodium ion is dominant at both Nakusp and Halcyon whereas at St. Leon calcium is slightly higher. The only other major cation of appreciable concentration is potassium, a reflection perhaps, of the alkaline mineralogical homogeneity of the Kuskanax Batholith. The higher calcium content at St. Leon is consistent with its higher sulphate concentration if these ions are attributable to dissolution of marine sulphates. Although no evaporites have been mapped in the area, it is possible that marine sulphates may occur in the minor limestone units which have been mapped regionally by Read et al. (1976). Such sources of gypsum could also have been glacially-transported, and deposited as part of the Quaternary deposits of the St. Leon and Nakusp areas. Regardless of the precise source of calcium and sulphate, the very low bicarbonate and high sulphate and calcium contents of St. Leon suggest a common ion effect involving calcium. This effect can lead to calcite saturation and precipitation, and a subsequent lowering of bicarbonate concentrations (Freeze and Cherry, 1979). Unfortunately, a sample of the mineral precipitating out of solution at the St. Leon vent was lost during airline transport from Vancouver, along with the ^{14}C sample for the hotspring. Mineral solubility data show saturation with respect to a number of species, notably the quartz

polymorphs, smectite-clays and kaolinite. St. Leon is the only hotspring at saturation with respect to calcite, supportive of the common ion effect and the scenario of calcite precipitation discussed above.

Table 3.3.2d *Mineral Solubility*

	Halcyon	St. Leon	Nakusp
Temperature °C	50.5	47.3	57.7
Mineral			
Calcite	-0.684	0.103	-0.211
Aragonite	-0.804	-0.018	-0.330
Dolomite	-1.773	-1.343	-1.076
Ca- Smectite	2.884	2.021	1.902
K- Smectite	2.300	1.364	1.215
Mg- Smectite	2.719	1.667	1.702
Na- Smectite	2.621	1.652	1.511
Talc	0.188	0.502	0.232
Kaolinite	3.283	2.415	2.439
Quartz	0.480	0.453	0.352
Chalcedony	0.230	0.204	0.097
Cristobalite (alpha)	0.121	0.091	-0.002
Anhydrite	-1.195	-0.786	-1.143
Gypsum	-1.107	-0.683	-1.106
Wairakite	-0.501	-0.217	0.872

** solubility is expressed as Log IAP/KT where IAP= ion activity product, KT=mineral solubility product*
Positive values indicate oversaturation; negatives indicate undersaturation
Values determined for hotspring discharge temperatures by Solmineq geothermal modelling software (Kharaka, 1988)

3.3.3 *Gas and dissolved gas*

Table 3.3.3a shows gas analyses for the Selkirk Range hotsprings. No visible gas discharge occurs at Nakusp so only dissolved gas was collected.

Table 3.3.3a ***Gas and Dissolved Gas*** ***(% volume @STP)***

Hotspring	Nitrogen	CO_2	Oxygen	CH_4	Helium
Halcyon (gas/diss. gas)	97.3	n.d*	2.49	trace	0.21
St. Leon (gas)	91.7	n.d	8.24	n.d	0.06
Nakusp (diss. gas)	84.0	n.d	16.0	n.d	0.02

* n.d. - not detected

The 8 % and 16 % by volume oxygen content, of St.Leon and Nakusp respectively, is interesting in that both of these hotsprings occur in, or adjacent to, coarse surficial Quaternary deposits. The oxygen volume approaching atmospheric concentration at Nakusp likely reflects open-system conditions (and/or mixing with meteoric waters) at some point prior to discharge in the boulder and cobble deposit which hosts the three main hotspring vents. Such conditions would also allow any methane, which may have been present in the Nakusp thermal waters, to degas prior to discharge. This assumption is supported by the helium gas content at Nakusp which is an order of magnitude lower than the content at Halcyon hotspring despite identical isotopic ratios (see Table 4.2.2a). St. Leon oxygen and helium gas concentration values are intermediate compared to the other two hotsprings.

3.3.4 Eh and Redox Conditions

Table 3.3.4.a shows the measured field Eh, and the value calculated from the sulphate-sulphide redox pair. The values for Nakusp and Halcyon are quite close, suggestive of redox conditions dominated by these two sulphur species. No sulphide was detected at the St. Leon hotspring.

Table 3.3.4a ***Eh Calculaton using the Sulphide - Sulphate Redox Pair***

To calculate Eh from the HS- - SO4-- redox couplet, the following equation can oe used:

Eh = E0 + 0.059/8 log((aSO4--(a9H+))/ aHS-); @25°C, E0=.3V

Chemical Activity and Eh

	HS-	SO4--	H+	log calc'n	Calc Eh (volts)	Field Eh (volts)
Halcyon	0.0005	0.002375	1E-08	-71.3232	-0.226	-0.185
St. Leon	na	0.002573	2.8E-09	na	na	-0.181
Nakusp	0.000107	0.001745	7.08E-09	-72.1353	-0.232	-0.212

The presence of 8% and 16% oxygen in gas and dissolved gas at St. Leon and Nakusp hotsprings (Table 3.3.3a) appears to be in contradiction with these reducing conditions. It is interesting that St. Leon has only half the oxygen of Nakusp coincident with about twice the bicarbonate and a complete lack of sulphide. The small amounts of O_2 gas present at these two springs would be oxidizing any sulphide present. The oxygenated waters of Nakusp have only a very small fraction of sulphide present, possibly the remnant of a larger preoxidized portion. The lower-temperature, higher Eh, sulphide-free St.Leon waters have a higher sulphate concentration (Table 3.3.2a). This matter is discussed further in the section on sulphur and carbon isotopes (Section 3.4.3).

3.4 Isotope Hydrogeology

3.4.1 Introduction

For this section on the Selkirk Range hotsprings, the same format, isotopic techniques, and sampling procedures, are followed as for the west coast Vancouver Island hotsprings. For background information on isotope hydrogeology in geothermal areas see Section 2.4.1 or Fritz and Fontes, 1980).

3.4.2 ^{18}O - deuterium

As discussed in Section 2.4.2, cold runoff samples were collected for determination of a regression line to represent the local meteoric water-line (LMWL). Sample locations are shown in Fig.3.1.2a. While no information on a local meteoric water-line for the immediate area was located in the existing literature, the regression-line plot shown in Fig 3.4.2a coincides well with the Global Meteoric Water Line (GMWL), and thus may be considered a reasonable approximation of a LMWL for the area.

The ^{18}O - deuterium plot shows good correlation between thermal waters and local run-off indicating local recharge for these hotsprings. At the same time, however, the thermal waters are distinct from the local runoff samples in that they are recharged at altitude and are not a blend of waters from different elevations. Additionally, all three springs have very similiar ^{18}O - D signatures suggesting a common recharge elevation or recharge area. No geothermal shift is evident, thus temperatures in excess of about 150°C are unlikely (Truesdell and Hulston, 1973).

Table 3.4.2a

	18O	D
Halcyon HS a	-18.85	-131.84
Halcyon HS b	-18.88	-141.00
H-1 (cold runoff 1	-17.35	-132.19
(H-2) St. Leon Cr.	-17.65	-134.40
H-3 (cold runoff 3	-17.59	-133.01
H-4 (cold runoff 4	-16.83	-122.90
Salmon Arm 1	-17.51	-134.00
Salmon Arm raln	-11.32	-82.00
N-1 Kuskanax Cr.	-17.86	-131.93
N-2 Raven Cr.	-17.60	-132.48
N-3 Gardner Cr.	-17.76	-132.77
N-4 Kuskanax Mtr	-17.93	-135.69
Nakusp H.S.	-18.68	-142.86
St Leon H.S.	-19.07	-141.01

Regression Statistics for Selkirk Series

Multiple R	*0.993573*
R Square	*0.987188*
Adjusted RSq	*0.985586*
Std. Error	*1.948877*
Observations	*10*

Analysis of Variance

	df	*Sum of Sqs*	*Mean Sq*	*F*	*Signif. F*
Regression	*1*	*2341.198*	*2341*	*616.40971*	*7.406E-09*
Residual	*8*	*30.38496*	*3.798*		
Total	*9*	*2371.583*			

	Coefficients	*Std Error*	*t Statistic*	*P-value*	*Lower 95%*	*Upper 95%*
Intercept	*9.5664*	*5.54049*	*1.726639*	*0.118*	*-3.209977*	*22.342825*
x1	*8.0699*	*0.32504*	*24.8276*	*1E-09*	*7.3203253*	*8.8193942*

Fig.3.4.2a

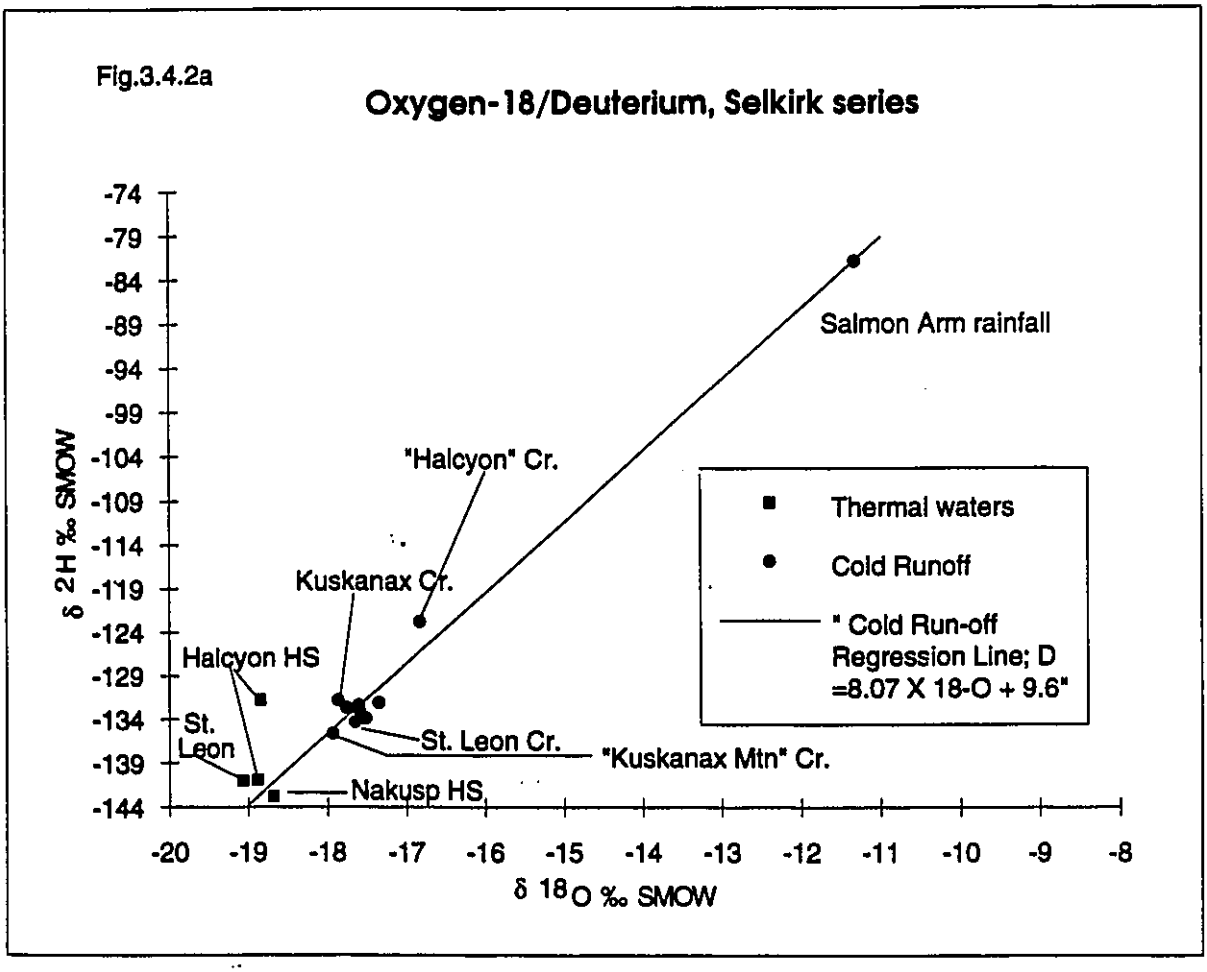

Table 3.4.2a O-18 - deuterium regression line for Selkirk hotsprings and cold run-off waters.

The bulk of the run-off samples in Fig 3.4.2a are clustered together between -17 and -18 ‰ and represent run-off waters from large catchment areas at a variety of altitudes. However, unlike the large volume run-off flow in Kuskanax Cr., St. Leon Cr. and the other run-off samples, the Halcyon Creek sample defines run-off from a small local creek adjacent to Halcyon hotsprings with headwaters at 1220 m elevation. For the three hotsprings, comparision to the Halcyon Cr. sample reveals an ^{18}O depletion of about 2 ‰ . Using the same altitude effect for ^{18}O as that described in Section 2.3.4, about -2.5 ‰ per kilometre:

-2.0/-2.5 ‰/1000 m = 800 metres (2625 ft.)

This calculation is based on one high $\delta\ ^{18}O$ end member and does not take into account seasonal variation. As this sample dwas collected in September (and is therefore less depleted) the calculated recharge elevation dwould be a maximum. Thus, the recharge elevation would be near 1220 + 800 m = ~2020 m (6600 ft.). Highland areas near these elevations occur both locally, near to each of these hotsprings, and toward the centre of the Kuskanax Batholith. For Halcyon hotspring, the Halcyon Mountain catchment area is in this range, its peak elevation ~2070 m (6789 ft; see Fig. 3.1 or Fig. 3.2.2).

The St. Leon hotspring waters are slightly more depleted than Halcyon hotspring ($\delta\ ^{18}O$ ‰ values of -19.07 and -18.85, respectively) perhaps indicative of a slightly higher recharge elevation. This scenario is consistent with peak elevations of ~2110 m (6920 ft.) near Mount Sanderson ~ 3km south of the hotspring. The Nakusp waters ^{18}O

values are slightly lower, but in the same range as the other two hotsprings. Potential recharge sites near ~ 1980 m (6500 ft.) can be found just south of Nakusp hotsprings.

Gat (1980) outlines how ^{18}O depletion due to altitude effects can vary from -1.5 to -5.0 ‰ per kilometre rise in elevation. If the altitude effect in Selkirk Range exceeded the -2.5 ‰/km depletion described for Mt. Meager (Clark et.al 1980) then recharge elevations could be higher than 1980 m (6500 ft).

Thus other highland areas, particularly those which include major faults, may be considered as potential recharge sites for these geothermal waters. One such area at ~7000 ft. is located about 13 km ENE of Halcyon, and another occurs in the region of Mount Steenhoff near the centre of the Kuskanax Batholith (Fig. 3.2.2). The former site may be the recharge area for Halcyon Hotspring. The latter area includes a 20 km long N-S aligned fault which commences just south of Mount Steenhoff and is overlain by the Kuskanax Cr. Quaternary deposit which hosts the Nakusp Hotspring. The same fault cross-cuts Kaslo Group rocks which also outcrop in close proximity to the St. Leon and Halcyon hotsprings. These potential recharge locations are consistent not only with the ^{18}O-D data, but also with the scenario of deeply circulating geothermal waters reflecting the alkaline rock geochemistry of the Kuskanax Batholith (Section 3.2.2). Additionally, these major faults may be connected with the Slocan Lake Fault and Columbia River Fault Zone (pers. comm. R.L. Brown) both of which undercut the batholith and could provide upward migration pathways for deep-seated volatile gases (see Section 3.2. and Section He).

3.4.3 *Sulphur Isotopes*

Sulphur is the dominant constituent in the thermal waters from all three Selkirk Range hotsprings, present both as sulphate and sulphide at Halcyon and Nakusp, and as sulphate at the St. Leon hotspring (Table 3.3.2b). Table 3.4.3a shows the isotopic and molar distributions of sulphur species for Halcyon, St. Leon and Nakusp. When sulphide and sulphate fractions are combined (for procedural details see Section 3.4.3) the ^{34}S isotopic signature of the weighted average is virtually the same for both Halcyon and Nakusp, +8.24 ‰ CDT and +8.46 ‰ CDT, respectively (see also Fig. 3.4.3a). Additionally, the ^{34}S value of +9.41 ‰ CDT for St. Leon sulphate is close to the weighted average of the other two hotsprings[1].

Table 3.4.3a* ***Sulphur Isotopes ****

	SULPHIDE (Calculated from Cd-acetate ppt.)					SULPHATE (Calculated from BaCl2 ppt.)			
	mg/l CdS (diss.HS-)	S mg/l	mg/l HS-	HS- mmols/l	delta S-34 sulphide	delta S-34 sulphate	mg/l BaSO4	mg/l SO4--	mmols SO4--
Halcyon	89	19.7	20.3	0.61	-12.43	11.06	1050	433	4.5
St.Leon	nd**	nd	nd	nd	nd	9.41	> 1500	nd	nd
Nakusp	18	4.0	4.1	0.12	-3.42	9.04	596	246	2.6

	Weighted delta S-34 (both HS-& SO4--)	mg/l SO4 if all HS- oxidizes	mg/l SO4 from BaSO4	Potential Total Sulphate	Analyzed mg/l SO4 Dionex
Halcyon	+ 8.24	60.7	432.6	493.3	435
St.Leon	+ 9.41	na	~ 600	na	535
Nakusp	+ 8.46	12.3	245.6	257.8	300

** - all Sulphur-34 figures as delta permil CDT values nd** - not detected na*** - not applicable*

[1] - Cadmium carbonate impurities, detected in the two sulphide samples, were not measured quantitatively, however their presence would increase the weight of sulphide. Thus the weighted average is quite possibly closer to +9.

These similarities are supportive of a common source of sulphur for all three Selkirk Range hotsprings. Isotopic signatures of various sources of sulphur were given in Fig. 2.4.3a. The ^{34}S values near δ +9.41 ‰ CDT fall within the range of limestones, present in the study area in the Milford Group, Kaslo Group, and Triassic-age Slocan group rocks. The lack of sulphide at St. Leon is interesting in that its waters have even less bicarbonate than the other two springs, only ~15 mg/l. Presumably, consumption of organics required for sulphate reduction, and the coincident incorporation of DIC related to organics, did not occur at St. Leon. ^{13}C isotopes support this and are discussed in the following section.

Fig. 3.4.3a

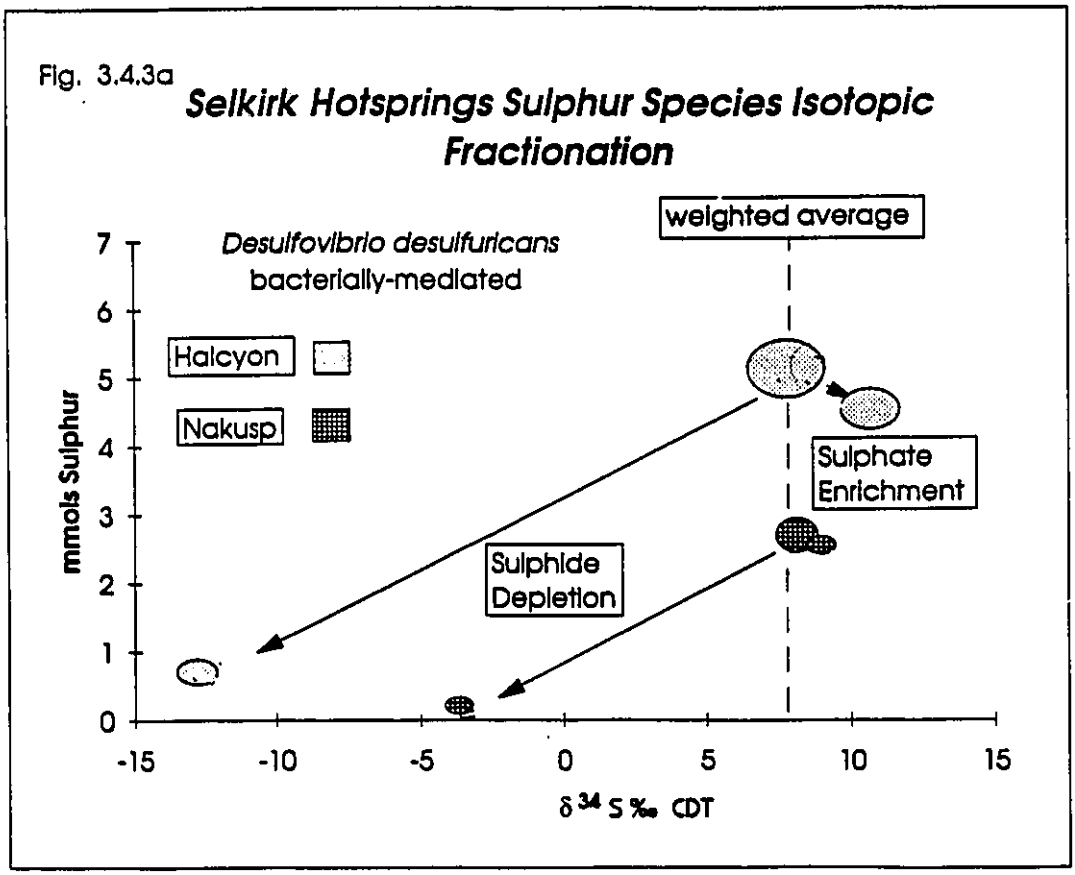

3.4.4 Tritium and Carbon Isotopes

As described in Section 2.4.4, tritium and carbon isotopes can be useful to characterize mean residence times of thermal waters. Table 3.4.4a shows the ^{13}C, ^{14}C and tritium isotope data for the Selkirk suite. For Nakusp the data are interesting in that they point to mixing of a thermal component with modern tritiated non-thermal waters and have "future" ages for ^{14}C, that is, >100 pmc. Halcyon hotspring ^{14}C data do not imply future ages but, like Nakusp, may be affected by introduction of DIC related to sulphate reduction. No ^{14}C data are available for the St. Leon hotspring due to loss of the ^{14}C sample during transport.

Selkirk Range Hotsprings Mean Residence Time Estimates

Table 3.4.4a ***Direct Application and Modified Pearson Correction***

Hotspring	*HCO3- (mg/l)*	*d13C‰ (PDB)*		*C-14 (pmc)*		*Direct Applic t=-8267 ln(pmc)*	*"q" factor**	*Modified Pearson "Age" -8267ln(pmc)q*	*Tritium (T.U.)*
Halcyon	48.80	-17.92	+/- 0.1	85.96	+/-.87	1251	0.9	1126	1.1 +/- 0.3
St.Leon	15.86	-10.34	+/- 0.1	nd	na	na	na	na	1.0 +/- 0.3
Nakusp	30.98	-20.67	+/- 0.1	108.99	+/-0.63	na	na	na	3.2 +/- 0.4

* In crystalline terrain q= ~ 0.9 - 1.0

Table 3.4.4b ***Correction for Reduced Sulphate***

Hotspring	*HCO3- mmols*	*d13C‰ (PDB)*		*C-14 (pmc)*		*"Desulfovibrio desulfuricans Sulphide" Corrected "pmc"*	*Sulphide Corrected "Age"*
Halcyon	0.80	-17.92	+/- 0.1	85.96	+/-.87	na	*na*
St.Leon	0.26	-10.34	+/- 0.1	nd	na	na	*na*
Nakusp	0.51	-20.67	+/- 0.1	108.99	+/-0.63	0.9922	65

For Halcyon, (2 x 0.61) mmols HS- neccessitates subtraction of more HCO3 than is present in the discharging waters
For Nakusp 0.12 mmols HS- produced from sulphate reduction, so 0.24 mmols of "future" C-14 are introduced (Section 3.4.4 in text).
To correct for this, (120 pmc x .24 mmols) was subtracted from (109 x .51 mmols). This then used as the numerator
and placed over the denominator of (0.51 - 0.24 mmols) to give corrected amount pmc. Thus pmc = 99.22

The ^{13}C data, which must be used in conjunction with the radiocarbon data for dating purposes (see Section 2.4.4) are different for all three springs and may be useful as an indicator of modification processes. Consider firstly the Halcyon hotspring data. A direct age-application of the ^{14}C data may be valid as the $\delta\ ^{13}C$ value near -18 ‰ PDB is close to a soil zone signature. Direct utilizaton of the decay equation yields a ^{14}C mean residence time of about 1250 years. Application of the Modified Pearson Age formula (Table 3.4.4a) (using a "q" factor for crystalline rocks of ~ 0.9) gives a corrected mean residence time near eleven hundred years.

The very low bicarbonate concentration at St. Leon is consistent with its ^{13}C signature and the complete lack of sulphide there. For, without incorporation of depleted organics into the DIC, the $\delta\ ^{13}C$ signature of -10.34 ‰ CDT may be more a reflection of water-rock interaction with, for example, minor limestone units present in the study area as mentioned in Section 3.4.3. It is noteworthy that the very low concentrations of bicarbonate, particularly for the St. Leon and Nakusp springs, can make for substantial modification of a pre-existing carbon isotope signature.

Such appears to be the case for the thermal waters of the Nakusp hotspring, where the following aqueous geochemical components are found:

1) 3 T.U. and 109 pmc

2) 0.21 mmols sulphide

3) -20.67 ‰ CDT value for ^{13}C

The 3 T.U. concentration is indicative of dilution of the Nakusp thermal component by a "modern" component (i.e. post-1950's recharged waters). The 109 pmc can be explained by a combination of modification processes including the addition of the diluting modern waters (which would also have >100 pmc). Additional potential input sources are from organics introduced via sulphate reduction, and incorporation of soil zone DOC from the Quaternary formation where the Nakusp hotspring discharges. The effect on the pmc due to sulphate reduction with modern carbon is shown in Table 3.4.4b.

As mentioned above, the low bicarbonate concentration in the Nakusp waters (~30 mg/l HCO_3^- final concentration) could facilitate major modification of a pre-existing geothermal ^{14}C component through addition of any soil zone modern carbon. Supportive of this is the ^{13}C signature of Nakusp (-20.7 ‰PDB) which is depleted compared to both Halcyon and St. Leon (-17.9 and -10.3 ‰ PDB respectively). The -20.67 ‰ PDB value is approaching the range of soil zone signatures which also have ^{14}C values in excess of 100 pmc and up to 120 pmc (see Section 2.4.4 or Gat, 1980). Thus, incorporation of soil zone carbon by diluting non-thermal waters may be lowering the ^{13}C signature of the Nakusp hotspring while simultaneously raising its ^{14}C pmc. Interestingly, the analysis reported by F.G. Wait (1888) (Fig 3.3.1a) included a trace amount of organic matter. While no unique solution exists for the derivation of a mixed water with 109 pmc at Nakusp, the above cited modifications could raise ^{14}C to the 109 pmc recorded in the sample.

3.5 *Geothermometry, Heat Flow and Depth of Circulation*

3.5.1 *Introduction*

The same geochemical, isotopic and geothermometric techniques employed for the hotsprings at Hotsprings Cove and Ahouset are generally applicable for the Selkirk suite largely as a result of similarities in these two terrains dominated by silicate rock. The presence of slightly higher concentrations of calcium in the Selkirk Range hotsprings facilites use of the Ca-Na-K geothermometer, although these estimates show little variance from the Na-K geothermometer estimates. The lithium geothermometer is also applied and provides estimates very similiar to the Na-Li geothermometer. The high levels of Li+ in the waters of Halcyon hotspring were part of the reason for its development as a health spa earlier this century (Elworthy,1925).

3.5.2 *Silica Geothermometers*

The homogeneity of the Kuskanax Batholith and the possibility of similiar characteristics of flow history for the three hotsprings is reflected in the consistency of their silica concentrations. Quartz and chalcedony geothermometer estimates shown in Table 3.5.2a. are in the 120° C and 95° C range, respectively.

Table 3.5.2a ***Silica Geothermometer Temperature Estimates (°C)***

	SiO2 (ppm)	Quartz*	Chalcedony**	Cristobalite***	Opal****
Halcyon	80.0	125	97	74	29
St.Leon	73.9	121	93	70	27
Nakusp	73.5	121	92	70	27

*T (°C) =(1309/(5.19-Log(ppm Silica)) } - 273.15 *(All formulae from Fournier,1981)*
**T (°C) =(1032/(4.69-Log(ppm Silica)) } - 273.15
***T (°C) =(1000/(4.78-Log(ppm Silica)) } - 273.15
****T (°C) =(731/(4.52-Log(ppm Silica)) } - 273.15

3.5.3 *Sodium-lithium and Lithium geothermometers*

Table 3.5.3a reveals the Na-Li-based geothermometer estimates for the Selkirk Range hotsprings. As mentioned above, the Li-based geothermometer (Fouillac and Michard, 1981) can also be used to estimate maxmum reservoir equilibrium temperatures. These calculations are included at the bottom of the table.

Table 3.5.3a ***Na-Li Geothermometer*** (after Fouillac and Michard, 1981)

Log (Na/Li)=1000T-0.38 (where Cl concentration < 0.3M; brackets denote molarity)

	Na (ppm)	mmolsNa	Li (ppm)	mmolsLi	log (na/li)	°K	°C
Halcyon	179	7.786	0.60	0.086	1.955	428	155
St.Leon	95	4.128	0.06	0.009	2.651	330	57
Nakusp	131	5.698	0.23	0.033	2.237	382	109

Lithium Geothermometer (after Fouillac and Michard, 1981)

Log (Li)=(-2258/T) + 1.44 (where Cl concentration < 0.2M; brackets denote molarity)

	Li (ppm)	mmolsLi	molsLi	log (mols Li)	°K	°C
Halcyon	0.60	0.086	0.000086	-4.0633	410	137
St.Leon	0.06	0.009	0.000009	-5.0352	349	76
Nakusp	0.23	0.033	0.000033	-4.4816	381	108

3.5.4 Sulphate-water geothermometer

Considered to be one of the most reliable geothermometers, the sulphate-water geothermometer was discussed in some detail in Section 2.5.4 along with possible complicating factors. Three of these factors are mixing with non-thermal or meteoric waters, sulphate reduction, and the lengthy residence times required for geochemical and isotopic equilibration. While the Halcyon hotspring estimate is in the range of other geothermometers (Table 3.5.4a) the estimate for Nakusp is below its 57.7° C discharge temperature .

Table 3.5.4a ***Sulphate Water Geothermometer*** (after Mitzutani and Rafter, 1969)

1000 ln alpha (SO4 - H2O)= 3.251(1million/°K X°K)-5.1

Where alpha = d 18O (SO4)+ 1000/ d 18O (H2O)+1000

	delta O-18 water	delta O-18 sulphate	Alpha (@)	1000 ln@	1000 ln@ plus 5.1	3.251/ 1000 ln@+5.1	X 1million	°K= sqrt	°C
Halcyor	-18.85	0.23	1.019447	19.2599	24.359899	0.13345704	133457	365	92
St.Leon	-19.07	5.23	1.024772	24.47055	29.570549	0.10994047	109940	332	58
Nakusp	-18.68	6.85	1.026016	25.68332	30.78332	0.10560914	105609	325	52

Similarly, the St. Leon hotspring sulphate-water geothermometer estimate is low, < 10° C above its 48.3° C discharge temperature. Sulphate reduction is occurring at both Halcyon and Nakusp and may be lowering their respective sulphate-water geothermometry estimates as a result of the enrichment in $^{18}O_{sulphate}$ which occurs coincident with the bacterially-mediated production of the sulphide phase.

3.5.5 Na-K, Na-K-Ca, and Log(√Mg-Li) geothermometers

The homogeneity and alkaline geochemistry of the Kuskanax Batholith, reflected in the consistent molar dominance of sodium, potassium and calcium cations in the Selkirk Range thermal waters, underline the importance of the Na-K and Na-K-Ca geothermometer temperature estimates (Table 3.5.5a and b). Errors in Na-K-based estimates, due to dilution or mixing with cooler but more saline waters (Fournier, 1981) do not apply here. The Na-K-Ca geothermometer makes a substantial correction to the Na-K geothermometer at Halcyon where it decreases the estimated temperature of equilibrium for these cationic species from 156° C to 133° C.

Table 3.5.5a ***Selkirk Hotsprings Na-K Geothermometer Estimates***

°K=855.6/(log(Na/K)+0.8573)*

	K (ppm)	Na (ppm)	°K	°C
Halcyon	7.9	179.0	387	114
Nakusp	5.7	94.9	412	138
St.Leon	7.1	131.0	403	130

* - after Fournier,1981

The log √Mg/Li geothermometer considered to be more accurate than other techniques by its authors Karaka and Mariner, (1988). While the Halcyon and St. Leon estimates are above boiling, 120° C and 115° C respectively (Table 3.5.5b), the Nakusp hotspring estimate of 68° C is only slightly above the discharge temperature of 58° C. All geothermometer temperature estimates are shown below in Table 3.5.5b.

Table 3.5.5b

Summary
Selkirk Range Hotsprings
Geothermometry Maximum Temperature Estimates (°C)

		Geothermometer								
	Discharge Temp	Sulphate Water	Quartz	Chalc'dy	Log sqrt(Mg)/Li	Na-K	Na-K-Ca	Li	Na/Li	Mean
Halcyon	50.5	92	125	97	120	156	133	137	155	127
St. Leon	48.3	58	121	93	115	130	130	76	57	98
Nakusp	57.7	52	121	92	68	138	136	108	109	103

As in Section 2.5, means of temperature estimates are shown. Of interest here is the grouping of temperature estimates into two sets, one set around ~ 90° C and the other between 115° C and 155° C. Though potentially contradictory, the two temperature "groups" may actually be indicative of two different depths of equilibrium (Fournier, 1981).

3.5.6 Heat Flow, Geothermal Gradient and Depth of Circulation

Although no downhole measurements of heat flow are published in the immediate study area, heat flow values from sites just east of Kettle River, ~40 km WSW of Nakusp, are high, near 90 mW/m^2 corrected for topographic effects (Davis and Lewis, 1984). The local geothermal temperature gradient in the study area is likely near ~ 29° C/km (pers. comm. Trevor Lewis). A depth of circulation near 3-4 km would therefore be required to attain temperatures between 90° C and 125° C in terrain free of topographic influences. Heat flow isotherms however tend to accentuate somewhat the surface topography. Thus beneath steeply inclined topographic features such as the Selkirk Mountains, the actual geothermal gradient values would be higher and meteoric waters need not penetrate so deeply to acquire a given amount of heat.

3.6 Summary

Data from the Selkirk Range hotsprings show a consistent geochemistry among the three hotsprings sampled in the Kuskanax Batholith. The sodium-sulphate waters of Halcyon and Nakusp contain a sulphide component, the lower temperature waters of the St. Leon hotspring do not. All thermal waters have a low bicarbonate content. ^{14}C values in excess of 100 pmc at the Nakusp hotspring imply incorporation of ^{14}C-active DIC from soil zone organics entrained during recharge. Possible additional ^{14}C-active input may be occurring due to sulphate reduction and incorporation of soil zone organics during mixing with non-thermal groundwaters near the discharge environment.

Sodium-sulphate waters of the Halcyon hotspring also have short mean residence times, according to ^{14}C activities, and a substantial sulphide concentration. Geothermometer estimates for all three springs are consistent. Of interest here is the grouping of temperature estimates into two sets, one set around ~ 90° C and the other between 115° C and 155° C. While the high heat flow and steep topography of the region may facilitate rapid flow sytem turn over times, the proximity to deep-seated regional faults, particularly the CRFZ in the case of Halcyon hotspring, are likely increasing the volume of volatiles in these locally-recharged thermal waters. This possibility is discussed further in Section 4.

4 *Regional Geotectonic Comparision of Geothermal Areas*

4.1 Introduction

The third objective of this study is a geotectonic comparision of southern Canadian Cordilleran geothermal systems. Insular and Omineca Belt hotsprings covered in sections 2 and 3 will be examined along with Coast Plutonic Complex geothermal areas at Mt. Meager- Pebble Creek and Harrison hotsprings. An overview of heat flow and tectonic settings is followed by a brief description of the Mount Meager -Pebble Creek area and discussion of hotspring helium isotope data from the three regions.

4.1.1 Heat flux and tectonic belts

The division of the southern Canadian Cordillera into five principal geologic and tectonic belts is shown in Fig.1.1. Surface heat flow in the Vancouver Island area of the Insular Belt is very low , about 25 mW/m^2 (Lewis, 1991) and is dominated by subduction of the young oceanic crust of the Juan de Fuca plate which acts as a heat sink and depresses isotherms under the island (Davis and Lewis,1984). Fig.4.1.2a shows heat flux and heat generation in the southern Cordillera, with contouring in the areas where sufficient data sets are available.

The very low heat flux and heat generation of the HSC area is evident as are the anomalously high values in the Mt. Meager-Pebble Creek area of the Coast Plutonic Complex (CPC). The CPC is comprised of a range of arc-related rocks and Pliocene/Pleistocene volcanics and intrusives related to the subduction of the Juan de Fuca

Range to the south are reflected in the marked increase in heat flow east of a line parallel to the trend of the Cascade arc volcanoes (Lewis et al.,1983). Heat flow measurements in the Mt.Meager geothermal area are as high as several hundred mW/m^2 (Lewis, 1991).

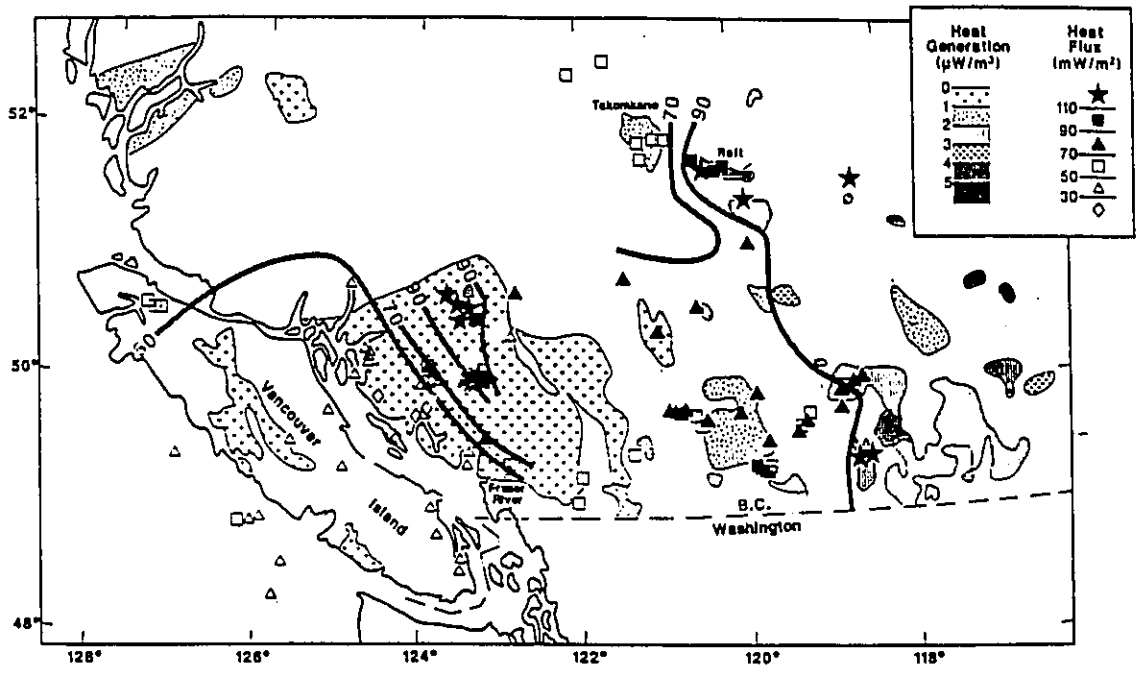

Fig.4.1.1a Heat flux and heat generation in Canadian Cordillera (after Lewis, 1991)

In the southern Canadian Cordillera, the Intermontane and Omineca Belts can be considered together as one heat-flow province[1] with a high heat flux. Geological and geophysical evidence points to a warm and thin crust in the area (Berry and Forsyth,

1 - Lewis (1991) describes heat flux as a combination of heat generated in the upper crust and heat flowing from the lower crust. Regions where a linear relation exists between the two can be called heat flow provinces.

geophysical evidence point to a warm and thin crust in the area (Berry and Forsyth, 1975). Omineca Belt heat flow values are very high, and average ~ 83 mW/m^2 (Lewis, 1991). Lewis considers that the 90 mW/m^2 contour (which passes in the vicinity of the Selkirk Range study area) bounds the higher heat-producing plutons to the northeast and may actually be the remnant plate boundary between ancestral North America and the Farrellon Plate (now the much smaller Juan de Fuca plate).

This hypothesis is consistent with the geomagnetic depth sounding inferences (Hyndman, 1963) referred to in Section 3.2.1, both of which point to the same conclusion, that this area is the "suture zone" where the accreted Cordilleran terrains have adhered to the continental margin. Although an Eocene thermal event could have been responsible for the high heat flow, the thin crust (30-40 km) and zone of uplift and extension in the region persists to the present, and may thus be better explained by alternate processes such as the continued flow of asthenospheric material toward the coastal subduction zone (Davis and Lewis, 1984).

4.2 Helium and Noble Gases in Hydrogeological Studies

4.2.1 Helium and the Noble Gases; Background

The noble gases xenon, krypton, radon, argon, neon and helium are unusual elements in a variety of ways. Their isotopic ratios vary widely with genetic history, they occur as monatomic gases, and, due to their stable electron configuration, they are very unreactive and volatile. From an analytical perspective, noble gases are relatively simple to extract, purify and analyze on a mass spectrometer provided certain procedures are adhered to (Mamyrin and Tolstikhin, 1984).

Helium, of all the noble gases, is particularly unique in a number of ways. It is (in addition to all the other characteristics cited for noble gases) the lightest of all elements except for hydrogen. This physical property, combined with its inertness, results in an extremely high volatility. It is the only gas known to escape from the planet into space. This phenomenon, known as helium escape, serves to delineate three distinct terrestrial reservoirs of helium: mantle, crustal and atmospheric.

These terrestrial reservoirs are in turn derived from three distinct *genetic* sources, each genetic type having its own characteristic isotopic gas ratio (Mamyrin and Tolstikhin, 1984). Discussion of these genetic sources of noble gases will focus primarily on helium, the principal hydrogeologic and isotopic tool used in this inquiry into tectonic influences on geothermal systems of the southern Canadian Cordillera.

Two isotopes of helium exist; ^3He and ^4He. The ratio of these two isotopes in terrestrial environments has been shown to vary over orders of magnitude depending on the contribution to the bulk gas volume from the three distinct genetic sources. These sources and their isotopic ratios are shown below:

1) **primordial** He; from nucleosynthesis fusion reactions; $^3He/^4He = \sim 2.4 \times 10^{-4}$

2) **radiogenic** He; produced through α decay $^3He/^4He = \sim 8 \times 10^{-12}$

3) **spallogenic** He; from cosmic ray bombardment of matter $^3He/^4He = 0.1 - 0.3$

The high ratio of ($^3He/^4He$) in spallogenic (or cosmogenic) helium presents a temptingly simple solution to explain high ratios observed in certain mantle-related processes. For, a simple mixing of radiogenic and spallogenic matter could yield He-isotope ratios over a broad range, including those related to primordial mantle sources. However, the concentration of atmospheric helium (5.24 ppm) is far below its predicted value when compared to other noble gases (see Appendix He). This is due to the phenomenon known as helium escape (Nicolet, 1957). The continual dissipation of helium into space has significant implications for mixing of terrestrial reservoirs, as despite its elevated helium isotope ratio (0.1 to 0.3), the depleted atmospheric concentration cannot account for the high $^3He/^4He$ in mantle hot-spots, volcanic fumeroles, oceanic ridges or even Coast Plutonic Complex geothermal waters.

Terrestrial reservoirs of helium

The incorporation of varying amounts of helium from different genetic sources results in a number of "standard" values for different components of the geosphere (Table 4.2.1a).

Geosphere component	$^3He/^4He$ Ratio	Genetic Source
mantle	3×10^{-5}	mainly primordial some crustal
crustal rock, gas and waters	1×10^{-8} to 5×10^{-8}	mostly radiogenic
materials from active tectonic areas	$\sim 10^{-6}$ to 10^{-7}	both radiogenic and primordial
atmosphere	$\sim 1 \times 10^{-6}$	all sources; depleted volume due to helium escape
Special cases; rocks rich in U-Th	$> 10^{-10}$	high radiogenic input

Table 4.2.1a Helium isotope ratios in geospheric reservoirs

This knowledge of distinctly defined terrestrial reservoirs facilitates studies pertaining to age, thermal history, and origin of geothermal waters. Anomalous elemental concentrations in certain terrains may directly affect helium isotopic ratios. Caution must

be exercised in terrains where rocks are enriched in minerals with high U-Th or Li content which can lower or raise the $^3He/^4He$ ratio, respectively, given sufficient time to decay. Groundwater in ancient granitic terrains will usually reflect the helium isotope ratio found in such rock types, namely a low R value ($^3He/^4He$) due to dissolution of radiogenically derived helium rich in the heavier isotope. This correlation has been used for uranium prospecting (Clarke and Kugler, 1973) Other possible influences on helium ratios come from decay of "bomb" or anthropogenic tritium or ^3H produced through in-situ activation (Andrews, 1985). Tritium decay can augment the light isotope component of helium and thereby skew He isotope ratios to give the impression of possible mantle contributions (Torgenson and Craig, 1982).

It is the chemical inertness, high volatility, and distinctive modes of origin tied to specific isotopic ratios which allows helium and noble gases to be applied in geothermal and hydrogeological studies as well as other areas of research such as volcanology.

4.2.2 Noble Gas Sample Purity

Table 4.2.2a shows the concentrations of both neon and helium in samples from Hotsprings Cove and Ahouset, as well as helium volume, He volume/He volume in air, and isotopic ratios for all samples from the three tectonic belts. The calculation of neon excess, used as a correction factor to account for the possible entrapment of air bubbles during sampling, was explained in Section 2.6 and is included here for completeness.

Table 4.2.2a Sample	Helium R/R air		Total He Vol cc STP/g x10-7		He Vol. R/Air	Total Ne Vol cc STP/g x10-7		X**	(R/R air)* corrected
Hotsprings Cove 1	0.27	+/- 1%	13.5	+/-.05	30.01	1.86	+/- 10%	25	0.24
Hotsprings Cove 2	0.27	+/- 1%	11.9	+/-.05	26.44	1.28	+/- 10%	32.1	0.25
Ahouset	0.28	+/- 1%	3.26	+/-.05	7.244	2.32	+/- 10%	4.85	0.09
Meager HS	6.54	+/- 0.22	3.90	+/- 7.7%	8.667	< 5 x 10-8	n.a.	n.a.	n.a.
EMR-1	6.01	+/- 0.09	130.00	+/- 20%	288.9	< 5 x 10-8	n.a.	n.a.	n.a.
Pebble Cr.	6.35	+/- 0.14	101.00	+/- 20%	224.4	< 5 x 10-8	n.a.	n.a.	n.a.
Harrison HS	1.44	+/- 0.04	120.00	+/- 20%	266.7	< 5 x 10-8	n.a.	n.a.	n.a.
Halcyon	0.06	+/- 0.02	176.00	+/- 20%	391.1	< 5 x 10-8	n.a.	n.a.	n.a.
St. Leon	0.10	+/- 0.01	51.00	+/- 20%	113.3	< 5 x 10-8	n.a.	n.a.	n.a.
Nakusp	0.06	+/- 0.04	16.70	+/- 20%	37.11	< 5 x 10-8	n.a.	n.a.	n.a.
Fresh water (air equilibrated s.l.)	1.00		0.45	n.a.	n.a.	1.8	n.a.	n.a.	n.a.

**** (R/Rair) corrected= ((R/R air) X) -1 / (X - 1)**

** where; X = (He/Ne)/(He/Ne) air,*
and where; (He/Ne) air = 0.29; includes atmospheric and radiogenic sources (Craig etal,1978a).

He dissolved in water in equilibrium with atmospheric Helium (5.24 ppm),
has a solubility of 4.5 X 10-8 cc/STP/gH20

Atmospheric Neon has a solubility of approximately 1.8 x10-7 @ STP
and a solubility of approximately 1.7 @ 50 C

Table 4.2.2a Noble gas data for southern Canadian Cordillera hotsprings

For the Coast Plutonic Complex (CPC) and Omineca Belt thermal waters, no precise qualitative measure of neon content was given due to analytical complications. However, neon aquisition data for these samples revealed a maximum possible atmospheric contamination of < 3%, indicative of good sample purity (pers. comm. Dr. Stephen Weiss). As discussed in Section 2.6, where precise neon data are not available, helium *volume* can provide a qualitative measure of sampling contamination or additional He input. This relates to the low atmospheric concentration (5.24 ppm) and low solubility of helium in water (4.5×10^{-8} cc/g H_2O at STP and 0 % salinity) ensuring that if substantial He is present (from radiogenic or mantle sources) then the effects of atmospheric "contamination" are negligible (Torgersen and Jenkins, 1982). In this regard, samples from all locations meet the volume criteria, ranging from 7 to 30 times atmospheric volume for Insular Belt samples, and up to 176 times atmospheric for Omineca and CPC thermal waters.

The lowest helium volumes for samples from the CPC and the Omineca Belt are for those at Meager Creek and Nakusp hotsprings. Both discharge from boulder and cobble-filled coarse surficial deposits where loss of volatile helium gas to the atmosphere is probable. Notably though, the Meager sample has a helium isotope ratio which is in close agreement with the adjacent shallow well values from EMR-1, as well as the value for Pebble Creek hotspring. Additionally, its helium gas concentration of ~8.7 times atmospheric is nearly twice the > 5 x volume recommended for sample purity.

The Nakusp hotspring helium gas sample has only about 10% the volume of the Halcyon Hotspring sample consistent with its discharge from a Quaternary boulder and cobble-filled river valley. Again gas loss to atmosphere prior to discharge through this surficial formation is possible. Regardless, the gas volume of more than 37 times atmospheric is almost an order of magnitude above the 5x atmospheric equilibrium value recommended as a reliable minimum for sample validaton using He-gas volume (Torgensen and Jenkins, 1982). In conclusion, all sample analyses are considered valid.

4.3 Mt. Meager and Pebble-Creek hotsprings of the Coast Plutonic Complex

4.3.1 Overview

The Mount Meager-Pebble Creek geothermal area defines the northern limit of the Cascade chain of volcanoes which includes Mt. Baker and Mt. St. Helen's (Souther, 1977). Basement granodiorites of the Coast Plutonic Complex underlay the silicic to intermediate volcanic rocks of the 16-km diameter Tertiary/Quaternary Mt.Meager volcanic complex which host the Meager Creek hotsprings (Read, 1979). The Pebble Creek hotsprings, located ~5 km east of the Meager hotsprings may be associated with both the Garibaldi Belt and the Pemberton Belt (PB) of Tertiary intrusives to the east (Fig.4.3.1a). Both belts are related to the subduction of the Juan de Fuca Plate (see cross section, Fig.4.3.1a) and intersect at the Salal Tertiary pluton just north of Pebble Creek (Lewis and Souther, 1978).

4.3.2 Description of geothermal discharges

Two principal geothermal anomalies, and two main shallow reservoirs have been identified in the area. Their isotope hydrogeology has been examined by Clark et al., (1982) and more recently by Ghomshei and Clark (1993). Geothermal waters upwell along the east-west striking Meager Creek Fault which dips ~ 55° N, and discharge at the Meager Cr. hotspring area which includes the shallow borehole, EMR-1 (Fig. 4.3.2a). These 45 - 55° C calcium-chloride thermal waters discharge up to 40 l/s from numerous vents in the boulder and cobble deposit on the south side of Meager Creek (Plate 4.3a). They have experienced up to 10% mixing with local shallow groundwaters recharged below the principal thermal water catchment area near peaks at the centre of the complex.

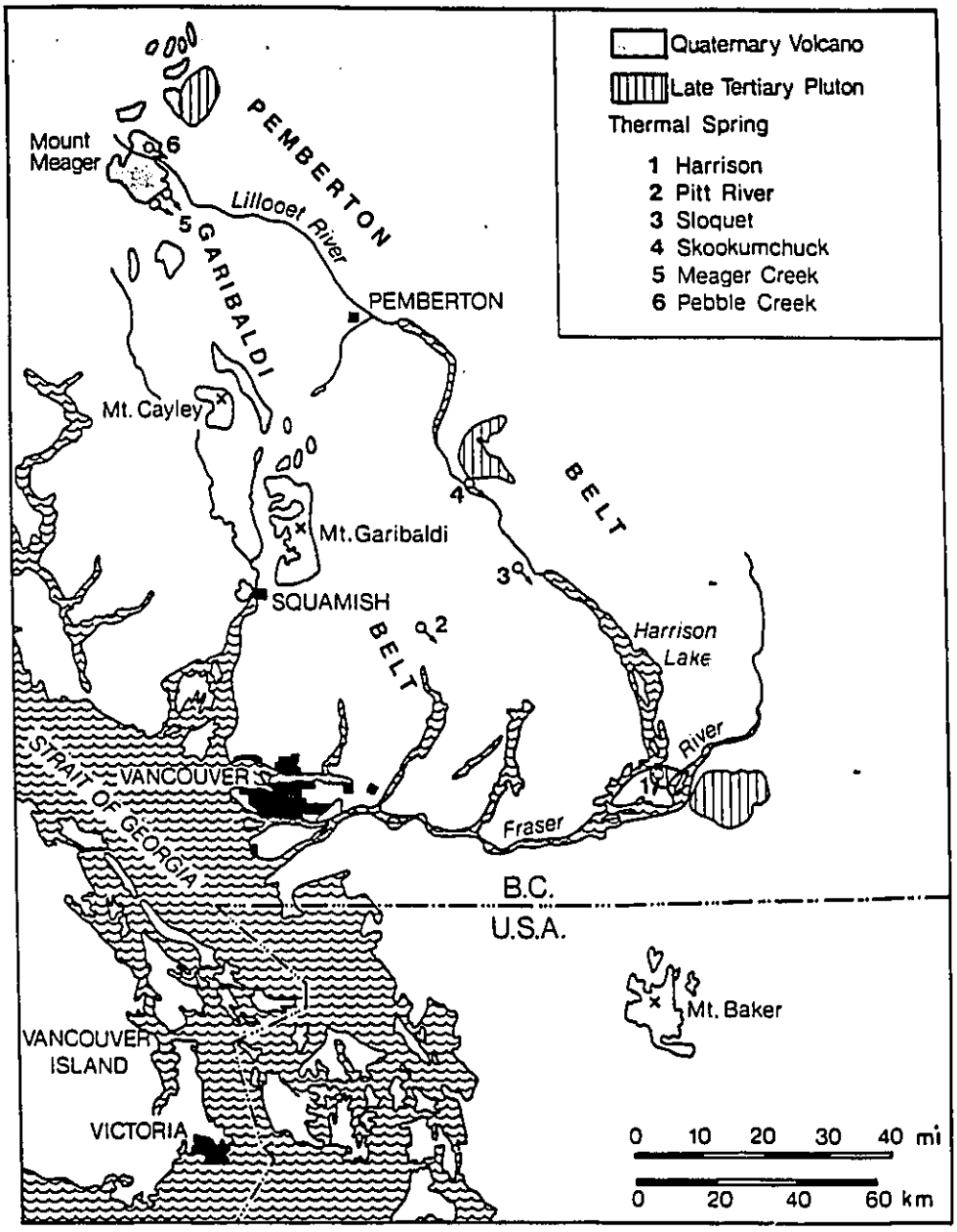

Fig. 4.3.1a Location of Mt.Meager, Garibaldi and Pemberton Belt hotsprings

(from Clark et al., 1982)

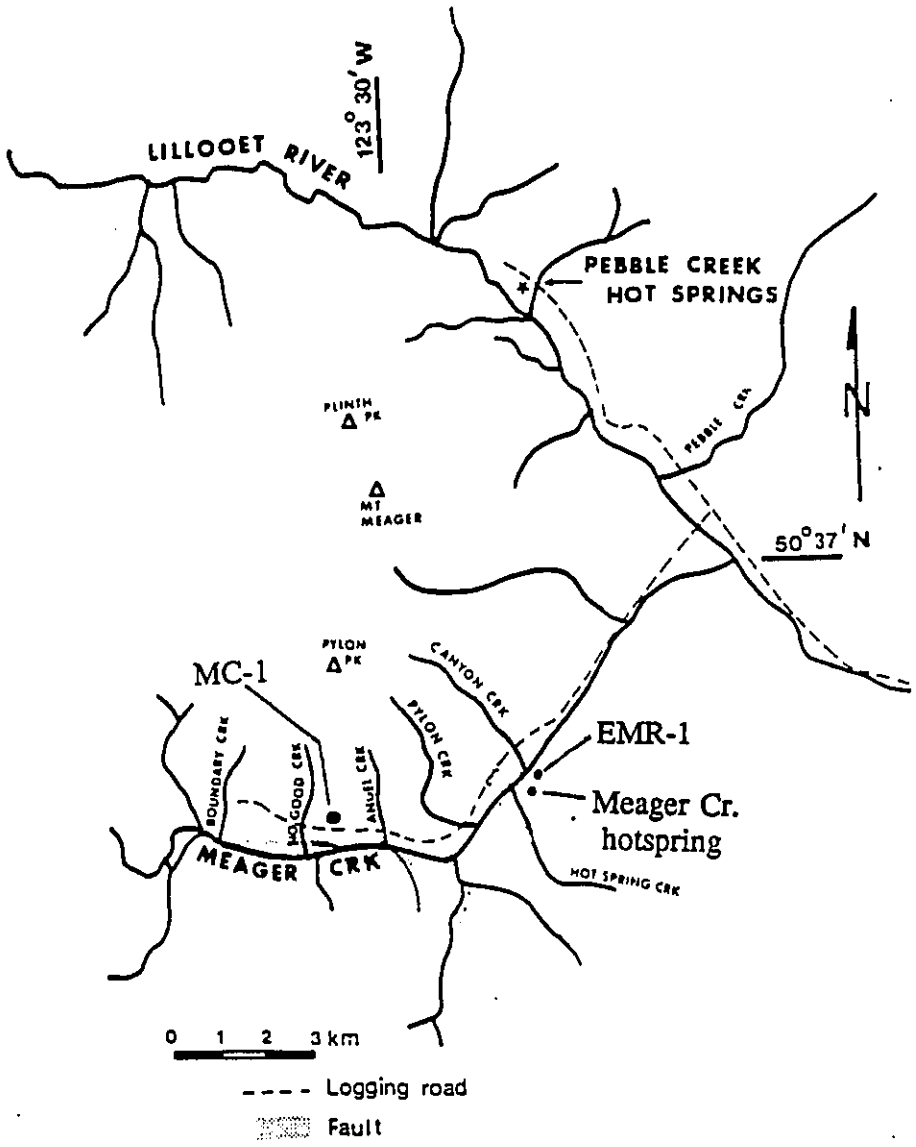

Fig.4.3.2a Location of Mt. Meager-Pebble Cr. geothermal sites sampled for helium gas

(after Clark et al., 1982)

Plate 4.3a (left) Looking east from main vent, Meager Cr. hotspring

Plate 4.3b (top) Copper tube helium gas sampler at Hotsprings Cove, Vancouver Island

The 60° C sodium-bicarbonate Pebble Creek thermal waters discharge at a rate of 5-10 l/s from a bedrock bench on the east side of the Lillooet River. They are more depleted in ^{18}O than the Meager Cr. thermal waters due to recharge by meteoric waters from the higher-altitude areas to the east. Maximum temperature estimates in the area of the Meager and Pebble Creek hotsprings are generally >140° C.

A third water type, of higher salinity and purported to be associated with deeper, more evolved, regional groundwater flow was extracted from the deep borehole, MC-1. MC-1 is the only flowing artesian, high-temperature deep-borehole in Canada; (Jessop et al., 1991). Down-hole temperature measurements taken from the borehole production zone were near 200°C (Ghomshei and Clark, 1993). Unfortunately the helium gas sample from MC-1 was lost during laboratory extraction.

4.3.3 Pemberton Belt fault-related hotsprings; Harrison Hotspring

The Tertiary intrusives of the Pemberton Belt which are associated with the Pebble Creek hotsprings, host other geothermal waters further south related to the Lillooet Valley fault system: the Sloquet, Skookumchuck, and Harrison hotsprings (Fig.4.3.1a). Although access to the Sloquet and Skookumchuck hotsprings was denied due to a major landslide and subsequent road closure, a helium gas sample was secured from Harrison hotsprings. The two natural springs at Harrison originally discharged underwater near shore, from bedrock-fissures in the lake-bottom (Elworthy, 1925). The site now features a concrete-enclosed basin about 2 m deep and 15 m^2. The 62° C NaCl - $NaSO_4$ waters are then piped a distance of ~200 m to one of the better known hotel/spas in British Columbia.

4.4 Regional Tectonic Trends

4.4.1 Consistency of $^3He/^4He$ ratios within each tectonic belt and implications

Insular Belt hotsprings

As shown in Table 4.2.2a and discussed in Section 2.6, the west coast Vancouver Island hotsprings have a consistent helium R/R_{air} value near 0.28 reflective of both the regional geologic setting and proximity to the dynamic tectonic environment of the subducting Juan de Fuca plate.

Coast Plutonic Complex hotsprings

R/R_{air} values >6 are consistent throughout the Mt. Meager-Pebble Creek area. Despite wide variations in the helium volume of these samples (see Table 4.2.2a) the ratio is constant. Other studies have shown a direct relationship between helium isotope ratios and geothermal reservoir temperatures. Geothermal systems with temperatures $>200^0$ C have R values considerably greater than unity while hot springs with T < 200^0 C show a sharp decrease (Craig et al., 1978a). The values >6 for the Meager-Pebble Creek geothermal area are consistent with the measured temperature of 200° C in the MC-1 well. The interesting aspect of these measurements is that all the Meager Cr. and Pebble Cr. sites are all consistently >6, even though previous geothermometric estimates at these sites (Clark et al. 1982) were in a lower temperature range. This finding suggests either that the R/R_{air} value has a broader spatial orientation than other geothermometers, or that higher temperature reservoirs exist closer to these sites. The latter possibility is particularly interesting for the Pebble Cr. site as it has been mapped as a geothermal

reservoir apart from the Meager Cr. geothermal system. Regardless, the data in this tectonic setting reveal a regionally consistent addition of volatiles to different locally-recharged geothermal systems.

The Harrison hotspring R/R_{air} value, although the only one available at present for the Pemberton Belt suite, is important in that the spatial consistency of the Meager-Pebble Cr. sites cannot be extrapolated to Harrison, which is likely associated with the Lillooet R. Fault-Harrison Lake Fault, not the Garibaldi Belt or the Mt. Meager volcanic complex.

Selkirk Range hotsprings

As in both the Insular belt and the CPC, consistent R/R_{air} values are found in the Omineca belt hotsprings. The variation between 0.06 and 0.10 is minimal if analytical precision given in Table 4.2.2a is considered. These values, unlike those from the other two belts, show a strong radiogenic signature, consistent with their tectonic setting in the 175 Ma old Kuskanax batholith. Nonetheless, the volume of helium gas at Halcyon (nearly 400 times atmospheric concentration) and the R/R_{air} near 0.06 means that ~24 times the atmospheric volume of helium gas is present. While it may be argued that this ratio simply reflects subsurface production of ^3He (see Section 4.4.1 or Appendix He), it is also possible to calculate contributions from two possible terrestrial reservoirs in the Omineca belt, crustal and mantle.

It is interesting that Halcyon hotsprings value of 391 times atmospheric volume surpasses all the CPC hotsprings as well as the EMR-1 borehole at Mt.Meager. Eqn.

2.6.2a, which was used to calculate contributions from two different helium sources for HSC, can be used in a similiar fashion for the Selkirk Range hotsprings. However, the ^{3}He-rich component used for the west coast Vancouver Island hotsprings was oceanic plate with a maximum R/R_{air} of 2.0 (see Section 2.6) The CPC helium R/R_{air} values exceeding 6, common in volcanic arc are indicative of a richer source of ^{3}He. Actual $^3He/^4He$ ratios for the upper mantle are in the range of 1 to 3 x 10^{-5} (Mamyrin and Tolstikhin, 1984), while crustal rocks range from 1 to 5 x 10^{-8}. Older batholithic rocks with radiogenic helium sources (such as those found in the Selkirks) are more likely to have ratios near ~ 2 x 10^{-8} (Mamyrin and Tolstikhin, 1984). Using these ratios and the measured ratio at Halcyon hotspring, it is possible to solve for the relative portions of mantle and crustal-derived helium gas in the same manner as in Section 2.6:

$\{^3He/^4He_{mantle} \times \text{Portion (P)}\} + \{^3He/^4He_{crustal} \times (P - 1)\} = \text{Actual } ^3He/^4He_{Halcyon}$ Eqn 4.4.1

Substituting in the values for these portions as described above;

$(2 \times 10^{-5} \times P) + (2 \times 10^{-8} \times (1 - P)) = 8.28 \times 10^{-8}$

Multiplying both sides by 10^8 and solving for the respective mantle and crustal portions:

$2000P - 2P - 2 = 8.28$; $P = 8.28/1998$; $P = .003143 = \sim 0.3$ %

Thus, while the contribution of mantle helium is unclear but appears to be minor, any such mantle addition may be considered significant in this tectonic regime, given the distance from the subduction zone.

4.4.2 Consistency of Cordilleran $^3He/^4He$ ratios in Canada and the United States

In addition to regional tectonic consistency, the helium data from geothermal areas in each tectonic belts in this study show good correlation with data from the United States. Fig. 4.4.2a summarizes data from this study and US data from Whelan et al., (1988).

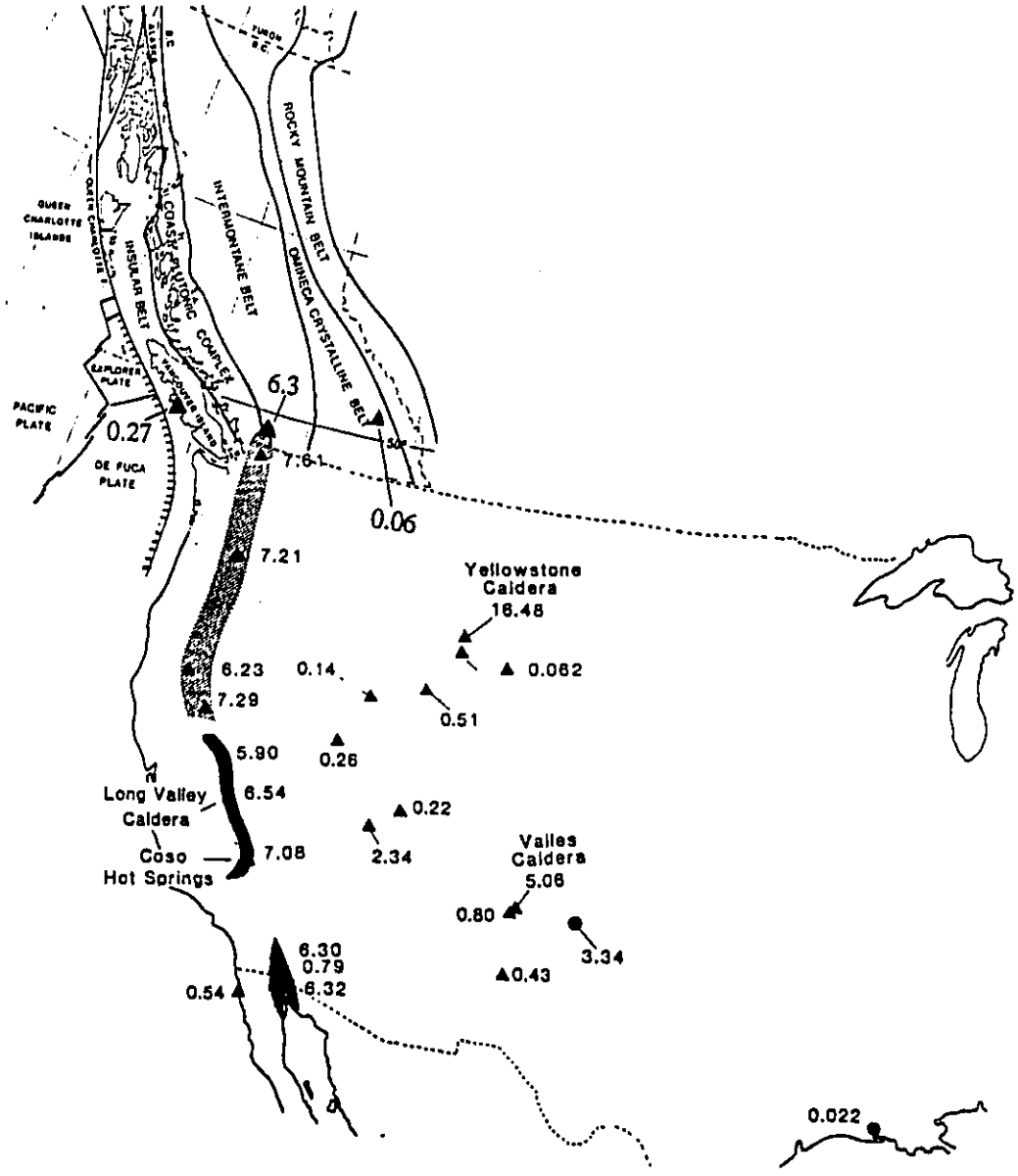

Fig. 4.4.2a Helium R/R_{air} values for geothermal waters in Canadian and U.S. Cordillera Canadian data from this study, Map modified after Whelan, (1988) and Lewis, (1991)

The consistency of the data within the tectonic belts of the Cordillera is exemplified by the consistency of the Mt. Meager-Pebble Cr. area data with other vocanic complexes of the Cascade Range to the south. All thermal waters have classic volcanic arc R/R_{air} signatures between 6 and 7. No coastal data points are shown by Welhan et al., (1988) except for the 0.54 R/R_{air} value for a hotspring in Baja, California. Omineca Belt values are similiar to those to the south, with the exception of the Yellowstone Caldera which relates to a mantle hotspot.

4.5 Summary of helium data and geotectonic implications

Findings from noble gas data in this study of hotsprings in the southern Canadian Cordillera reveal a number of consistent trends. Helium R/R_{air} values, for instance, can vary widely from one tectonic belt to the next, while $^3He/^4He$ ratios are consistent for geothermal systems in the same tectonic setting, irrespective of differences in their noble gas volume.

The volume of helium gas present in the thermal waters of Halcyon hotspring is nearly 400 times the atmospheric concentration, reflecting radiogenic input from the Kuskanax Batholith and proximity to the Columbia River Fault Zone. Although influx of mantle helium cannot be ruled out in this area, the contribution from deep-seated sources is likely <1 %.

Mt. Meager-Pebble Cr. area geothermal waters have classic volcanic arc helium signatures, R/R_{air}= ~6. These data are consistent with those for Cascade Range volcanic

centres to the south and reflect the high regional heat flux and proximity to the subducting Juan de Fuca Plate. Thermal waters of Harrison hotspring have markedly lower R/R_{air} values than the Mt. Meager area geothermal systems, consistent with differences in geotectonic setting within the Coast Plutonic Complex.

Insular Belt hotsprings at Hotsprings Cove and Ahouset reflect both the local geology and input from deep-seated regional volatiles. The -2.83 ‰ PDB signature of Ahouset and its R/R_{air} value of 0.28 are consistent with data from HSC which reveal the presence of a methane component and ~11% subduction-related helium gas. The presence of deep-seated volatiles in these Insular Belt hotspring waters are a reflection of frequent local seismic activity, and proximity to deep-seated regional faults and the subducting Juan de Fuca plate.

This study reveals how geothermal systems of the southern Canadian Cordillera can reflect both locally-derived meteoric processes and water-rock interaction, and regional geotectonic processes as characterized by input from deep-seated volatile components.

4.6 Future research suggestions

Findings of this study invite further research on a number topics, which relate both to regional tectonic implications from noble gas data, and to geothermal research focusing on more specific sites in the Canadian Cordillera.

For the Hotsprings Cove geothermal system, carbon and hydrogen isotope analyses of the methane gas component would clarify the source of carbon used in sulphate reduction processes which influence the ^{14}C-based mean residence time estimates. Similiarly ^{36}Cl analyses of these thermal waters would clarify questions concerning seawater intrusion, and sources of bromide and chloride.

Future research on Insular Belt hotsprings could also include, for Hotsprings Cove and Ahouset, a periodic sampling program involving repeat measurements of noble gases including helium, neon, and radon gas. Radon gas measurements from HSC and Ahouset could provide valuable information related to seismic events, particularly when considering findings from this study which suggest that subduction-related volatiles are emanating from these geothermal vents following upward migration along deep-seated regional faults. If these hotsprings are in fact a window on tectonics and subduction-related processes, their potential use as an earthquake analysis or prediction tool should not be overlooked. Other coastal hotsprings further north, including those at Knight Inlet and in the Queen Charlotte Islands area, could be added to this small dataset which may be seen as a starting point for Insular Belt geotectonic studies using noble gases.

The Selkirk Range hotspring data from this study was collected over a two day period, and must be viewed as a reconnaissance-style overview of these very interesting thermal waters. Future geothermal research in this area should include the Halfway River hotspring, located between the Halcyon and St. Leon springs. Isotopic data from both the

Halfway River and St. Leon hotsprings may clarify the some of the processes occurring in all of these Kuskanax Batholith hosted hotsprings, where ^{14}C-based mean residence times are remarkably short, contrary to qualitative estimates based on helium gas volume. The massive volumes of helium gas present in the Halcyon hotspring, along with its proximity to the Columbia River Fault Zone, invites further sampling and research concerning the possible upward migration of deep-seated volatiles in this area of the Cordillera.

For Coast Plutonic Complex hotsprings, the elevated helium isotopic signatures at Meager and Pebble Creek support the prospects of economically-viable electrical power production. Extension of the helium gas dataset to include the deep borehole MC-1, and other regional geothermal occurrences such as Skookumchuck and Sloquet hotsprings, may help delineate further the extent of high-temperature reservoirs. Helium systematics of all southern Cordilleran thermal waters studied in this project are very interesting and should be expanded to look at correlations with tectonics on a larger regional scale throughout the Cordillera.

References

Andrews, J.A. (1985), "Natural production of tritium in permeable rocks," Nature vol. 298, pp 361-363.

Arnorsson, S., (1975), "Application of the silica geothermometer in low-temperature hydrothermal areas in Iceland", Amer. J. Sci.,vol. 275, pp 763-784.

Bentkowski, W.H., and T.J. Lewis, (1989), "Thermal measurements in Cordilleran boreholes of opportunity, 1984-1987", G.S.C. Open File 2048.

Berry, M.J., and D.A. Forsyth, (1975), "Structure of the Canadian Cordillera from seismic refraction and other data: Can. J.Earth. Sci. 12, pp 182-208.

Bodvarsson,G., (1960), "Exploraton and exploitation of natural heat in Iceland," Bull. Volcan., vol. 23, pp 241-250.

Bottomley, D.J., J.D. Ross, W.B. Clarke (1984), "Helium and neon isotope geochemistry of some groundwaters from the Canadian Precambrian Shield", Geochem. Cosmochem. Acta, Vol. 48, pp 1973 - 1985.

Brown, R.L., Geologist Ottawa Carleton Geoscience Centre, Carleton University, Ottawa, Ont., personal communication, (December 15, 1993).

Brown, R.M., (1961), "Hydrology of tritium in the Ottawa Valley," Geochem. Cosmochem. Acta, vol. 21., p 199.

Chiba, H. and H. Sakai (1985), Oxygen isotope exchange rate between dissolved sulphate and water at hydrothermal temperatures," Geochem. Cosmochem. Acta, vol. 49, pp 993-1000.

Clapp, C.H., (1913),Sharp Point hotspring, Vancouver Island," G.S.C. Sum. Rept. pp.80-83.

Clague, J.J. (1977), "Quadra sand: a study of the Late Pleistocene geology and geomorphic history of coastal southwest B.C.: G.S.C. Paper 77-17.

Clark,I.D., P.Fritz, F. Michel and J.G. Souther (1982), "Isotope hydrogeology and geothermometry of the Mt. Meager geothermal area", C.J.E.S. vol. 19, pp. 1454-1473.

Clark I.D. (1985), "Geochemistry, Isotope Hydrogeology, and Geothermometry of Hotsprings in the Northern Coastal Area of British Columbia", unpublished report to GSC, Energy, Mines and Resouces Canada, April 1985.

Clarke, W.B. and G. Kugler (1973), "Dissolved Helium in Groundwater: A Possible Method for U and Th Prospecting," Econ. Geol. 68., pp. 243-251.

Conway, K.W., J.V. Barrie, B.D. Bornhold (1990), "Surficial Geology of the Vancouver Island Continental Shelf, Nootka Sound to Strait of Juan de Fuca, Offshore British Columbia", G.S.C. Open File 2432.

Craig, H., (1961), "Isotopic variations in meteoric waters," Science, vol. 133. pp 1702-1703.

Craig, H. and W.B.Clarke, (1970), Oceanic ^{3}He: Contribution from cosmogenic tritium," Earth Planet. Sci. Lett., 6: pp. 213- 220

Craig, H., and J.E. Lupton (1976), "Primordial neon helium and hydrogen in oeanic basalts," Earth Planet. Sci. Lett. 31, pp. 369-385.

Craig, H., J.E. Lupton and Y. Horibe (1978a), "A mantle component in Circum-Pacific Volcanic gases", *in* Terrestrial Rare Gases (Eds.E.C. Alexander and M. Ozima), Cent. Acad. Publ., Japan.

Davis, E.E., and T.J. Lewis (1984), "Heat flow in a back-arc environment: Intermontane and Omineca Crystalline belts, southern Canadian Cordillera", Can. J.Earth. Sci. 21, pp 715-726.

Davis, E.E., and Villager, (1992), "Proceedings of the Ocean Drilling Program, Initial Reports, vol. 139.

Dawson, G., (1888-89), "Geological Survey of Canada, Ann. Rept., New Series,Vol. IV, pt.B, p12.

Drever, J.I., (1988), "The gechemistry of natural waters," Prentice Hall Publ., Englewood Cliffs, New Jersey, second edition, 437 pp.

Edmonds, W.M., R.L.F. Kay, D.L. Miles, and J.M. Cook, "The Origin of Saline Waters in the Carnmenellis Granite, Cornwall, U.K.: Further Evidence from minor and Trace Elements", in Salinle water and gases in crystalline rocks, Eds., Fritz, P., and S.K. Frapé; Geological Association of Canada Special Paper 33, 1987,pp. 127-143.

Egboka, B.C.E., (1980), "Bomb tritium in shallow sand aquifers," Ph.D. thesis, University of Waterloo, Waterloo, Ont., 197 pp.

Elworthy, R.T. (1925), "Hotsprings in Western Canada Their Radioactive and Chemical Properties", Mines Branch, Dept. of Mines, Canada., Bulletin 669.

Environment Canada, (1980), "Canadian Climatic Normals, 1951-1980, Temperature and Precipitation, British Columbia", Atmospheric Environment Service.

Faure, G., (1987), "Principles of Isotope Geology", 2nd edition, John Wiley and Sons, Toronto, Ont., 589 p.

Fouillac, C. and G.Michard, (1981), "Sodium/Lithium ratio in water applied to geothermal reservoirs", Geothermics vol.10, pp 55-70.

Fournier, R.O.,(1981), "Application of Water Geochemistry to Geothermal Exploration and Reservoir Engineering" in Geothermal Systems: Principals and Case Histories, Eds., Rybach, L. and L.P.J. Muffler, John Wiley and Sons, Toronto.

Fournier, R.O. and J.J. Rowe, (1962),"The solubility of cristobolilte along the three phase curve, gas plus liquid, plus cristobolite," Am. Minerlaolgist, vol. 47, pp 897-902.

Fournier, R.O. and J.J. Rowe,(1966), "Estimation of underground temperatures from the content of water from hotsprings and wet-steam wells", Amer. J. Sci.,264 pp 685-697.

Freeze, R.A., and J.A. Cherry, (1979), "Groundwater," Prentice Hall Publ., Englewood Cliffs, New Jersey, First edition, 604 pp.

Fritz, P. and J.Ch. Fontes, (1980), "Handbook of Environmental Isotope Geochemistry, Volume 1, The Terrestrial Environment, A," Fritz, P. and J.Ch. Fontes, Eds., Elsevier (1980), Amsterdam.

Fritz, P.,and S. Frape, (1982), " Saline groundwaters in the Canadian Shield-A first overview", Chem. Geol., vol. 36, pp179-190.

Gabrielse, H. (1991), "Structural styles, Chapter17, in Geology of the Cordilleran Orogen in Canada, H. Gabrielse and C.J.Yorath (ed); G.S.C., Geology of Canada, no. 4, pp 571-675.

Gabrielse, H., J.W.H. Monger, J.O. Wheeler, and C.J. Wheeler (1991), "Tectonic Framework", in Geology of the Cordilleran Orogen in Canada, H. Gabrielse and C.J.Yorath (ed); G.S.C., Geology of Canada, no. 4, pp 15-28.

Gat, J.R., (1980), "The isotopes of hydrogen and oxygen in precipitation. Chapter 1 in Handbook of Environmental Isotope Geochemistry, Volume 1, The Terrestrial Environment, A., Fritz, P. and J.Ch. Fontes, Eds., Elsevier (1980), Amsterdam, pp. 22-44.

Gieskes, J.M. and J.R. Lawrence, "Alteration of volcanic matter in deep sea sediments: evidence from the chemical composition of interstitial waters from deep sea drilling cores", Geochemica and Cosmochemica Acta. Vol. 45, pp1687-1703.

Ghomshei, M.M., and I.D.Clark,(1993), "Oxygen and Hydrogen in deep thermal waters from the south Meager Creek geothermal area, B.C.", Geothermics, vol. 22, no.2, pp. 79-89.

Heaton, T.H.E. and J.C. Vogel (1981), " "Excess air" in groundwater", J. of Hydrology 50, 201 -216.

Heier, K.S. and G.K. Billings (1969), Lithium in Handbook of Geochemistry, Vol. III, Springer Verlag, Berlin.

Hyndman, R.D. (1963), Electrical conductivity in the Earth's upper mantle: M.Sc. thesis , U.B.C., Vancouver, B.C.

Hyndman, R.D., R.R. Riddihough and, R. Herzer, (1979), "The Nootka Fault Zone - A new plate boundary off western Canada; Geophys. J. of Royal Astronomical Society, vol. 58, pp 667-683.

Hyndman, R.D., C.J. Yorath R.M. Clowes and E.E. Davis, (1990), "The northern Cascadia subduction zone at Vancouver Island: Seismic structure and tectonic history," C.J.E.S. vol. 27, pp 313-329.

Hyndman, R.D. and K.Wang, (1993) "Thermal Constraints on the Zone of Major Thrust Fault Failure: the Cascadia Subduction Zone", J. of Geophysical Research, Vol. 98, pp 2039-2060.

Hyndman, R.D., Senior geophysicist, Pacific Geoscience Centre, Sidney, B.C., personal communication, November, 1993.

Irwin, H., C.D. Curtis, and M.Coleman, (1977), "Isotopic evidence for source of diagenetic carbonates formed during burial of organic rich sediments", Nature vol. 269, pp.209-213.

Jeletzky, J.A. (1954), "Tertiary rocks of the Hesquiat-Nootka area, west coast of Vancouver Island, B.C.; G.S.C. Paper 53-17, 65 pp.

Jessop,A.M., M.M. Ghomshei, and M.J. Drury, "Geothermal energy in Canada", Geothermics vol. 20, pp. 369-385.

Krouse, H.R., (1980), "Sulphur isotopes in our environment", Chapter11 in Handbook of Environental Isotope Geochemistry, Volume 1,the Terrestrial Environment, A., Fritz, P. and J.Ch. Fontes, Eds., Elsevier (1980), Amsterdam, pp. 22-44.

Karaka and Mariner, (1988), Solmineq geothermal modelling software program.

Kennedy, G.C.,(1950),"A portion of the system silica-water", Econ.Geol., vol. 45 pp 629-653.

Lajoie, J.L. and B. Caner, (1970), Geomagnetic induction anomaly near Kootenay Lake - a strike slip feature in the lower crust?; Can. J. Earth. Sci., vol. 7, pp. 1568-1579.

Lewis, T.J., W.H. Bentkoski, and E.E. Davis, (1983), "The variation in measured heat flow, Jervis Inlet, B.C., Geological Association of Canada, Program with Abstracts, vol. 8.

Lewis, T.J., and J.G. Souther, (1978), "Meager Mountain, B.C. - a possible geothermal energy resource; Earth Physics Branch, Geothermal Series No. 9.

Lewis, T. J., W.H. Bentkowski, E.E. Davis, J.G. Souther, and J.A. Wright, (1988), "Subduction of the Juan de Fuca Plate: thermal consequences," J. Geophys. Res., vol. 93, pp 15,207-15,225.

Lewis, T.J., (1991), "Heat flux in the Canadian Cordillera", in Slemmons ,D.B., E.R.Engdahl, M.D.Zoback, and D.D. Blackwell, eds., Neotectonics of North America: Boulder, Colorado,Geological Society of America, Decade Map Volume I.

Lewis, T.J., Senior Geophysicist, Geological Survey of Canada, Pacific Geoscience Centre, Sidney, B.C., personal communication April 2, 1993.

Mamyrin, B.A. and L.N. Tolstikhin, (1984), "Helium Isotopes in Nature," Elsevier, New York 273 pp.

Mahon, W.A.J.,(1976), "Review of hydrogeochemistry of geothermal systems. Prospecting, development, and use. United Nations Symposium on the Development and Use of Geothermal Resources vol. 1, pp. 775-783.

Mathews, J.W. (1991), "Physiographic evolution of the Canadian Cordillera, Chapter 11 in Geology of the Cordilleran Orogen in Canada, H. Gabrielse and C.J.Yorath (ed); G.S.C., Geology of Canada, no. 4, p. 403-418.

Mazor. E. (1972), "Paleotemperatures and other parameters deduced from noble gases dissolved in groundwaters; Jordan Rift Valley, Israel", Geoch. Cosmochem. Acta 36, 1321 - 1336.

Mazor. E. (1979), "Noble gases in a section across the vapour dominated geothermal field in Larderello, Italy," Pure Appl. Geophys., vol. 117, pp 262-275.

Mazor, E. and A. Bosch, (1989), "He as a tool for groundwater dating in the range of 10^4 - 10^8 years," *in* Isotopes of Noble Gases as Tracers in Environmental Studies, IAEA, Vienna.

Mazor. E. (1991), "Applied chemical and isotopic groundwater hydrology," Open University Press, Celtic Court, 22 Ballmoor, Buckingham MK18 1XW. First Edition.

McDonald, J., D. Pollock and B. McDermot (1978), "Hotsprings of Western Canada A Complete Guide", Labrador Tea Company, Vancouver, B.C.

McKenzie, W.F., and A.H. Truesdell (1977), "Geothermal reservoir temperatures estimated from the oxygen isotope compositions of dissolved sulphate and water from hotsprings and shallow drillholes," Geothermics, vol. 5, pp 51-61.

Mitzutani, Y., (1972),"Isotopic composition and underground temperature of the Otake geothermal water, Kyushu, Japan",Geochem. J.(Japan), Vol. 6, no. 2, pp 67-72.

Mitzutani, Y. and T.A. Rafter (1969), "Oxygen Isotope composition of sulphates; part 3. Oxygen isotopic fractionation in the bisulphate ion-water system", New Zealand J. Sci., vol.12, no. 1, pp 54-59.

Morrison, P.and J. Pine, (1955), "Radiogenic Origin of the Helium Isotopes in Rocks," ANN. N.Y. Acad. Sci., 62: 69-92

Muller, J.E., B.E.B. Cameron and K.E. Northcote, "Geology and mineral deposits of Nootka Sound map-area, Vancouver Island, B.C., G.S.C. Paper 80-16, 53 pp., with accompanying map 1537 A.

Muller, J.E. and D.J.T. Carson (1969), "Geology and mineral deposits of Alberni map-area, B.C. (92F); G.S.C. Paper 68-50, 52 pp., with accompanying map; 17-1968.

Nicolet, M. (1957), "The aeronomic Problem of Helium," ANN. Geophys., 13:1-21

N.S.B.G., Nevin Sadlier-Brown Goodbrand Ltd.,(1988), "An Evaluation of Geological and Geochemical Data on the Sharp Point Hotsprings, Maquinna Prov. Park", unpublished report for B.C. Ministry of Parks.

Parrish, R.R., and J.O. Wheeler, (1983), "A U-Pb zircon age from the Kuskanax Batholith, southeastern, B.C.", C.J.E.S., vol.20,pp 1751-1756.

Pearson, F.J. and B.B. Hanshaw (1970), "Sources of dissolved carbonate species in groundwater, and their effects on ^{14}C dating," *in* Isotope Hydrology 1970, IAEA, Vienna, vol. 2, pp 95-109.

Pierre, C.,(1980), "Sedimentation and Diagenesis in Restricted Matine Basins", Chapter 8 in Handbook of Environental Isotope Geochemistry, Volume 3,the Terrestrial Environment, A., Fritz, P. and J.Ch. Fontes, Eds., Elsevier (1980), Amsterdam, pp. 22-44.

Poreda, R. and H.Craig, (1989),"Helium isotope ratios in circum-Pacific volcanic arcs," Nature, vol. 338, pp 473-477.

Read, P.B.,(1973), "Petrology and structure of Poplar Creek map-area, B.C.", G.S.C. Bulletin 193.

Read, P.B., and W.O. Wheeler (1976), "Lardeau west-half, G.S.C. Open File map 432.

Read, P.B. and R.L. Brown, (1981), "Columbia River Fault Zone; southeastern margin of the Monashee and Shushwap Complexes, southern B.C.," C.J.E.S. vol. 18, pp. 1127-1145.

Read, P.B., Woodsworth, G.J., Greenwood, H.J., Ghent, E.D., and C.A. Evenchick, (1991) "Metamorphic Map of the Canadian Cordillera, G.S.C. Map1714A; in Geology of the Cordilleran Orogen in Canada, H. Gabrielse and C.J.Yorath (ed); G.S.C., Geology of Canada, no. 4.

Reesor, J.E. and J.M. Moore, "Petrology and Structure of the Thor-Odin gneiss dome, Shushwap Metamorphic Complex, B.C.", G.S.C. Bull. 195.

Riddihough, R.R., and R.D. Hyndman (1991), "Modern plate tectonic regime of the continental margin of western Canada, Chapter 13 in Geology of the Cordilleran Orogen in Canada, H. Gabrielse and C.J.Yorath (ed); G.S.C., Geology of Canada, no. 4, p. 435-455.

Roddick, J.A. (1965), "Vancouver North , Coquitlam, and Pitt Lade map areas, British Columbia, with special emphasis on the plutonic rocks; GSC Memoir 335, 276 pp.

Souther, J.G. and E.C. Halstead (1973), "Mineral and Thermal Waters of Canada", G.S.C. Paper 73-18.

Souther, J.G., (1977), "Volcanism and tectonic environments in the Canadian Cordillera- a seecond look," *in* Volcanic Regimes in Canada, W.R.A. Baragar, L.C. Coleman and J.M. Hall (eds.) Geol.Assoc. Can. Special Paper 16, pp 3-24.

Souther, J.G., and C.J. Yorath, (1991) "Neogene assemblages," Chapter 10 in Geology of the Cordilleran Orogen in Canada. H. Gabrielse and C.J.Yorath (ed); G.S.C., Geology of Canada, no. 4, pp. 373-401.

Souther, J.G.Stevenson, J.S. (1950), Geology and mineral deposits of the Zebellos mining camp, British Colmbia; B.C. Dept. of Mines Bull. 27, 145 pp.

Torgersen, T. and W.J. Jenkins (1982), "Helium isotopes in geothermal systems: Iceland, The Geysers, Raft River and Steamboat Springs", Geochemica et Cosmochemica Acta, Vol. 46, pp 739 - 748.

Wait, F.G.(1898), "Geological Survey of Canada, Ann. Rept., Vol. XI, pt.R, p54.

Wanless, R.K., Stevens, R.D., Lachance, G.R., and R.N.D. Delabio (1974), "Age determinations and geological studies; K-Ar isotopic ages, Rpt. 12, GSC Paper 74-2, 72 pp.

Wanless, R.K., Stevens, R.D., Lachance, G.R., and R.N.D. Delabio (1978), "Age determinations and geological studies; K-Ar isotopic ages, Report 12, GSC Paper 74-2;72 pp.

Waring, G.A.(1965) "Thermal Springs of the United States and other Countries of the World - A Summary", U.S.G.S. Prof. Paper 492.

Weiss, Dr. S.,Institut für Hydrologie, GSF-Forschungszentrum für Umwelt und Gesukndheit, Neuherberg, F.R. Germany, personnel communication, (January 20, 1992).

Welhan, J.A., R.J. Poreda, W. Rison, and H. Craig, (1988), "Helium Isotopes in Geothermal and Volcanic Gases of the Western United States. Journal of Volc. and Geothrm. Res., vol.34, pp. 185-199

Wetherhill, G.W., (1975), Radiometric chronology of the early Solar System. Annual Review Nuclear Science, 16:283-328

Williams, P.M. (1971), "The distribution and cycling of organic matter in the ocean", in Organic Compounds in aquatic environments, Faust, S.D and J.V.Hunter, Eds., Marcel Dekker publ., New York , pp 145-164.

Yorath, C.J., Senior research scientist, Pacific Geoscience Centre, Sidney, B.C., personal communication, (April 14, 1993).

Appendix A

Regression Statistics for HSC-Mate Island NaCl (ppm)Mixing Line

Regression Statistics for NaCl (ppm)

Multiple R	*0.9995*
R Square	*0.99901*
Adjusted R Square	*0.99876*
Standard Error	*0.0511*
Observations	*6*

				Y=mx+b	*x*	*Residuals*
	Intercept	*-0.258349*	*-0.258349*	*0*	*0.0208687*
	x1	*1.0026687*	*4.053126*	*4.3*	*-0.024957*
					0.0040882

Analysis of Variance

	df	*n of Squares*	*Mean Square*	*F*	*Significance F*
Regressio	*1*	*10.526729*	*10.5267294*	*4031.2905*	*3.686E-07*
Residual	*4*	*0.010445*	*0.00261126*		
Total	*5*	*10.537174*			

	Coefficients	*Standard Er*	*t Statistic*	*P-value*	*Lower 95%*	*Upper 95%*
Intercept	*-0.2583*	*0.0452009*	*-5.715577*	*0.0022917*	*-0.383848*	*-0.132851*
x1	*1.00267*	*0.0157919*	*63.4924446*	*1.835E-08*	*0.9588232*	*1.0465143*

Regression statistics for seawater mixing lines

SO4--Regression line		*y=mx+b*	x
Intercept	-0.893961592	*0.002947*	0.9
x1	0.996565267	*3.391269*	4.3

Regression Statistics

Multiple R	0.998125663
R Square	0.996254839
Adjusted R Sqt	0.995318549
Standard Error	0.098858734
Observations	6

Borate Regression line		y=mx+b	x
Intercept	-1.231849	0.02841	0.9
x1	1.400287	5.069443	4.5

Regression Statistics

Multiple R	0.9943933
R Square	0.9888181
Adjusted R Square	0.9776361
Standard Error	0.0227261
Observations	3

Regression Statistics for NaCl (mmols) plot

Multiple R	0.994918336
R Square	0.989862494
Adjusted R Sq	0.987834993
Standard Error	0.224022212
Observations	7

Regression Statistics Br-Cl

Multiple R	0.9999134
R Square	0.9998268
Adjusted R Square	0.9997403
Standard Error	0.0142837
Observations	4

Appendix He

Note: This section is synthesized from information in Mamyrin and Tolstikhin (1984) unless otherwise referenced.

The three genetic sources of helium gas are:

1) **primordial;** from nucleosynthesis fusion reactions; $^3He/^4He = \sim 2.4 \times 10^{-4}$
2) **radiogenic;** produced through α decay $^3He/^4He = \sim 8 \times 10^{-12}$
3) **spallogenic;** from cosmic ray bombardment of matter $^3He/^4He = \sim 0.1 - 0.3$

Other noble gases also have specific isotopic ratios resulting from the same three modes of origin. Table 1 (after Mamyrin and Tolstikhin) quantifies these relationships.

TABLE 1

Isotope composition of primordial, radiogenic and spallogenic light noble gases

Gas	$^3He/^4He$	$^{20}Ne/^{22}Ne$	$^{21}Ne/^{22}Ne$	$^{40}Ar/^{36}Ar$	$^{38}Ar/^{36}Ar$
Primordial	$3 \cdot 10^{-4}$	12—13	0.03	10^{-4}	0.17—0.18
Radiogenic	$2 \cdot 10^{-8}$	0	0.3—1.0	10^{7}	1
Spallogenic	$2 \cdot 10^{-1}$	0.9	0.95	0.01	0.65

The following section summarizes the evidence which led to delineation of the three principal genetic typesof helium.

1) Primordial helium

Radiometric chronology data points to an absolute age for Earth of approximately 4.5 billion years, while meteorites ages are generally in the range of 4.5 to 4.7 billion years. The assumption that meteorites were a part of the protomatter of planet earth has been substantiated largely through the study of carbonaceous chondrites. The latter are deemed to be one of the principal contributors, along with gas-rich and other meteorites, of volatile and primordial gases to earth's accreting mass about 4.5 billion years ago. [4]

The $(^3He/^4He)_{prim}$ ratio (based again on trapped primordial carbonaceous chondrite gases and the relationship between helium primordial ratio and $^{20}Ne/^{22}Ne$) has been calculated to be near 2.4×10^{-4}.

2. Radiogenic helium

Most terrestrial rocks have $^3He/^4He$ ratios near 2×10^{-8}, typified by older granitic rocks where the presence of uraniferous minerals has led to α-decay. Alpha particles need only add two electrons to become ^4He atoms, thus in Uranium fission reactions, the heavy isotope of helium quantity produced over a time (t) is given by the equation:

$$^4He = {}^{238}U\ [\exp \lambda_\alpha t\text{-}1] \times N_\alpha \times N_\alpha^1$$

where: N = 8 = #He atoms formed to U family decay

$N^1_\alpha = 2$ adds contributions from Th and actino U.

$\lambda_\alpha = 0.153 \times 10^{-9}/yr$

The light isotope of helium however is also produced by U-fission as shown by the equation (Kugler and Clarke, 1972):

$$^3He = {}^{238}U\ [\exp \lambda_\alpha t\ \text{-}1\ ] \times (\lambda_f/\lambda_\alpha) \times Y\ (^3H,\ ^3He)$$

where: $\lambda_f = 8.6 \times 10^{-17}$ /yr

$Y\ (^3He,\ ^4He) = 2.2 \times 10^{-4}$ atoms/fission.

Thus the ratio of $^3He/^4He$ produced by the radioactive decay of uranium is:

$$^3He/^4He = (\lambda_f/\lambda_\alpha) \times Y(^3He,^4He)/N^1_\alpha = 8 \times 10^{-12}$$

This figure, is more than three orders of magnitude less than the observed ratio. Even though addition of primordial helium (retained since planetary accretion) could augment the calculated ratio somewhat, a more likely, and demonstrated, contribution from lithium can occur through three separate reactions; neutron, alpha and γ reactions:

(1) $^6Li + n \rightarrow \alpha + {}^3H\ \beta^-\ {}^3He$

(2) $^7Li + \alpha \rightarrow {}^8Be + {}^3H$

and (3) $^7Li + \gamma \rightarrow {}^4He + {}^3H$

Of the above three reactions only reaction (1) is considered to be of major significance in supplying ^3He atoms and thereby raising the helium isotope ratio.

Although a detailed examination of the ($^3He/^4He$) formula which incorporates this reaction is beyond the scope of this study, the net effect is important, for values of between 1 and 3 x 10^{-8} are calculated (Morrison and Pine, 1955) which are in close agreement with measured values. The ubiquitous occurrence of lithium in most rock-types is a principal factor. Older granitic rocks, where the above decay reactions and accumulation of helium have had time to occur, have $^3He/^4He$ ratios indicative of radiogenic production of helium (eg. 0.06 Selkirk ratio). Further, the presence of a portion of the ^3He in lithia-rich geothermal waters, such as those of the Halcyon hotspring, can be at least partially attributed to this source.

3. Spallogenic helium

The ($^3He/^4He$) ratio for spallogenic helium is the highest in nature about 0.1 to 0.3. This type of helium is produced when matter is bombarded by cosmic rays. The latter are composed largely of protons but include raw atomic nuclei ranging in weight and size from helium through to iron. Although evidence suggests that cosmic rays also come from outside the solar system the bulk of our source is the sun.

The high ratio of ($^3He/^4He$) in cosmogenic helium presents a temptingly simple solution to explain high ratios observed in certain mantle-related processes. For, a simple mixing of radiogenic and spallogenic matter could yield He-isotope ratios over a broad range including those related to primordial mantle sources. Such however is not the case, and can be explained largely through the phenomenon of helium escape.

The observed concentration of atmospheric helium (5.24 ppm) is far below its predicted value when compared to other noble gases. First demonstrated by Nicolet (1957), helium escape drains the atmospheric sink of He so that even though the ratio of He-isotopes remains very high, the content of helium in air is very low. This continual helium dissipation into space has significant implications for studies of mixing of terrestrial reservoirs, as despite

into space has significant implications for studies of mixing of terrestrial reservoirs, as despite the elevated isotopic ratio (0.1 to 0.3), the depleted atmospheric concentration, cannot possibly account for the high ratios of helium found in mantle hop-spots, volcanic fumeroles, oceanic ridges (Craig and Clarke, 1970) or other even geothermal waters of the Coast Plutonic Complex.